ANNUAL REPORT

2017-2018

Nuclear Chemistry

Czech Technical University in Prague

CONTACTS

Department of Nuclear Chemistry

Břehová 7
115 19 Praha 1
Phone: +420 224 358 207
Fax: +420 222 317 626
E-mail: kjch@fjfi.cvut.cz
http://www.jaderna-chemie.cz/

Czech Technical University in Prague

DEPARTMENT OF NUCLEAR CHEMISTRY

NUCLEAR CHEMISTRY

Annual Report 2017-2018

Editors: John, J.; Vopálka, D.; Múčka, V.; Kozempel, J.

Reports are available from: Marie Kotasová (kotasova@fjfi.cvut.cz), Břehová 7, 115 19 Praha 1, Czech Republic or download from: http://www.jaderna-chemie.cz/

EDITORIAL

Dear Reader, this is the sixth in the series of the CTU Nuclear Chemistry Annual Reports that became a well-established periodical with bi-annual periodicity and established structure and format. The period covered by this issue (2017 – 2018) can be generally rated as a busy period in the life of the department during which foundations for the new quantitative and qualitative growth were laid.

This ongoing growth has been connected with the fact that, after many years of developments of the regions, the European structural and investment funds (ESIF), specifically the European regional development fund and European social fund, were opened for the institutions located in Prague and Central Bohemian region, too. The department has been successful – either as a part of the faculty or together with external partners – in applying for resources to significantly develop its infrastructure and also for partial increase in the staff numbers. The full list of the ESIF projects is given in the respective chapter later in this report, here I would like to pinpoint only the two most important research-directed ones – CTU project CAAS – "Center for Advanced Applied Sciences", and the project RAMSES – "Ultra-trace Isotope Research in Social and Environmental Studies Using Accelerator Mass Spectrometry" – awarded to a consortium led by the Institute of Nuclear Physics AS CR, Řež.

From the point of view of the operation of the Department of Nuclear Chemistry (DNC), the most important fact is that there was a significant shift in the policy of the Czech grant agencies that now make it possible to apply not only for operational expenses but also for personal costs. Since the funding of DNC is strongly research driven (more than two thirds of the annual budget come from grants and research funds) this was reflected significantly in the overall numbers of staff. From the starting value of 21.5 FTE in January 2017, the department grew to 34.7 FTE in December 2018. A significant part of this increase has been distributed among young researchers – in particular PhD students. Great news for the future is that three young researchers were promoted to the academic staff during the period. From the qualification structure point of view, promotion of Ján Kozempel to the associate professor should be mentioned here. The three DNC young associate professors are now taking the lead in both the research and teaching activities and should be a guarantee of the future development of the department. This is exemplified e.g. by the fact that they are the leaders of the three big ESIF research project – chemistry part of CAAS is led by Václav Čuba, RAMSES by Mojmír Němec and CAP – Centre of Applied Photovoltaics – by Ján Kozempel. As usually, the good news is accompanied also by some bad ones. In this case, it is the sad news that the former professor at DNC – Prof. Milan Pospíšil – passed away on the 29th July 2018. You will find more details in a short obituary at the end of this editorial.

Another important event during the period covered was the leading role of DNC in organisation of the international 18th Radiochemical Conference held in 2018 traditionally in the Western Bohemian spa of Mariánské Lázně (http://www.radchem.cz/). Again, it was organised as a part of the regular bi-annual series of pan-European nuclear chemistry conferences guaranteed by the Division of Nuclear and Radiochemistry of the EuChemS. The largest ever audience – 334 participants from 36 countries – made the conference a clear success. The booklet of all accepted abstracts was published as a special issue – Vol 16, No 2 (2018) – of the open access journal Czech Chemical Society Symposium Series and is available at http://www.ccsss.cz/index.php/ccsss/issue/viewIssue/14/30. Full texts of the selected contributions are collected in a special issue of the Journal of Radioanalytical and Nuclear Chemistry (Volume 318, Issue 3).

Similarly to the previous period, the research in nuclear chemistry at the DNC was organised in four research groups that, for the purpose of this Report, may be referred to as "Speciation and Migration", "Separation and Radioanalytics", „Radiation Chemistry" and "Radiopharmaceutical

Chemistry". Selection of short reports characterising the research topics in more detail forms the body of this Annual Report. To summarise briefly, one can state that the research activities of the DNC continued to cover the majority of the fields within the traditional definition of nuclear chemistry – radiochemistry including its separation methods, radioanalytical chemistry, radiotracer techniques and chemistry of the actinides, radiation chemistry including its applications, e.g., in radiation initiated preparation of solids inclusive nanoparticles or in bioradiation chemistry, environmental radiochemistry and radioecology, or radiopharmaceutical chemistry. In these fields, the CTU has been a partner in several big international EURATOM H2020 integrated projects such as CEBAMA or GENIORS; thus, most of the research is performed in close collaboration and co-ordination with the major European institutes and universities. As usually, the main national collaborations included the ÚJV Řež a.s., Nuclear Physics Institute of the AS CR, or Research Centre Řež, all three located in Řež near Prague, Institute of Physics of the AS CR, Radioactive Waste Repository Authority of the Czech Republic (SÚRAO), and many others. Full list of publications, conference contributions, and research reports can be found in the respective section below.

The Department Seminar continued to be organised as an open seminar together with the Working Group of Nuclear Chemistry (WGNC) of the Czech Chemical Society and continues to attract an average of 30–40 participants each month. If approved by the speaker, opening lectures by invited experts are recorded and archived using the SlidesLive™ system. These recordings are publicly available at https://slideslive.com/seminar-kjch-fjfi-cvut-v-praze and contribute tremendously to the visibility of our department and nuclear chemistry in general. The invited speakers and the topics of their talks are listed in a dedicated section of this Annual Report.

In the field of international cooperation in education, the earlier Euratom FP7 CINCH and CINCH-II projects, co-ordinated by DNC CTU, were succeeded by the Euratom H2020 MEET-CINCH project aiming at setting-up "A Modular European Education and Training Concept In Nuclear and Radio Chemistry" (http://www.cinch-project.eu/). In this project, CTU remained a partner under coordination of the Gottfried Wilhelm Leibniz University Hannover (Germany). As an example of the tools developed in these programmes, the CINCH Moodle e-learning management platform is described in a dedicated article in the Education section below. Among the important activities, the existing set of modular hands-on courses in nuclear chemistry for the customers from both academia and industry are periodically run and further developed.

Similarly to the previous Editorials, it can be concluded that the department is marching on strongly and the core activities and productivity have been mostly taken over by a strong group of highly competent and motivated young nuclear chemists in their late early 40s who still remain backed by the older generation. This team represents one of the most important units of the Czech nuclear community. Taking in account the variety and number of research grants, the Department of Nuclear Chemistry continues to resemble rather a small research institute than a typical university department.

As usually, we hope that you will find this report interesting, and that it may help to further promote both our national and especially international collaboration. We hope that all potential new collaborators will find the environment in our research groups as convivial and inspiring as our current colleagues do.

Jan John

Head, DNC

OBITUARY

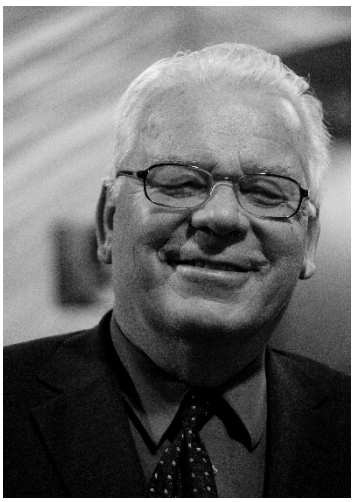

Prof. Milan Pospíšil, a renowned radiation chemist, our friend and dear colleague, passed away on the 29th July 2018 in the age of 81 years. He was born on the 15th March 1937 in Semily. After graduating from the chemistry high school in Pardubice, he studied nuclear chemistry at the Faculty of Nuclear Sciences and Physical Engineering of the CTU where he graduated in 1962. Since the graduation till his retirement in 2016, he was an academic at the Department of Nuclear Chemistry, where he served for many years as the registrar. Here he was also promoted to associated and later inaugurated to full professor of Nuclear Chemistry.

During his more than 50 years spent at DNC, he shared his activities equally between the science and teaching. His papers, especially those from the field of the kinetics of reduction processes influenced by ionizing radiation, found lively interest both in national and international scientific community. In parallel to teaching the courses of Chemistry of special elements, Instrumental methods of research and analysis, and Practical exercises in instrumental methods, he supervised many doctoral, diploma and bachelor students. In addition to being a leading scientist and excellent teacher, he was a friend and often even conferee of his students with whom he maintained very friendly and empathic relations. Even after his retirement, he stayed in touch with the department and faculty.

He will be remembered with love and gratitude by all who knew him.

God rest his soul!

CONTENTS

EDUCATION AND MANAGEMENT

- Courses Taught
- Projects and Management

Courses Taught

List of Courses in the Academic Years 2017/2018 and 2018/2019

Title, credits (ECTS), semester (W - October to mid-January, S - March to mid-June), cycle (B – bachelor, M – master, D – doctorate), lecturer(s)

• Chemistry for Nuclear Engineering	4	S	B	Drtinová, B.; Silber, R.
• Fundamentals of Construction and Function of Nuclear Power Plants	3	S	B	Bílý,T.*; Sklenka, L.*; Frýbortová, L*;
• General Chemistry	6	W	B	Motl, A.
• General Chemistry 1	3	W	B	Motl, A.
• General Chemistry 2	3	S	B	Motl, A.
• Instrumental Methods of Research 1	3	S	B	Zavadilová, A. ; Vlk, M.
• Ionising Radiation Detection	2	S	B	John, J.
• Laboratory Practice in the Instrumental Methods of Research	2	S	B	Zavadilová, A. ; Vlk, M.
• Measurement and Data Handling	3	W	B	Vetešník, A.; Vopálka, D.
• Nuclear Chemistry 1	3	S	B	Čuba, V.; John, J.
• Nuclear Chemistry 2	4	W	B	John, J.; Čuba, V.
• Physical Chemistry 1	5	W	B	Múčka, V.; Silber, R.
• Physical Chemistry 2	5	W	B	Drtinová, B.; Silber, R.
• Practical Exercises in Ionising Radiation Detection	3	S	B	Němec, M.; Čubová, K.; Špendlíková, I.; Semelová, M.
• Practical Exercises in Radiochemical Techniques	2	W	B	Němec, M.; Čubová, K.; Špendlíková, I.; Semelová, M.
• The Theory of the Electromagnetic Field and Wave Motion	4	S	B	Vetešník, A.

* External teacher

• Application of Radionuclides 1	3	W	M	Mizera, J.*
• Application of Radionuclides 2	3	S	M	Mizera, J.*
• Applications of Radiation Methods	2	S	M	Múčka, V.
• Astrochemistry	2	S	M	Ferus, M.*
• Chemistry of Radioactive Elements	2	W	M	John, J.
• Chemistry of the Pharmaceuticals	3	S	M	Smrček, S.*
• Decomissioning of Nuclear Facilities	2	S	M	Čubová, K.
• Determination of Radionuclides in the Environment	2	S	M	Němec, M.
• Environment Chemistry and Radioecology	2	W	M	Filipská, H.; Vopálka, D.
• Glykoconjugates and Immunochemistry	3	S	M	Pompach, P.*
• Introduction to Photochemistry and Photobiology	2	W	M	Čubová, K.; Juha, L.*
• Isotop Syntheses	2	S	M	Kozempel, J.;°Vlk, M.
• Modelling and Simulation of Radionuclide Migration in Environment	3	W	M	Vetešník, A.; Vopálka, D.
• Physical Chemistry 3	2	W	M	Čuba, V.
• Physical Chemistry 4	5	S	M	Múčka, V.; Bárta, J.; Silber, R.
• Physical Chemistry 5	2	W	M	Silber, R.
• Practical Exercises in Nuclear Chemistry	4	W	M	Čubová, K.; Němec, M.
• Practical Exercises in Radiation Chemistry	3	S	M	Bárta, J.; Čuba, V.
• Practical Exercises in Radiation Methods in Biology and Medicine	4	S	M	Kozempel, J.; Vlk, M.
• Practical Exercises in Radioanalytical Methods	4	S	M	Němec, M.; Čubová, K.; Špendlíková, I.; Semelová, M.
• Practical Exercises in Separation Methods in Radiochemistry	3	W	M	Němec, M.; Čubová, K.; Špendlíková, I.; Semelová, M. .
• Protection of Environment	2	W	M	Filipská, H.
• Radiation Chemistry	4	S	M	Motl, A.
• Radiation Methods in Biology and Medicine	2	W	M	Čuba, V.
• Radioanalytical Methods	3	S	M	John, J.
• Radiobiology	2	S	M	Davídková, M.

* External teacher

• Radionuclide Production	2	W	M	Lebeda, O.*
• Radiopharmaceuticals 1	2	W	M	Lebeda, O.*
• Radiopharmaceuticals 2	2	W	M	Kozempel, J.; Moša, M.*; Vlk, M.
• Radiopharmaceuticals Technology	2	S	M	Kozempel, J.; Vlk, M.
• Separation Methods in Nuclear Chemistry 1	3	W	M	Němec, M.
• Separation Methods in Nuclear Chemistry 2	2	S	M	Němec, M.
• Structure Analysis 1	3	S	M	Kozempel, J.; Vlk, M.
• Structure Analysis 2	2	W	M	Kozempel, J.; Vlk, M.
• Technology of the Fuel Cycles of Nuclear Power Stations	2	W	M	Čubová, K.; Štamberg, K.
• The Chemistry of Operation of Nuclear Power Plants	2	W	M	Drtinová, B.; Silber, R.
• Theoretical Basics of Radiation Chemistry	2	W	M	Juha, L.*
• Toxicology	2	W	M	Kozempel, J.; Vlk, M.
• Trace Radiochemistry	3	S	M	Filipská, H.; John, J.

* External teacher

• Advanced Nuclear Chemistry	D	John, J.; Čuba, V.
• Applications of Radiation Chemistry in Chemical Industry, Agriculture and Medicine	D	Múčka, V.
• Application of Radionuclides	D	Mizera, J.*
• Biosyntheses of Labelled Compounds	D	Smrček, S.*
• Chemistry of Actinoids and Transactinoids	D	John, J.
• Experimental Nuclear Chemistry	D	John, J.; Čubová, K.; Němec, M.
• Instrumental Radioanalytical Methods and their Application for Monitoring the Environmental Contamination	D	Kučera, J.*
• Labelled Compounds	D	Smrček, S.*; Kozempel, J.
• Modelling and Simulation of the Migration Processes in the Environment	D	Vetešník, A..; Vopálka, D.
• Nuclear Data, Targetery and Preparation of Radionuclides	D	Lebeda, O.
• Nuclear Power Plants	D	Sklenka, L.; Bílý, T.
• Photochemistry and Radiation Chemistry	D	Juha, L.*; Čubová, K.; Čuba, V.
• Radiation Removal of Liquid and Gaseous Contaminants	D	Múčka, V.
• Radioanalytical Chemistry	D	Němec, M.; John, J.
• Radionuclides in Biological Sciences	D	Smrček, S.*
• Radiopharmaceuticals	D	Lebeda, O.*; Moša, M.*
• Separation Methods	D	Němec, M.
• Technology of Nuclear Fuels	D	Štamberg, K.; Čubová, K.
• Transport Processes	D	Vopálka, D.

* External teacher

Projects and Management

CINCH MOODLE E-LEARNING PLATFORM

Bartl, P; Semelová, M.; Němec, M.; John, J.; Šácha, M.; Omtvedt, J. P.[1]; Fournier, C.[2]; Evans, N.[3]; Macerata, E.[4]; Platts, L.[5]; Štrok, M.[6]

[1]University of Oslo, Norway; [2]Leibnitz University of Hannover, Germany;
[3]Nottingham Trent University, UK; [4]Polytechnic University of Milano, Italy;
[5]National Nuclear Laboratory, UK; [6]Jozef Stefan Institute, Slovenia

INTRODUCTION

CINCH Moodle e-learning platform has been developed within the CINCH II project and is administered by the CTU team. Its purpose is to serve as a universal platform for hosting e-learning courses across the NRC Network. In addition, it provides password-protected access to other relevant resources such as open acces teaching materials, webinars. video-lectures, learning texts etc.

STRUCTURE

The platform is logically ordered into Themes containing the main Courses that constist of Topics. Each topic may be filled with Resources and/or Activities of various kind offered by the platform. Such organized structure provides complete courses containing complex student-teacher environment, i.e. learning materials, video-lectures, tests or a forum. Moreover, topics may be conditionally locked to prevent a student from skipping them, which results into a chronologically ordered study plan.

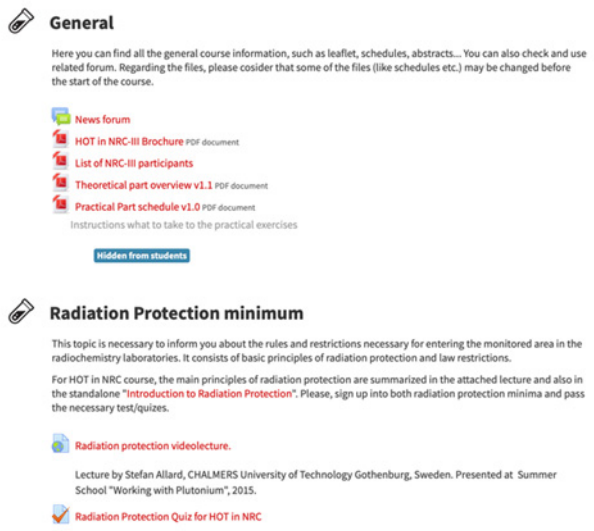

Fig. 1. A screenshot of a blended-learning Hands-on-training in Nuclear Chemistry 2018 course, developed by the CTU.

Currently, the CINCH Moodle utilizes the following sturcture. The first two themes contain complex courses mostly developed within the CINCH-series of projects, the other themes mediate contact to materials developed by the third parties:

- Summer Schools
  - Contains four courses
  - Each based on a summer school, including lectures and tests
- Learning and Training Courses
  - Contains 9 courses
  - Usually cover a fundamental learning course or supplement ongoing hands-on training course
- NucWik Content
  - Contains 4 courses
- NAMP Radiochemistry Webinars
  - Contains 1 course with URL links to cycles of webinars on various NRC topics
- GEN IV Webinars
  - Contains 1 course with URL links to a cycle of webinars on generation IV nuclear reactors
- *Materials and Modules (hidden section)*
  - *Material storage for the course creators*
- *Courses Playground (hidden section)*
  - *Training section for the course creators*

FUNCTIONS

One of the most flexible fuctions of the whole CINCH Moodle are Activities that may be associated with the Topics. Fig. 2 shows a partial list of activities available at the platform. Among those are several communication channels (e.g. Chat or Forum, couple of interactive learning tools (e.g. Lesson or Glossary), and mainly several tools for examination (Quiz and Assignment).
Furthermore, enrolled students may be rewarded, along with his or her total mark within a course, by a certificate for clearing the course with exceptional score or a badge for meeting some special conditions.

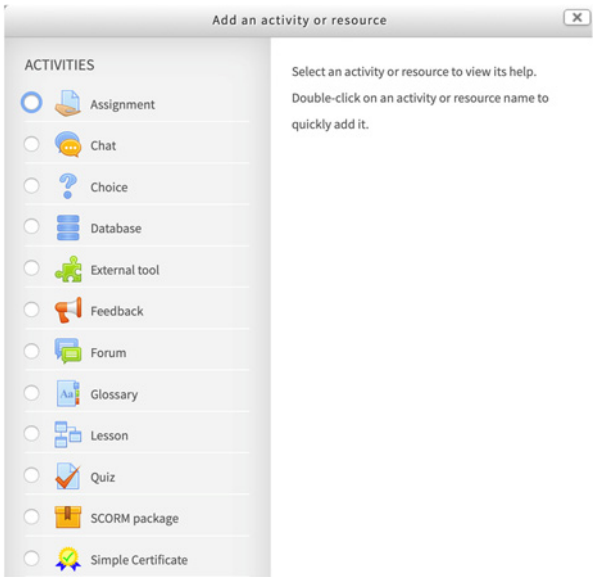

Fig. 2. A screenshot of a partial list of activities the platform offers.

SUMMARY

The CINCH Moodle platform has been successfully tested and proven to be a powerful tool for both the students and teachers. It has a solid course-base nowadays and continues to grow. . It is available at https://moodle.cinch-project.eu/.

This development and administration has been supported by the MEET-CINCH project (H2020 Euratom grant No. 754 972).

18th RADIOCHEMICAL CONFERENCE – RADCHEM 2018

Němec, M.; Mizera, J.[1]; John, J.; Kučera, J.[1]

[1] Nuclear Physics Institute, Academy of Sciences of the Czech Republic, Řež

The 18th Radiochemical Conference – RadChem 2018, was held in the Casino conference centre in Mariánské Lázně, Czech Republic, on the 13-18th May 2018. As usual, the conference was co organized by the Czech Chemical Society, Ioannes Marcus Marci Spectroscopic Society, and Department of Nuclear Chemistry, Faculty of Nuclear Sciences and Physical Engineering, Czech Technical University in Prague (DNC FNSPE CTU). Since 2010, the RadChem series has been organised on behalf of the Division of Nuclear and Radiochemistry of the European Chemical Society (EuChemS). Traditionally, RadChem 2018 was organised in cooperation with the IAEA and sponsored by the IUPAC. Since the previous conference, the number of participants increased again – RadChem 2018 was attended by 334 participants from 36 countries from all parts of the world, from which the most represented countries were the Czech Republic, Germany, Russia, China, France Japan and Slovakia. A new feature for RadChem series was the large number of Chinese participants (18)

and significantly increased French representation (17). In total, 356 contributions were presented at the meeting – 157 lectures, including 7 plenary and 14 invited, and 199 posters The scientific programme was accomplished, except for the plenary lectures, in two parallel sessions. The poster presentations were organised into topical sessions and spread over three days to give the participants ample time for the discussion with the authors.

RadChem 2018 was honoured by being selected as the host of the celebration of the 50th anniversary of the Journal of Radioanalytical and Nuclear Chemistry. The anniversary was commemorated in a lecture "Fifty years of the Journal of Radioanalytical and Nuclear Chemistry" delivered by JRNC editor, dr. Zsolt Révay, during the Sunday evening opening session. The conference itself covered most of the topical issues in the field of nuclear- and radiochemistry in a total of nine sessions including: Radionuclides in the Environment and Radioecology, Nuclear Analytical Methods, Chemistry of Actinide and Trans-actinide Elements, Radiation Chemistry, Production and Application of Radionuclides, Separation Methods and Speciation, Chemistry of Nuclear Fuel Cycle and Radiochemical Problems in Nuclear Waste Management, Radiopharmaceutical Chemistry and Labelled Compounds, and Education. As usually, our thanks are due to all the Session Organisers and to the International Advisory Board for their help and support.

The full conference programme is available at the conference web page (http://www.radchem.cz), the booklet of all accepted abstracts was published as Vol. 16, No 2 (2018) – of the journal Czech Chemical Society Symposium Series and is available (open access) at http://www.ccsss.cz/index.php/ccsss/issue/viewIssue/14/30. Full texts of the contributions that have been selected based on the results of a standard peer-review procedure are collected in a special issue of the Journal of Radioanalytical and Nuclear Chemistry (Volume 318, Issue 3).

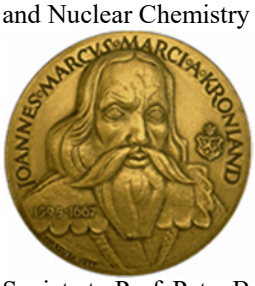

Two prestigious scientific awards were presented during the block of the opening plenary lectures. The first was the Ioannes Marcus Marci Medal for excellence in and significant contribution to spectroscopy awarded by the Ioannes Marcus Marci Spectroscopic Society to Prof. Peter Bode (Delft University of Technology, The Netherlands) in recognition of his excellent results in the field of instrumental radioanalytical methods, especially neutron activation analysis, and in chemical metrology. Prof. Bode delivered a laurate lecture on the topic „Quo Vadis, neutron activation analysis?"

The second appraisement was the Vladimír Majer Medal Award presented by the Nuclear Chemistry working group of the Czech Chemical Society to Prof. Jukka Kalevi Lehto, former Head of the Laboratory of Radiochemistry at the Department of Chemistry, University of Helsinki, Finland, in recognition of his international contributions to ion exchangers development for radioactive waste treatment and investigation of geological and environmental behaviour of radionuclides.

Every day after the demanding conference scientific programme, the participants could have enjoyed a rich social and cultural programme. Besides the Welcome Reception celebrating the 50th Anniversary of JRNC on Sunday mentioned above, every evening played its specific role. The Beer Party on Monday evening presented the Czech cuisine and selection of local beers. On Tuesday night, concert of Jiří Pavlica's Hradišťan Dulcimer Band (http://www.hradistan.cz/en) took place. Wednesday afternoon trips were directed to historical monuments and nature beauties of the surroundings of Mariánské Lázně and were followed by a joint celebration dinner in Teplá monastery. Finally – following the new tradition established at the previous conference – on Thursday evening amateur musician group, composed of the conference participants, gave concert with a folk-rock programme. Traditionally, the last of the social events was the Singing Fountain performance at the spa colonnade.

Next in this series, the 19th Radiochemical Conference – RadChem 2022, has been scheduled for spring 2022 (https://www.radchem.cz/).

RESEARCH REPORTS


Speciation and Migration


Separation and Radioanalytics


Radiation Chemistry


Radiopharmaceutical Chemistry

Speciation and Migration

IMPACT OF CARBONATION ON THE UPTAKE OF RADIUM BY CEMENTITIOUS MATERIALS

Kittnerová, J.; Lange, S.[1]; Drtinová, B.; Deissmann, G.[1]

[1]Forschungszentrum Jülich GmbH, Germany

INTRODUCTION

^{226}Ra is a long-lived radionuclide originating mainly from the decay of ^{238}U in spent nuclear fuel. According to the Swedish nuclear safety case and with respect to the direct disposal of spent nuclear fuels, ^{226}Ra can be a main contributor to long term dose (i.e. 100,000 years). Cementitious materials are widely used as structural support in deep geological repositories and, depending on the repository concept, as backfill for waste conditioning or as component in waste containers. The mobility of radium in cementitious systems is controlled by the solubility of radium-bearing phases under highly alkaline conditions, diffusion, inter-face processes such as surface complexation, or incorporation of radionuclides into solid phases. For the assessment of the long-term safety of a repository, the retardation mechanisms of radionuclides on cementitious materials within the engineered barriers need to be fully understood. However, the cementitious barriers will change over time in terms of phase and pore water composition, e.g. due to leaching/alteration by groundwater. One of the main processes that needs to be considered is carbonation of the hardened cement paste during the operational and post-closure phase of the repository. Due to carbonation, calcium-silicate-hydrates (CSH), which are the major constituents of hardened cement paste with high immobilization potential for many radionuclides, will be transformed into calcite and amorphous silica, lowering the alkalinity and promoting also the corrosion of rebars.

In this study we addressed the effects of carbonation on the uptake of radium on various cementitious materials by performing a comparative study on the radium retention potential for fresh and altered (carbonated) materials.

EXPERIMENTAL

Different cementitious materials were used including three hardened cement pastes (HCP CEM I, HCP CEM II, and VTT, a low pH HCP comprising CEM I, blast furnace slag, silica fume, and quartz filler [1]) and two concretes (C CEM I and C CEM III). All materials were used as crushed powders. Carbonation of the cementitious materials was performed in an autoclave under a pressure of about 30 bar of CO_2 at room temperature for 24 hours under several millilitres of solution, which was used for pH measurement. The materials were characterized prior and after carbonation by X-ray diffraction analysis (D4 Endeavor, Bruker AXS GmbH). The radium uptake was determined in static batch experiments (^{226}Ra concentration $5 \cdot 10^{-7}$ mol·L^{-1}) lasting for three weeks, using liquid-to-solid ratios of 25, 100 and 200 L·kg^{-1}. Leachate from HCP CEM I was used as solution for all materials except for VTT; here a leachate from the VTT was prepared. For sorption experiments on carbonated materials, the carbonated solution was used. The ^{226}Ra concentrations in the liquid phase at the end of the sorption experiments were determined by gamma spectrometry (HPGe detector, GLO510P, DSG: Detector System GmbH with Gamma-Vision version 6.01.). The ^{226}Ra uptake by the cementitious materials is characterized in terms of the distribution ratio R_d between liquid and solid phases.

The predicted pH decrease was confirmed for all materials after 24 hours of carbonation. The XRD analyses were used as proof of the carbonation. Comparison of the spectra prior and after carbonation revealed a decrease in the portlandite ($Ca(OH)_2$) content and an increase of the calcite ($CaCO_3$) content, shown for HCP CEM II in Figure 1.

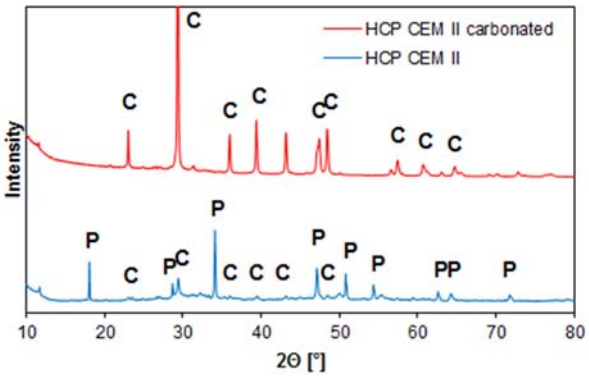

Fig. 1. XRD analysis of HCP CEM II prior and after carbonation. C – Calcite, P – Portlandite.

RESULTS

In the sorption experiments, in all cases the ^{226}Ra uptake on altered materials was found to be higher compared to the fresh materials. For fresh HCP and concrete prepared from ordinary cements, the R_d values in average ranged from 60 to 100 L·kg^{-1}. The highest ^{226}Ra uptake was observed for the VTT low pH HCP with R_d values of about 1500 to 2500 L·kg^{-1}, all results comparable to those determined by Lange et al. [2]. The significantly higher ^{226}Ra uptake in the systems with VTT is probably due to the lower system pH and the lower Ca/Si ratio of the CSH. The altered, carbonated materials show generally R_d values for ^{226}Ra in the range of 2000 to 10000 L·kg^{-1}, including the altered VTT, which in this case is not the most sorbing material. These results indicate that the experimental carbonation resulted mainly in the conversion of portlandite without destroying the CSH phase completely, but decreasing its Ca/Si ratio. According to Lange et al. [2] during carbonation of CSH, R_d for ^{226}Ra may first increase due to the decreasing Ca/Si ratio before it finally drops after complete carbonation, since the uptake of ^{226}Ra by calcite is significantly low.

REFERENCES

[1] Vehmas, T. et al (2017) KIT SCIENTIFIC REPORTS 7734, 101-111.

[2] Lange, S. et al. (2018) Appl Geochem 96, 204-216.

The research leading to these results has received funding from the European Union's Horizon 2020 research and innovation program under grant agreement No 662147 (Cebama).

STUDY OF RADIUM UPTAKE BY CEMENTITIOUS MATERIALS RELEVANT FOR LILW DISPOSAL IN THE CZECH REPUBLIC

Drtinová, B.; Kittnerová, J.; Vopálka, D.

INTRODUCTION

The uptake of radium ^{223}Ra (gained via ^{227}Ac/^{227}Th/^{223}Ra generator) used instead of ^{226}Ra isotope on three cementitious materials: a hardened cement paste HCP CEM II/ A-S 42.5 R (hydration for six months) and two types of concrete (both actually used in the storages of radioactive waste in the Czech Republic) under various conditions was studied. The aim of the research was to collect data enabling the preparation of methodology necessary for a case study of LLW-ILW repository Bratrství located in Czech Republic with engineered barriers based on cementitious materials.

The ^{223}Ra has a half-life of 11.43 days, decaying to ^{219}Rn with a half-life of only 4 s, which does not interfere with the measurement of radium. The short half-life of generated radon enables to work more safely in comparison to the use of ^{226}Ra with its relatively long-lived daughter ^{222}Rn. On the other hand, the short half-life of ^{223}Ra can be considered also as a disadvantage limiting the time of experiments.

EXPERIMENTAL AND RESULTS

All three cementitious materials were studied by X-ray diffraction (Rigaku Mini Flex 600). The comparison of measured spectrum with the database ICDD PDF-2 (version 2013) of the measuring system enabled to identify four crystalline mineral phases in HCP, namely calcite $CaCO_3$, portlandite $Ca(OH)_2$, hydrotalcite $Mg_6Al_2CO_3(OH)_{16}\cdot 4(H_2O)$ and ettringite $Ca_6Al_2(SO_4)_3(OH)_{12}\cdot 26H_2O$, and two phases in concretes, namely portlandite $Ca(OH)_2$ and quartz SiO_2.

Sorption experiments were carried out in a carrier-free arrangement (with Ra concentration between 4.7×10^{-13} and 1.8×10^{-12} mol·L^{-1}), i.e. nearly in the absence of change of solution composition caused by uptake of Ra sorption via ion exchange. Varying conditions included the temperature, the liquid-to-solid ratio *V/m*, and the composition of the starting solution which was either Portlandite water (saturated $Ca(OH)_2$) or synthetic cement pore water CPW. Equilibrium sorption experiments were evaluated using a distribution coefficient K_d (also via non-linear equilibrium models, namely the Langmuir and Freundlich isotherms).

Investigation of the sorption kinetics proved that sorption proceeds quite quick and equilibrium is reached within one day for all studied materials. Through equilibrium sorption experiments (96 hours) the change of the liquid phase from the saturated $Ca(OH)_2$ to the synthetic cement water CPW resulted into the distribution coefficient K_d increase. The increasing of the temperature in which the experiments were performed from 22 to 80 °C had an interesting effect on the behavior of the HCP (Fig. 1) and one concrete material. The K_d firstly decreased followed by increase with increasing phase ratio. Within verifying of this trend at 50 °C and 65 °C for HCP, milder trend with smaller phase ratios was observed.

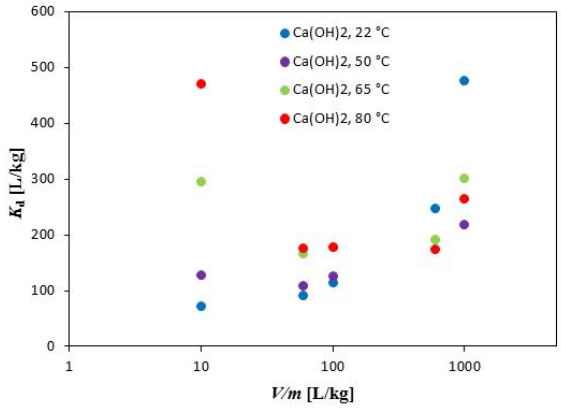

Fig. 1. Dependence of determined K_d values describing ^{223}Ra uptake on hydrated cement paste in the Portlandite water $Ca(OH)_2$ on the phase ratio *V/m* at different temperatures.

The distribution coefficient of ^{226}Ra (with initial concentration about 10^{-8} mol·L^{-1}) on HCP (type CEM I) was set at 140 L/kg for degraded HCP (phase ratio 1:200) at pH 12.5 [1]. The CEM I type of cement is contained in our concrete sample, which at this *V/m* ratio produced K_d values of about 235 L·kg^{-1} (1:100) and 427 L·kg^{-1} (1:600), both at 22 °C.

To summarize the results of radium retention on cements, K_d values ranged from 72 to 574 L·kg^{-1} in $Ca(OH)_2$ at temperatures between 22 and 80 °C. At the same temperatures, in the case of HCP, the K_d values were found to be within range 73 to 478 L·kg^{-1}, in systems with $Ca(OH)_2$ saturated solution as the liquid phase. In CPW, the values were 103-764 L·kg^{-1}.

REFERENCES

[1] Tits, J. et al. (2006) Radiochim Acta 94, 637-643.

The research leading to these results has received funding from the European Union's Horizon 2020 Reasearch and Training Programme of the European Atomic Energy Community (EURATOM) (H2020-NFRP-2014/2015) under grant agreement n° 662147 (CEBAMA). This contribution is partially a result of Radioactive Waste Repository Authority project „Research support for Safety Evaluation of Deep Geological Repository".

COMPARATIVE STUDY OF HTO DIFFUSION ON INDIVIDUAL AND COUPLED SYSTEMS OF COMPACTED BENTONITE AND FRESH ORDINARY PORTLAND CEMENT PASTE

Rosendorf, T.[1]; Hofmanová, E.[1]; Vopálka, D.; Vetešník, A.; Červinka, R.[1]

[1]ÚJV Řež, a. s., Czech Republic

INTRODUCTION

Determination of diffusion coefficients of radionuclides is fundamental for the performance assessment of radioactive waste disposal in deep geological repositories (DGR). During the long-term evolution of DGR, the alkali-leachates from cementitious materials will induce changes in compacted bentonite (mineralogy, cation exchange capacity, population of exchangeable cations, swelling, hydraulic conductivity) that may affect radionuclides migration [1-2]. The radionuclide transport on the interface of compacted bentonite and cementitious materials has been rarely investigated. The main aim was to understand how processes at the interface of bentonite and cementitious materials affect the transport properties of bentonite. Under the same experimental conditions, HTO through diffusion experiments were performed on individual materials (bentonite or fresh hardened cement paste) and compared to experiments in the coupled system [3].

EXPERIMENTAL

Bentonite and montmorillonite powder ("BaM", Keramost, a. s., CZ) was compacted in the diffusion cell (length 15 mm, diameter 30 mm) to a dry density 1.3-1.6 g cm^{-3}. Fresh hardened cement paste from CEM II/A S 42.5R (Lafarge Cement, a. s., CZ) mixed with distilled water in w/c of 0.66 (after 28 days of hydration cut into cylinders "HCP", length 10 mm, diameter 36 mm–coupled or 44 mm–individual system). The experiments consisted of three steps [3]:

(1) Samples were saturated in groundwater SGW-UOS separately for 6 weeks and coupled before the start of the through diffusion experiments.

(2) Realization of through diffusion experiments (TD) of HTO lasting 14 days (BaM) or 28 days (HCP and coupled system HCP/BaM and BaM/HCP); concentration evolution in both reservoirs, concentration profile in BaM, determination of porosity (gravimetric difference of dry and wet BaM or HCP; in advance for HCP: mercury intrusion porosimetry or fitted using GoldSim).

(3) Evaluation of diffusion experiments using the diffusion module was prepared in the GoldSim program.

RESULTS

The TD experiments were evaluated by fitting the experimental concentration data from both reservoirs and a concentration profile (without a concentration profile of HCP). In total six TD experiments were performed on compacted BaM (individual system) with different dry densities. The HTO effective diffusion coefficients on compacted BaM from individual and coupled systems "BaM/HCP" and "HCP/BaM" were in a great agreement. The determined values were compared to other bentonites – Kunigel V1 and FEBEX in Fig. 1 that were obtained under similar conditions.

HTO effective diffusion coefficients on HCP samples were determined in the range (2-3)·10^{-11} m^2s^{-1} with fitted porosity 0.67-0.71 (individual system) and (1-2)·10^{-11} m^2s^{-1} with fitted porosity 0.40-0.70 (coupled system), however the porosity determined by gravimetry and MIP were 0.50-0.52 and 0.37-0.40, respectively.

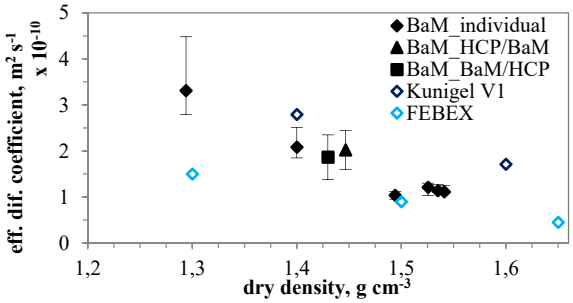

Fig. 1. HTO effective diffusion coefficients on compacted BaM (individual and coupled systems). Comparison with Kunigel V1 [4] and FEBEX [5].

The measured concentration profiles of HTO relative activity concentration in the coupled system is shown in Fig. 2. Model predictions (based on data from the individual system) provided good agreement in "BaM/CEM" series datasets from the inlet reservoir. In "HCP/BaM" series, a smaller decrease of HTO activity concentration in the inlet was observed than expected. These observations lead us to the conclusion that the diffusion parameters of BaM were set correctly, unlike HCP [3].

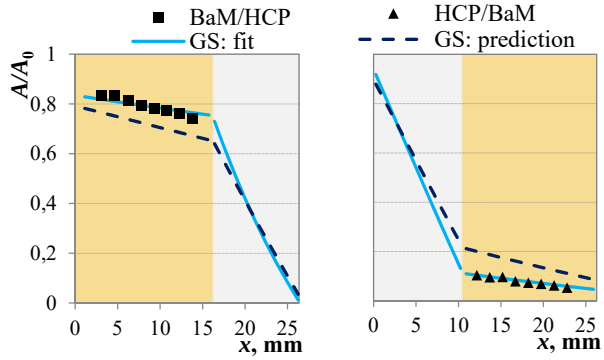

Fig. 2. Experimental, GoldSim (GS) fitted and predicted (from the individual system) HTO concentration profiles in the coupled system.

REFERENCES

[1] Melkior, T. et al. (2004) App Clay Sci 26, 99-107.
[2] Karnland, O. et al. (2007) Phys Chem Earth 32, 275-286.
[3] Rosendorf T. et al. (2018) J App Geo 97, 102-108.
[4] Sato, H. et al. (1992) MRS Proc 294, 403.
[5] García-Gutiérrez, M. et al. (2004) Appl Clay Sci 26, 65-73.

This research is partially the result of Radioactive Waste Repository Authority (SURAO) project "Research support for Safety Evaluation of Deep Geological Repository" and partially the result of the Grant Agency of the Czech Technical University in Prague, grant No. SGS16/250/OHK4/3T/14.

MODELLING AND INTERPRETATION OF DIFFUSION EXPERIMENTS OF STRONTIUM AND RADIUM THROUGH CEMENTITIOUS SAMPLES

Vopálka, D.; Baborová, L.; Kittnerová, J.

INTRODUCTION

A sophisticated tool for evaluation and modelling of diffusion experiments was implemented in the GoldSim environment [1]. This model enables, after improvements performed, to evaluate through-diffusion experiments in steady and non-steady states and with variable concentration in the inlet and outlet containers. The three data sets describing each diffusion experiment could be evaluated simultaneously, i.e. break-through and depletion curves, and tracer concentration profile in a porous layer cementitious plug [2].

MODEL DESCRIPTION

The quasi-stationary state of the modelled type of through-diffusion experiment is attained when the downstream and upstream mass flows are the same. In the case of the same working reservoirs volumes, the changes of concentration in both reservoirs should be then opposite, but numerically also the same. So, if concentration in output container is presented as a reminder to the unity (relative concentration in the input reservoir prior the diffusion starts), the quasi-stationary state can be characterized by the constant distance between curves corresponding to concentrations in both working reservoirs. From results of modelling of through-diffusion experiments with variable concentration of studied species in the inlet and outlet containers presented in Fig. 1 it is seen that the quasi-stationary state is reached, for the experiment, in which no sorption was assumed, after approximately 10 days. In turn 50 days are needed in the experiment with K_d = 10 L·kg^{-1}, while the experiment with. K_d = 50 L·kg^{-1} does not reach steady-state conditions.

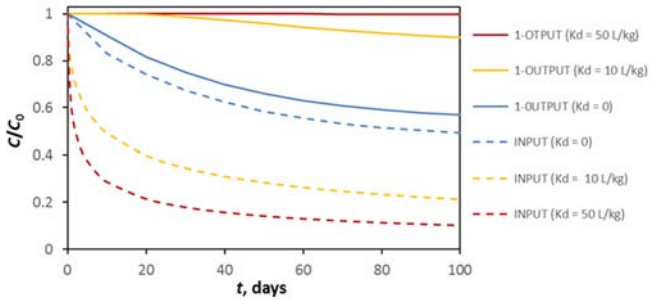

Fig. 1. Modelled time dependences of concentrations in input and output containers (60 mL); parameters of the layer: diameter 50 mm, width 10 mm, porosity 0.5, $D_p = 1 \cdot 10^{-10}$ m^{2}s^{-1}) for three values of distribution coefficient K_d.

EVALUATION OF EXPERIMENTS

The verified modelling tool was applied to the evaluation of diffusion experiments performed with radium and strontium over 0.5 cm wide layers, formed by pressed crushed hydrated cement paste (CEM II), carried with portlandite equilibrated water or with synthetic cement pore water. Isotope ^{223}Ra was carrier free, strontium (C_0 = 3.5·10^{-4} mol·L^{-1}) was labelled by ^{85}Sr. In this case, only our original method of evaluation was used, as diffusion experiments with ^{223}Ra did not reach stationary state. The model took into account the presence of separating filters and eliminates their influence on the values of diffusion coefficients corresponding to the studied layer of pressed crushed cement paste.

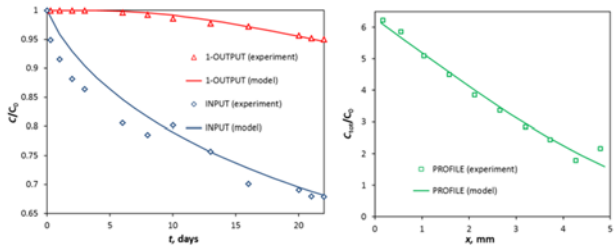

Fig. 2. Results of Sr (labelled by ^{85}Sr) through-diffusion experiment, which lasted 22 days, in portlandite equilibrated water and its optimal fit.

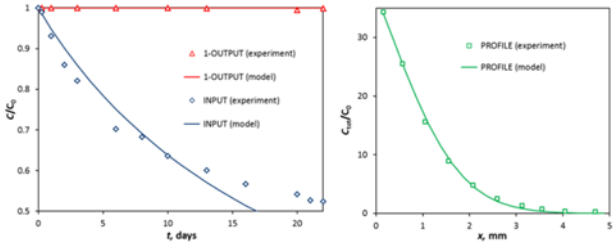

Fig. 3. Results of ^{223}Ra through-diffusion experiment of, which lasted 22 days, in portlandite equilibrated water and its optimal fit.

Fig. 2 and Fig 3 show the experimental results of Ra and Sr diffusion in portlandite equilibrated water and model curves corresponding to the optimal fits. The quality of fits demonstrates that the model description assuming the linearity of the sorption model and reversibility of the sorption process might be valid for the retarded diffusion transport of both Sr and Ra.

RESULTS

The results of diffusion experiments were in agreement with results of batch experiments, in which similar K_d values (about 10 L·kg^{-1} for Sr and about 100 for Ra) were obtained for both tracers for lower values of phase ratio *V*/*m*.

REFERENCES

[1] Vopálka, D. et al. (2006) MRS Proceedings, 932, 983-989.
[2] Vopálka, D. et al. (2017) KIT Scientific Reports 7734, 281-285.

The research leading to these results has received funding from the European Union's Horizon 2020 Research and Training Programme of the European Atomic Energy Community (EURATOM) (H2020-NFRP-2014/2015) under grant agreement n° 662147 (CEBAMA) and partially it is a result of Grant No. SGS16/250/OHK4/3T/14 provided by the Grant Agency of the Czech Technical University in Prague.

SORPTION OF Sr AND Cs ONTO CZECH NATURAL BENTONITE – EXPERIMENTS AND MODELLING

Baborová, L.; Vopálka, D.; Červinka, R.[1]

[1]ÚJV Řež, a.s., Fuel Cycle Chemistry Dpt.

INTRODUCTION

Sorption of Sr and Cs on clay materials is usually described as non-specific and reversible process with fast sorption kinetics, which suggest that the main sorption mechanism is ion exchange. Generally, in clay minerals, ion exchange takes place on the surfaces, mainly in the clay mineral interlayer space, called layer sites. The electrical charge of these sites is pH independent and is related to the cation exchange capacity of the material (CEC). Therefore, sorption mechanism is affected mainly by ionic strength, composition of solution and cation exchange complexes. An important competing cation for Sr^{2+} is Ca^{2+} due to its similar hydrated radius and valence, whereas for Cs^{+} it is K^{+}. However, in trace concentrations, sorption characteristics of Cs, namely the high value of distribution coefficients, slower kinetics and irreversibility present another sorption mechanism. It is assumed that specific sorption sites, sometimes called frayed edge sites (FES), located at the edges of minerals [1], are responsible for these phenomena. In this study, for modelling of Sr sorption on bentonite one-site ion exchange model was considered, due to the observed linear sorption isotherm, whereas two-site ion exchange/surface complexation model for Cs sorption was proved to be more appropriate for modelling of observed non-linear shape of sorption isotherm.

EXPERIMENTAL

Data from batch experiments with Sr and Cs on Czech natural Mg/Ca bentonite with a commercial name ‘‘Bentonite and Montmorillonite’’ (BaM) which were performed in two background electrolytes, $CaCl_2$ and NaCl respectively, of the same ionic strength (I_s = 0.1 mol·L^{-1}) are presented. Several values of solid-to-liquid ratios (m/V, [g·mL^{-1}]) and a range of tracer total concentrations (C_0, [mol·L^{-1}]) were tested. The total concentration was controlled by non-active carrier ($SrCl_2 \cdot 6H_2O$ and CsCl) and the distribution between solid and liquid phase was assessed with the use of radioactive tracers (^{85}Sr and ^{137}Cs), concentration of which were not higher than $5 \cdot 10^{-9}$ mol·L^{-1}. Ion exchange was modelled using Gaines–Thomas convention, the modelling was realized in the PhreeqC programming environment. The initial solution in the model contained the selected background electrolyte and the mass of exchanger according to given solid-to-liquid ratio, in which the real CEC and initial occupation by Ca^{2+}, Mg^{2+}, Na^{+} and K^{+} was respected. Surface complexation was modelled based on Guy-Champan equation. Because the minor sorption mechanism of Cs on clay material is specific and pH independent [1] and the pH in all of the experiments was in the range between 7 and 9, the protonation of surface sites was not considered.

RESULTS

Sorption of Sr in both electrolytes showed a linear trend in the given concentration range. The model of ion exchange was able to predict the dependence on m/V in NaCl background electrolyte (right graph in Fig. 1). The model prediction for $CaCl_2$ background electrolyte was satisfactory, (left graph in Fig. 1), though the model predicted slightly lower K_d values and opposite dependence of K_d on m/V.

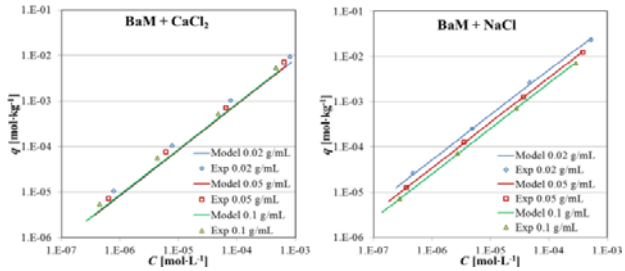

Fig. 1. Sorption isotherms of Sr on bentonite BaM (points) in $CaCl_2$ background electrolyte (left) and NaCl background electrolyte (right) and prediction of ion exchange model (lines) for three solid-to-liquid ratios.

The sorption isotherm of Cs was non-linear (Fig. 2) with distribution coefficients being higher in lower range of Cs total concentration. Sorption of Cs was lower in NaCl electrolyte, compared to $CaCl_2$ electrolyte. This suggests that Na^{+} is relatively stronger competitor for Cs^{+} than Ca^{2+}. This agrees with the findings of many authors, e.g. [2], though it cannot be explained by one-site ion-exchange model which predicts an opposite behaviour. It appears that two-site model allowing the competition between Cs and the other cations would be convenient, as it was showed previously [3]. The problem presents the unknown selectivity coefficients of minor sorption sites for Ca^{2+} and Na^{+}. Therefore, surface complexation model without the competition was applied.

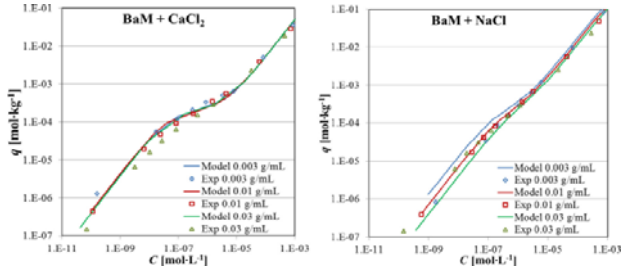

Fig. 2. Sorption isotherms of Cs on bentonite BaM (points) in $CaCl_2$ background electrolyte (left) and NaCl background electrolyte (right) and prediction of ion exchange/surface complexation model (lines) for three solid-to-liquid ratios.

REFERENCES

[1] Pusch, R. and Karnland, O. (1996) Eng Geol 41, 73-5.
[2] Bostick, B.C. et al. (2002) Environ Sci Technol 36, 2670-2676.
[3] Vopálka, D. et al. (2015) J Radioanal Nucl Chem 304, 429-304.

This work is partially a result of Radioactive Waste Repository Authority Project ‘‘Research Support for Safety Evaluation of Deep Geological Repository’’ and partially a result of Grant No. SGS16/250/OHK4/3T/14 provided by the Grant Agency of the Czech Technical University in Prague.

INVESTIGATION OF COPPER(II) ADSORPTION ON SLOVAK BENTONITE JELŠOVÝ POTOK

Viglašová, E. [1]*; Daňo, M.; Galamboš, M.* [1]*; Krajňák, A.* [1]*; Rosskopfová, O.* [1]*; Rajec, P.* [1]

[1]Comenius University in Bratislava, Slovak Republic

INTRODUCTION

The most commonly used chemical spray in agriculture, is solution of $CuSO_4 \cdot 5H_2O$. The main advantage of this compound is destroying ability for different kinds of fungi, plants or animals, which are possible vermin of vine yards. However, the copper is biogenic element, higher content is very toxic for vineyards and human body. One of the methods for copper removing its adsorption [1,2].

EXPERIMENTAL

Adsorption experiments were studied through radiotracer technique using ^{64}Cu (prepared by $^{64}Ni(p,n)^{64}Cu$) as a tracer, in aerobic and static conditions at laboratory temperature. Volume activity of ^{64}Cu was equal to 2 MBq·mL^{-1}. Influence of pH on Cu(II) adsorption and adsorption parameters were determined after adding 3 mL of aqueous phase to 30 mg of bentonite Jelšový potok (J250) (particle size ~250 µm) in a plastic tube and mixing both phases in laboratory rotator (250 rpm). Then, the suspension was centrifugated at 6000 rpm for 10 min and an aliquot volume of the supernatant was measured on a gamma NaI(Tl) detector.

RESULTS

The characteristics of Cu(II) ionic species predominant at a specific solution pH may play an important role in adsorption process of Cu(II) on bentonite because of surface functional groups ionization and alteration of the solution composition. In the range of pH = 3 – 8, the adsorption percentage (*R*) reached various values.

Decrease in amount of adsorbed Cu(II) on studied samples at pH 3 was observed, which is explained by competitive influence of H^+ ions and presence of relatively small number of available sites. In aqueous systems, the bentonites surface groups are protonated in different extents. Therefore, the concentrations of surface species changed under different pH values. There is possibility that the decrease was caused also by lower values of pH where the layer bentonite structure is being disrupted (pH under 3.5).

With increasing pH, the negatively charged groups or deprotonated groups increase and the hydrolysis of Cu(II) also increases. In the pH range between 4 and 6, the R values are approximately constant (R = 96–97%). These values proved that aside from the basic adsorption mechanism, which is the ion exchange, for higher pH then 7, the values of *R* decrease and complex-forming reaction with the surface bentonite groups take place.

Based on the chemical speciation of Cu(II) in water solutions, Cu(II) exists in the forms of Cu^{2+}, $Cu(OH)^+$, $Cu_2(OH)_2^{2+}$, $Cu(OH)_2^0$, $Cu(OH)_3^-$ and $Cu(OH)_4^{2-}$ at various pH values. The copper is presented in the solution mainly in the form of Cu^{2+} ions up to the pH 6.5 and the adsorption is established by ion exchange process, copper does not precipitate in this pH region. The positively charged $Cu(OH)^+$ and $Cu_2(OH)_2^{2+}$ hydrolytic products appear in the pH range of 7 – 11, while $Cu(OH)_2$ starts to precipitate at pH 6.5 and above the pH 9 it is dominant form of precipitation.

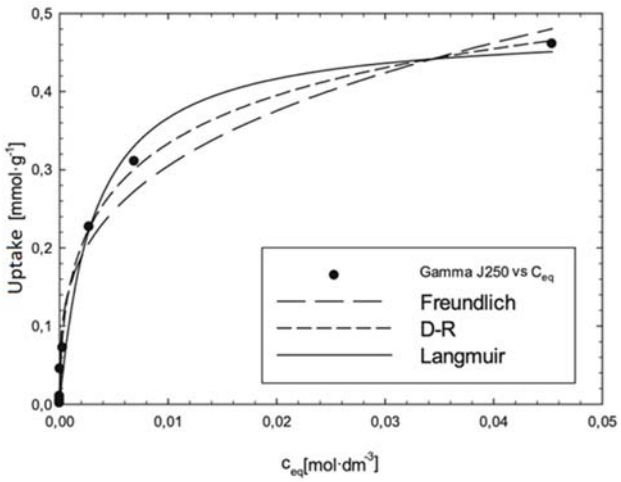

Fig. 1. Adsorption of Cu^{2+} onto bentonite J250 ($pH_{initial}$ = 5).

The results of Cu(II) adsorption onto J250 were plotted according to the Langmuir, Freundlich and Dubinin-Rasushkevich (D-R) models (Fig. 1). The equilibrium adsorption isotherms express the mathematical relations between the quantity of adsorbate and equilibrium concentration of adsorbate remaining in the solution at constant temperature. The coefficient of determination (R^2) for the chosen three isotherms are shown in Tab. 1.

Tab. 1. Coefficients of determination (R^2) and maximum uptake of Cu(II).

Isotherm model	R^2
Langmuir	0.9925
Freundlich	0.9904
Dubinin-Radushkevich	0.9987
uptake (Langmuir)	0.45 mmol·g^{-1}

The isotherms are appropriate in their own merits in describing the potential of bentonite Jelšový potok for removal of Cu(II) ions. It can be also concluded from the value of R^2 that the Dubinin–Radushkevich isotherm fits the data the best followed by the Langmuir isotherm and Freundlich isotherm.

REFERENCES

[1] Vanek, G. (2012) Vinič a víno 12(3), 77-81.
[2] Juang, K.W. et al. (2012) Environ Sci Pollut Res 19, 1315-1322.
[3] El-Araby H. et al. (2017) J Geos Environ Prot 5, 109-152.

This work was supported by the Grant of the Slovak Research and Development Agency APVV project no. SK-AT-2015-0003 and Agency of the Ministry of Education, Science, Research and Sport of the Slovak Republic and Slovak Academy of Sciences VEGA project no. 1/0507/17.

MODELLING OF TRANSPORT PROCESSES IN THE ROCK ENVIRONMENT USING IN-SITU EXPERIMENTS

Vetešník, A.; Reimitz D.; Vopálka D.

INTRODUCTION

Migration group of Department of Nuclear Chemistry focuses, among others, on modelling migration of radionuclides with GoldSim software [1]. To improve our skills in modelling we have participated in SKB Task Force on Modelling of Groundwater Flow and Transport of Solutes. In particular, we participated in the Task 9, which focuses on the realistic modelling of coupled matrix diffusion and sorption in heterogeneous crystalline rock matrix at depth. The ultimate aim of this task is to develop models that in a more realistic way represents retardation in the natural rock matrix at depth.

MODEL

Our conceptual model of WPDE-1 and WPDE-2 (Water Phase Diffusion Experiment) of the REPRO (Through Diffusion Experiment) project at the ONKALO underground rock in Finland is depicted in Fig. 1. The rock matrix was modelled as a network of finite volumes. We assumed that a rock matrix is composed from three homogenous parts connected in a series along axis of annular slot (light and dark brown regions in Fig. 1). We represented rock matrix using cylindrical geometry which allowed within Goldsim simulation framework to model diffusion in a radial and a height directions. This simplification neglects rock heterogeneities on the plane perpendicular to the axis of the cylinder. We assumed the Fickian character of diffusion transport, and the surface sorption was not considered.

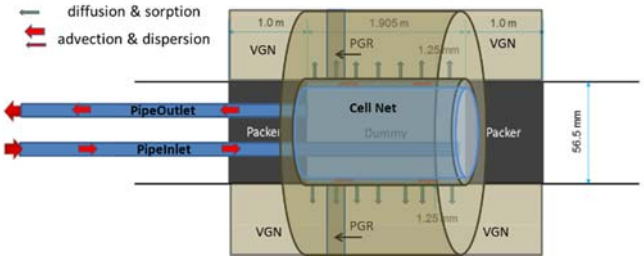

Fig. 1. The graphical representation of the conceptual model. Inlet and outlet PEEK tubing were modelled by two Pipe pathways. An annular slot and rock matrix were modelled by Cell pathway network of a cylindrical geometry.

RESULTS

We calculated central predictions for WPDE-1 and WPDE-2 experiments as well as upper and lower predictions for a set of selected uncertain parameters. We calculated the upper and lower predictions by assigning intervals of values to some of important transport parameters. We performed with these values the interval analysis, i.e. we calculated breakthrough curves for all combination of min-max values and then we determined the upper prediction as a maximum of all calculated breakthrough curves at given time point, and the lower predictions as minima of all calculated breakthrough curves. The upper and lower predictions cannot thus be identified with an individual breakthrough curve.

Fig. 2 shows the upper and lower predictions calculated for WPDE-1 experiment and Fig. 3 shows the upper and lower predictions calculated for WPDE-2 experiment. In both cases, the calculated breakthrough curves were most sensitive to changes of the dispersivity in annular slot, α_S, within assumed range. The breakthrough curves of Na-22, Sr-85, and Ba-135 were sensitive also to a rock matrix transport properties (ε, D_e, K_d) of VGN.

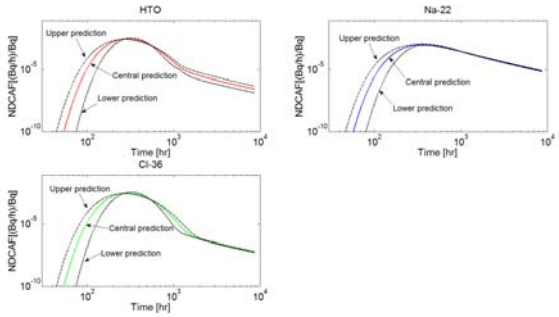

Fig. 2. Central prediction, upper and lower predictions of WPDE-1 experiment.

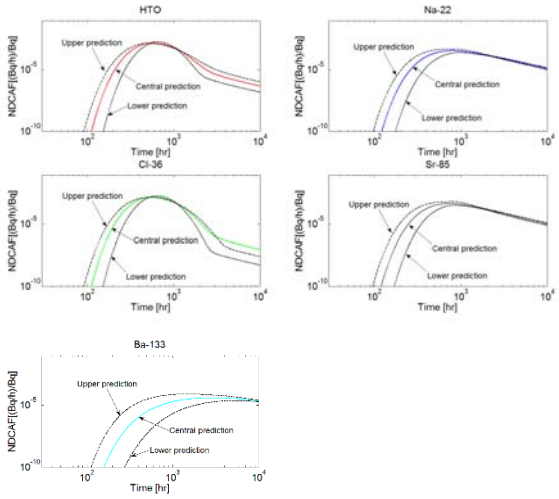

Fig. 3. Central prediction, upper and lower predictions of WPDE-2 experiment.

CONCLUSIONS

We implemented within Goldsim simulation framework a model of WPDE-1,2 experiments using the network of Cell pathways of the Contaminant Transport Module. It turned out that it is necessary to adjust Cell Net geometry to avoid numerical errors. The values of some of parameters will be optimized using GoldSim's optimization feature which fits automatically model parameters to experimental data.

REFERENCES

[1] GoldSim (2014) GoldSim Contaminant Transport Module User's Guide. GoldSim Technology Group, version 6.4., 373 p.

[2] Löfgren, M. et al. (2015) Task 9: increasing the realism in solute transport modelling-modelling the field experiments of REPRO and LTDE-SD. SKB, 44 p.

This work is a result of Radioactive Waste Repository Authority Project ''Research Support for Safety Evaluation of Deep Geological Repository''.

MOLECULAR MODELLING MEETS ENVIRONMENTAL PROTECTION

Višňák, J.[1,2]; Sobek, L.[3]; Hoth, N.[4]

[1]Dept. of Chemical Physics and Optics, Faculty of Mathematics and Physics, Charles University; [2]J. Heyrovský Institute of Physical Chemistry; [3]Czech Physical Society; [4]TU Bergakademie Freiberg, Dept. of Mining and Special Constructions, Germany

INTRODUCTION

First-principles based Computational Chemistry Modelling is of importance for reliable predictions of both thermodynamic and spectroscopic properties of uranyl(VI) complex species in aqueous solutions. Our proceedings contribution [1] presenting application for the UO_2^{2+} - XO_4^{2-} - H_2O (X = S, Se) systems have been followed by study tailored for interpretation of U(VI) natural water samples TRLFS spectra [2]. Methodology [3], [4] incorporating spin-orbit coupling and discrete solvent model is able to overcome previous insufficiencies [2] in accurate predictivity of phonon-less excitation energy T_{00} and allows incorporation of several vibrational modes. That constitutes a first-principles based proof, the chromophore (UO_2^{2+})-localized symmetric stretching mode is responsible for aqueous uranyl(VI) complex species spectra overal shape (peak spacing corresponds to its vibrational frequency ω_{gs} and peak areas to single-mode harmonic Franck-Condon factors with difference between U-O equlibria bond lengths ΔR). Results will be presented for $[UO_2(H_2O)_5]^{2+}$(aq) ambient temperature luminescence (TRLFS) spectrum simulation.

COMPUTATIONALS [3,4]

To probe solvent configuration space, Classical Molecular Dynamics computation (with FF adopted from [5]) involving complex and 4000 surrounding water molecules have been performed (p1, Fig.1). Snapshots from the CMD trajectory have been partitioned into three regions (Fig. 2) and computed: 1. Ground electronic state normal modes (p3,p5) (The inner-most "region 1" optimized, "region 2" considered as explicit but frozen, "region 3" as point-charges), 2. Excited electronic state normal modes (p2,p4), 3. Double-harmonic Franck-Condon profile (p6). Results from all snapshots were averaged (p12). For normal mode computations scalar RECP/B3LYP+D3/def-TZVPP method has been used, but each snapshot spectrum origin (T_{00}) corrected by spin-orbit resolved SORECP/TD-DFT/XALDA/def-TZVPP (p10), several XC functionals.

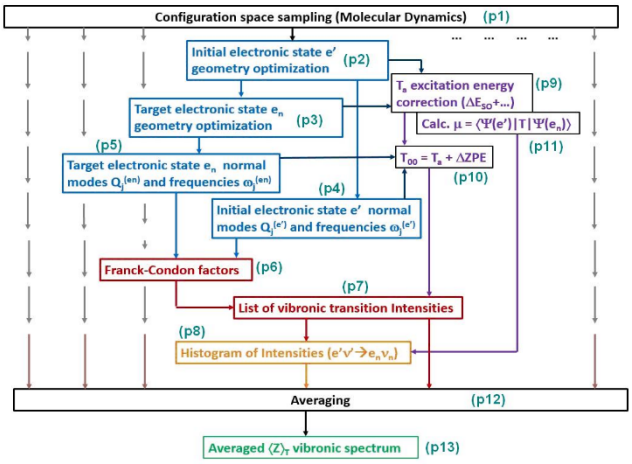

Fig. 1. Vibrationally resolved spectra simul. workflow.

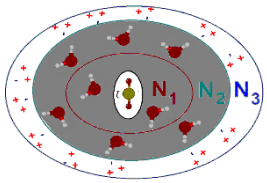

Fig. 2. Studied system formal partitioning. For details and used software [3],[4]; the TT1 settings: $N_1 = 0$, $N_2 = 5$; the TT3 settings: $N_1 = 5$, $N_2 = 12$.

RESULTS

Multimode simulated spectra have been fitted to an effective single-mode model in a same way as measured TRLFS spectra with most prominent parameters compared (Tab. 1).

Tab. 2. Spectroscopic par. (TT1 settings [4] left | TT3 right).

	T_{00} [cm^{-1}]	ω_{gs} [cm^{-1}]	ΔR [pm]	T_{00} [cm^{-1}]	ω_{gs} [cm^{-1}]	ΔR [pm]
TD-HF	20615	882	5.10			
LBα/B3LYP	20506	919	5.26	20583	891	4.75
CAM-B3LYP	20014	842	5.49	20129	894	4.75
B3LYP	18357	873	5.30	18399	890	5.32
Experiment	20485	867	5.57			

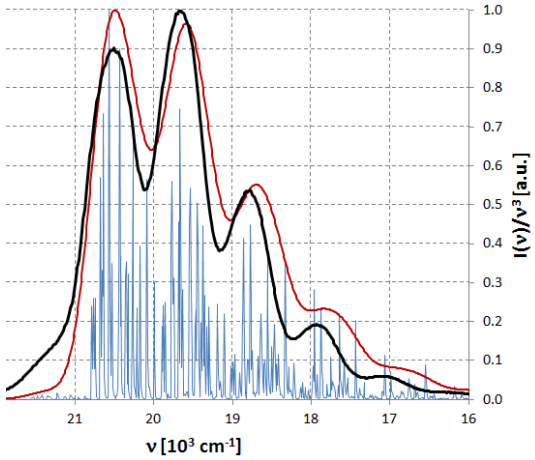

Fig. 3. Simulated spectra for $[UO_2(H_2O)_5]^{2+}$(aq), T_{00} correction: LBα/B3LYP SAOP functional, histogram (blue), gauss. smoothed (red), exper. data (black).

REFERENCES

[1] Višňák, J. et al. (2016) EPJ Web Conf 128, 02002.
[2] Višňák, J. et al. (2017) EPJ Web Conf 154, 01029.
[3] Višňák, J. (2018), PhD Thesis, CTU in Prague.
[4] https://arxiv.org/ftp/arxiv/papers/1811/1811.10456.pdf
[5] Pomogaev, V. et al. (2013) PCCP 15, 15954-15963.

Computational resources were provided by the CESNET LM2015042 and the CERIT Scientific Cloud LM2015085, "Projects of Large Research, Development, and Innovations Infrastructures". Czech Science Foundation project # 18-24563S.

Separation and Radioanalytics

A NEW POTENTIAL FLUORIDE TARGET MATRIX FOR ^{236}U DETERMINATION IN ENVIRONMENTAL MEDIA BY ACCELERATOR MASS SPECTROMETRY

Prášek T.; Němec M.

INTRODUCTION

Research of the fluoride target matrices for anthropogenic ^{236}U determination by Accelerator Mass Spectrometry (AMS) has been recently focused on uranium tetrafluoride in particular [1]. Although the compound itself appears to provide promising results in caesium sputtering ion source of AMS, its practical application in routine analytical process still faces two major problems that have not been fully solved yet. First of them is connected to complicated preparation of the pure compound from aqueous solutions, where the product usually contains significant amount of oxidic impurities, mostly UO_2. Second problem refers to the continuity of the whole analytical process of ^{236}U determination with preceding steps of natural samples pre-concentration and subsequent treatment, which usually leads to an acidic uranium concentrate. Trace amounts of uranium in the samples also require for a suitable non-isotopic carrier to be employed in the matrix preparation procedure. In this respect, a new fluoride target matrix preparation method aimed at the determination of ^{236}U has been developed, more suitable for trace concentrations of uranium contained in natural samples than the methods published so far.

EXPERIMENTAL

Proposed fluoride target matrix preparation scheme is shown in Fig. 1.

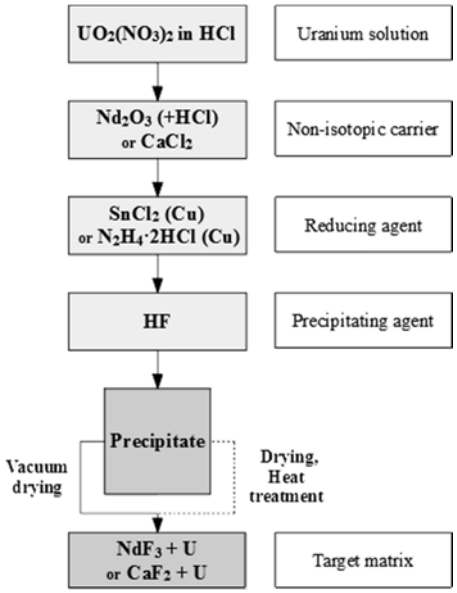

Fig. 1. Preparation scheme of the new potential fluoride target matrix for ^{236}U AMS determination.

The procedure starts from solution of uranium salt in HCl, simulating conditions of an acidic eluate from natural sample treatment. Subsequently, non-isotopic carrier in the form of Ca^{2+} or Nd^{3+} is added and either $SnCl_2$ or $N_2H_4 \cdot 2HCl$ is used as a reducing agent for uranium at presence of Cu^{2+} ions and temperature 80 °C. Uranium is then co-precipitated with the carrier as fluoride by adding concentrated HF. The resulting precipitate is washed, dried and pressed into a target holder, with possible additional heat treatment of the matrix. Applicability of the preparation method was tested on a series of samples analysed with Liquid Scintillation Counting (LSC), X-Ray Powder Diffraction (XRPD) and AMS device at VERA laboratory, University of Vienna.

RESULTS

For all the samples, separation of uranium from the initial acidic solution measured with LSC was nearly quantitative, exceeding 99 % in most cases. By comparing the results of XRPD analysis with ICDD-PDF2 database, the matrices prepared were identified as either calcium-uranium fluoride or neodymium fluoride with slightly deviated diffraction lines, suggesting incorporation of uranium into the crystalline structure of the carrier compound. No observable oxidic contamination was present. Regarding the sputtering process in AMS caesium ion source, the total yield of UF_5^- ions was chosen as the main criterion for matrix evaluation and comparison (Fig. 2). Although the standalone target samples provided lower yield values than both the reference oxidic and fluoride matrices (less than 0,06 %), combination of better performing NdF_3-based samples with PbF_2 lead to a major improvement, reaching almost 5 %. These results exceed the ionisation efficiency for the reference samples 20 – 40 times and could mean a significant progress for analytical applications.

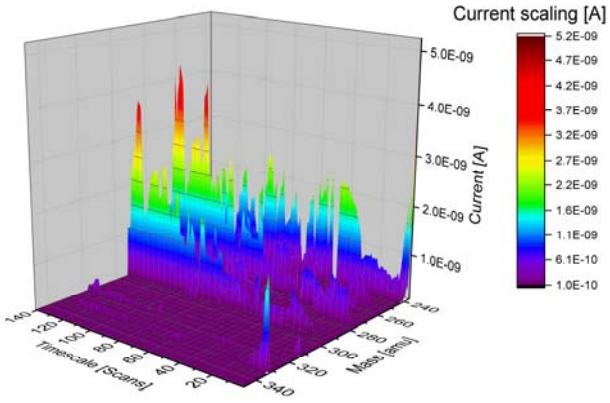

Fig. 2. Complete AMS record of NdF_3-based sample, UF_5^- peak in the foreground (333 amu).

REFERENCES

[1] Xianggao Wang, Kejun Dong, Ming He, Shaoyung Wu, Shan Jiang (2013) Nucl. Tech. 182, 235-241

We would like to acknowledge colleagues from laboratory VERA, University of Vienna, for their cooperation on the research and the opportunity to analyse performance of the target samples within AMS device.
This research was supported by the Grant Agency of the Czech Technical University in Prague (SGS18/192/OHK4/ 3T/14) and Project RAMSES (CZ.02.1.01./0.0/0.0/16_019/0000728)

SEPARATION OF Fe AND Co FROM MEDIA USED IN DECONTAMINATION PROCESSES USING IONIC LIQUIDS

Čubová, K.; Semelová, M.; Němec, M.; Straka, M.[1]

[1]ÚJV Řež, Czech Republic

INTRODUCTION

Ionic liquids (ILs) are salts with the melting point below 100°C, many of them are liquid even at room temperature (RTIL) [1]. Due to their enhanced selectivity, the use of ILs in liquid-liquid extraction seems to be a very promising way for the separation of metals and radionuclides from the solutions resulting from the processes of decontamination and decommissioning or treatment of an industrial waste. Two-step separation process consisting of extraction of radionuclides from the decontamination solutions by using the ionic liquids, followed by the separation of radionuclides from ionic liquids by electrodeposition was proposed and tested. The mentioned process was successfully applied to separation and concentration of ^{59}Fe and ^{60}Co (as representatives of the main activation products) from simulant of a decontamination solution. The patent application for this process was submitted in 2018.

EXPERIMENTAL

Liquid-liquid extraction

Five different ionic liquids were tested as the organic phase. High-purity grade (99%) 1-alkyl-3-methylimidazolium bis(trifluoromethansulfonyl) imide ionic liquids (marked as [$C_n$mim][NTf_2], where n = 2,4,6 and 10), tributylmethylammonium bis (trifluoromethanesulfonyl) imide (marked as [Tbma][NTf_2]) and methyltrioctylamonium bis (trifluoromethanesulfonyl) imide (marked as [Mtoa][NTf_2]) were purchased from Iolitec, Germany. For the comparison, chloroform was also used. 8-hydroxyquinoline (8-HQ) was used as the extractant.

Aqueous phase of total volume of 1 mL was prepared as follows: HNO_3 concentration from 0.001 to 5 mol/L or phosphate or borate buffers or oxalic acid (H_2Ox) (0.01 and 0.005 mol/L) or citric acid (H_3Cit) (0.01 and 0.005 mol/L) or mixture of both of them (0.01 mol/L H_2Ox and 0.005 mol/L H_3Cit). The aqueous phase was spiked with ^{59}Fe or ^{60}Co respectively.

Equal volumes (1 mL) of both phases were contacted and shaken for 30 minutes at laboratory temperature. Aqueous and organic phases were then separated by centrifugation (5 min at 2500 rpm). Aliquots of the volume 750 µl of both phases were taken for the measurement. Aqueous and organic phases were measured with well-type NaI(Tl) scintillation detector. The equilibrium pH value was measured after the experiment.

Electrodeposition

For electrochemical characterization of the organic phase, cyclic voltammetry was used. Screen-printed platinum electrodes were purchased from Drop Sense (ref. 550). Voltammetric experiments were carried out at the room temperature and potential speed 50 mV/s. Following potentiostatic electrodeposition was carried out at the potential of -1.4 V. The layer formed on working electrode was analysed by SEM/EDAX, ^{60}Co was again measured with well-type NaI(Tl) scintillation detector.

RESULTS

The extraction was studied in the pH range of aqueous phase from 0 to 10 (for Fe) and from 0 to 8 (for Co). In the pH range from 3 to 8, almost 100% of extraction was achieved for Fe and for Co, and almost 100% extraction was reached from pH above 3 into all the ionic liquid tested at 8-HQ concentration 0.1 mol/L. Good results were obtained for all [$C_n$mim][NTf_2]; [Tbma][NTf_2]) and [Mtoa][NTf_2] provided lower extraction yields in all experiments. Oxalic and citric acid and their mixture were used as the aqueous phase to test the possibility of extraction of radionuclides from organic complexing agents media. In such mixture and in the presence of 0.5M 8-HQ, practically 100 % extraction was achieved for both ^{59}Fe and ^{60}Co. As for reextraction by electrodeposition, more than 99.8 % of ^{60}Co was deposited on the working electrode. SEM images show a regular and compact surface structure. Similarly, galvanostatic electrolysis on a gold electrode and potentiostatic electrolysis on a glass-graphite electrode were tested, both resulting in the formation of a compact layer of metallic cobalt. By this step, ionic liquid was recycled and can be re-used.

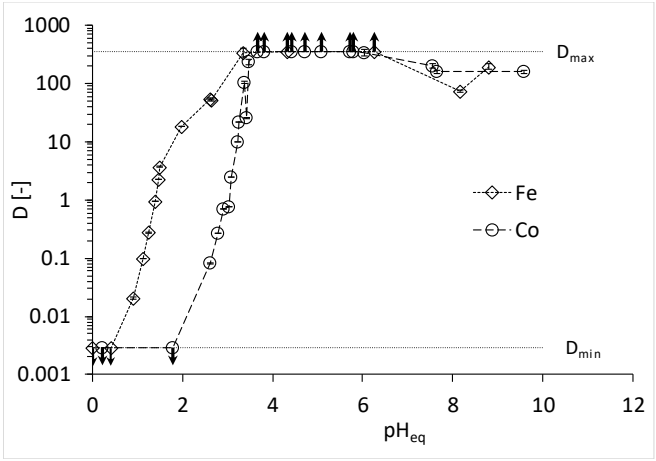

Fig. 1. The dependence of distribution ratio D of cobalt and iron extraction into 0.1M 8-HQ in [C4mim][NTf2] on the equilibrium pH value.

REFERENCES

[1] Zhou, Y, et al. (2015) Extraction of Metal Ions with Task Specific Ionic Liquids: Influence of a Coordinating Anion. Sep. Sci. Technol. 50(1) 38-44

This work was carried out within grant project of the Technology Agency of the Czech Republic TH01020381 and within the Center for advanced applied science, project number CZ.02.1.01/0.0/0.0/16_019/0000778, supported by the Ministry of Education, Youth and Sports of the Czech Republic

COOPERATION WITH UNIVERSITY OF OSLO AND DEPARTMENT OF ACCELERATORS (NPI CAS) WITHIN CANAM INFRASTUCTURE

John, J.; Omtvedt, J. P.[1]; Němec, M.; Bartl, P.; Čubová, K.; Semelová, M.; Wulf, S.[1]; Štursa, J.[2]

[1]University of Oslo – Department of Chemistry, Oslo, NOR
[2]Nuclear Physics Institute, Czech Academy of Sciences – Department of Accelerators, Řež, CZE

INTRODUCTION

Centre of Accelerators and Nuclear Analytical Methods (CANAM) is a large research infrastructure for the investigation of various scientific tasks using accelerated ion beams or neutrons. Within this infrastructure, the Department of Nuclear Chemistry started to cooperate since fall 2017 with professor Omtvedt's research group from the University of Oslo (UiO) and with the Department of Accelerators at the Nuclear Physics Institute of the Czech Academy of Sciences (NPI CAS). This cooperation has resulted in one week of open access beam time biannually at the cyclotron U-120M in Řež and building a joint CTU/UiO/NPI laboratory at the cyclotron facility. Currently, liquid-liquid extraction of homologues of super-heavy elements is studied with two systems – fast microfluidic aqueous/organic extraction and aqueous/ionic liquid extraction.

CYCLOTRON U-120M

Isochronous cyclotron U-120M is a powerful tool operated by the Department of Accelerators, NPI CAS. For our purposes, the cyclotron is tuned to accelerate positively charged helions-3, so the X(^{3}He, x^0n)Y reaction may occur. Helions are generated internally via molybdenum PIG source. The beam is extracted using external channel, where beam energies between 18-52 MeV and intensities up to 2 μA can be obtained.

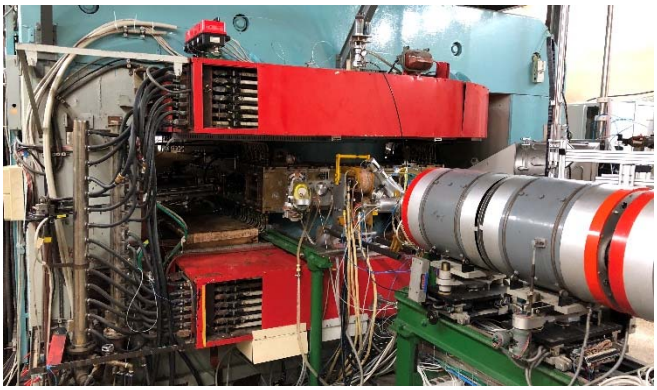

Fig. 1. Isochronous cyclotron U-120M.

GAS-JET TRANSPORT SYSTEM

The reaction products are recoiled into gas-jet recoil transfer chamber, provided by University of Oslo, as well as the whole gas-jet transport system. In more detail, KCl aerosols produced in a tube furnace from its crystalline form at ca 650 °C are carried in a helium stream into the recoil-transfer chamber (the rear part of the target chamber), where reaction recoil products are collected. Consequently, the product-carrying aerosols are cumulated at the direct-catch assembly and further chemically processed [1].

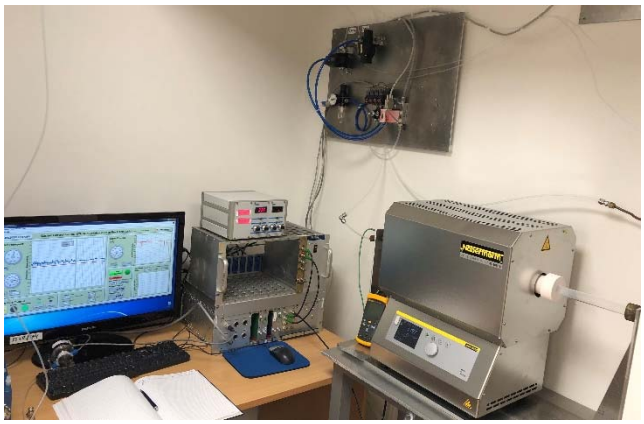

Fig. 2. Gas-jet transport system control centre.

At this point, the direct catch represents first discontinuity in the process. Alternatively to the direct catch method, the membrane degasser (MDG) developed by UiO is available. However, it is not suitable for CTU's approach based on the application of microfluidic extraction due to high-volume of the solution produced by the MDG. However, this discontinuity is planned to be eliminated by installation of a Particle Into Liquid Sampler (PILS) arriving in 2019 [2].

SHE HOMOLOGUES EXTRACTION

As the two experimental approaches studied at the CTU are described in separate articles by K. Čubová and P. Bartl within this annual report, this section focuses on our goals. Currently, implementing PILS into the system is the key step. PILS is expected to decrease the solution volumes by at least one order of magnitude and thus allow direct connection with microfluidic extraction (or with a future dynamic system for extraction by ionic liquids). In this way, a continuous system is going to be created consisting of the following steps – production of radionuclei, aerosol transport of the recoiled nuclei, fast gas flow into slow liquid flow conversion coupled with aerosol dissolution, dynamic microextraction and phase separation. To complete the process, an on-line detection system will have to be implemented at the end.

REFERENCES

[1] Even, J. et al. (2011), Nucl. Instrum. Methods Phys. Res. A, 638, 157 – 164.
[2] Orsini, D. A. et al. (2003), Atmos. Environ., 37, 1243 – 1259.

This work has been carried out within the CANAM infrastructure, Project Number LM2015056, and within the Centre for advanced applied science, Project Number CZ.02.1.01/0.0/0.0/16_019/0000778, both supported by the Ministry of Education, Youth and Sports of the Czech Republic.

FAST MICROFLUIDIC LIQUID-LIQUID EXTRACTION STUDIES OF Sg HOMOLOGUES

Bartl, P.; Němec, M.; John, J.; Omtvedt, J.P.[1]; Štursa, J.[2]

[1]University of Oslo – Department of Chemistry, Oslo, NOR
[2]Nuclear Physics Institute, Czech Academy of Sciences – Department of Accelerators, Řež, CZE

INTRODUCTION

The periodic law is a generally known principle forming the current shape of the periodic table of elements. However, relativistic effects start to apply on orbiting electrons when the relativistic increase in mass exceeds 10% (Z > 56). When it comes to super-heavy elements (SHEs), this increase is so dominant that it may severely affect the element's chemical behaviour, thus disrupting the validity of the periodic law. [1] Therefore, chemical studies involving SHEs are of very high interest. There are, unfortunately, several features of SHEs obstructing such studies, e.g. very short half-life and extremely low production rate. Therefore, gas-phase chemistry experiments results are often favoured for their speed. However, chemical information obtained from liquid-phase chemistry is irreplaceable, despite its usually slower kinetics and difficult experimental setup.

RESULTS AND EXPERIMENTS

Recent results of microfluidic liquid-liquid extraction of W (as homologue of Sg) from diluted nitric acid into Cyanex®600 (Cy600) in 1% *n*-octanol and kerosene obtained by the new CTU/UiO/NPI collaboration at CANAM facility (see the preceding report) are reported here. Microfluidic slug-flow method developed at the NE Division, ANL was utilized. [2] Isotopes of tungsten (^{176}W and ^{177}W) were produced at the U-120M cyclotron in Řež via (^{3}He, *x*n) reaction on ^{nat}Hf target.

First, microfluidic slug-flow capillary technique and batch technique were compared. The graph on Fig. 1 shows comparison of batch and microfluidic extractions in terms of tungsten D-values dependency on contact time. Based on the slope ratio, microfluidics appears to be more than 30 times faster than common lab rotator-mixer, thus demonstrating enhanced mass transfer properties in favour of microfluidics.

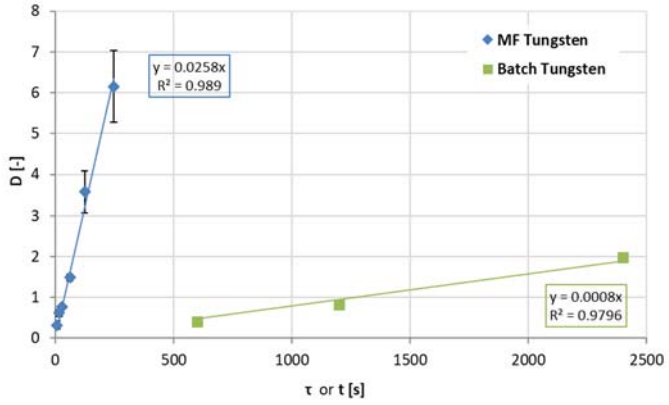

Fig. 1. Non equilibrium D(W) dependency on contact time for the 0.5M Cy600/0.5M HNO_3 system. Slug-flow microfluidics (blue) vs. Grant Bio PTR30 rotator-mixer (green).

In parallel, the choice of Cy600 as a group 6 fast extracting agent was justified by comparison with widely used HDEHP extractant. Fig. 2 shows both higher affinity towards tungsten (higher D-values) and faster kinetics in favour of Cy600 over HDEHP. Unfortunately, the generated activity was not sufficient for achieving very high D_{max}-values.

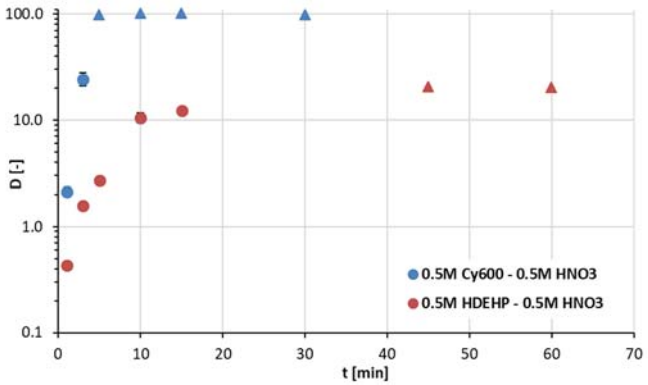

Fig. 2. Non-equilibrium D(W) dependency on contact time for the 0.5M Cy600/0.5M HNO_3 (blue) and the 0.5M HDEHP/0.5M HNO_3 (red) system. Triangular data points indicate D_{max}.

Consequently, dependency of W equilibrium distribution ratio on Cy600 concentration was explored, aiming at the slope analysis unveiling the extraction mechanism. As shown in Fig. 3, log D(W) dependency on log c(Cy600) shows linear trend for constant c(HNO_3). Since the slope of the trend is equal to almost one, it may be assumed that 1:1 W:Cy600 complexes are the extracted species. Again, D-values getting too high appear to be an issue.

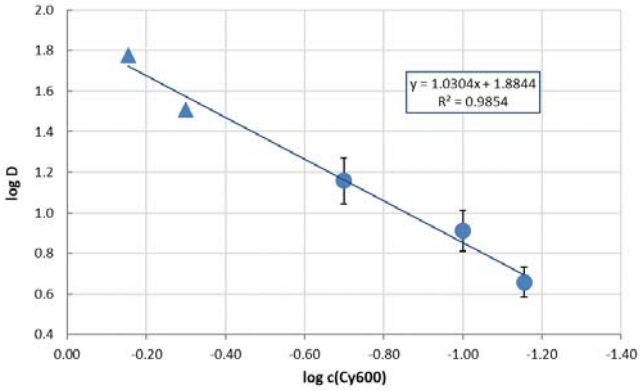

Fig. 3. log D(W) dependency of log c(Cy600).

REFERENCES

[1] Pyykkö, P. (1988), Chem. Rev., 88, 563 – 594.
[2] Nichols, K.P. et al. (2011), J. Am. Chem. Soc., 133, 15721 – 15729.

This work has been carried out within the CANAM infrastructure, Project Number LM2015056, and within the Centre for advanced applied science, Project Number CZ.02.1.01/0.0/0.0/16_019/0000778, both supported by the Ministry of Education, Youth and Sports of the Czech Republic.

EXTRACTION OF THALLIUM AND INDIUM ISOTOPES AS THE HOMOLOGUES OF NIHONIUM INTO THE IONIC LIQUIDS

Čubová, K.; Semelová, M.; Němec, M.; John, J.; Milačić, M.; Omtvedt, J.P.[1]; Štursa, J.[2]

[1]Department of Chemistry, University of Oslo, Norway
[2]Nuclear Physics Institute, Czech Academy of Sciences, Řež, Czech Republic

INTRODUCTION

Chemical studies of Superheavy Elements (SHEs) are one of today's great challenges with respect to understanding the periodic table at "the deep end". Because of their very short half-lives and complicated production, experimental confirmation of their predicted chemical properties (especially for those with Z > 108) is difficult [1,2]. Extraction of thallium and indium, as the homologues of nihonium, from HCl solutions into hydrophobic ionic liquids was studied.

EXPERIMENTAL

Short-lived thallium and indium isotopes were produced by irradiating Au and Ag self-supporting target foils with natural isotopic composition (10 and 15-µm thick, Goodfellow AU000160 and AG000180, respectively) using the U-120M cyclotron at the Nuclear Physics Institute of the Czech Academy of Science in Řež near Prague. The aerosols carrying the radionuclides were dissolved by washing the collector filter with the HCl solution to be used directly as the aqueous phase for liquid-liquid extraction experiments. The 1.4-h ^{196m}Tl and 58-min ^{108}In were used to determine the amount of Tl and In in the different phases of the liquid-liquid extraction experiments. No carriers were added for either Tl or In and the extractions were performed separately for these two elements.

In the extraction experiments [3], concentrations of hydrochloric acid and $NaClO_2$ as an oxidation agent in the aqueous phase were optimised. As the organic phase, two different ionic liquids were selected: 1-hexyl-3-methylimidazolium bis(trifluoromethylsulfonyl)imide [C_6mim][NTf_2] and tributylmethylammonium bis(trifluoro methanesulfonyl)imide [Tbma][NTf_2]. Aqueous phase of a total volume of 1 mL was prepared constituting a mixture of HCl at concentrations: 0.2; 0.5; 0.75; 2.5; 3.75 mol/L; and $NaClO_2$ at concentrations: 0; 2; 4; 6; 8; 16; 24 mmol/L. The $NaClO_2$ was added to the aqueous phase and mixed just before contact with the equal volume of the organic phase. In all the experiments, equal volumes of both phases were contacted and violently shaken by a vortex shaker for 4 min at 3000 rpm at ambient temperature. Aqueous and organic phases were then separated by centrifugation (30 s at 3000 rpm). Aliquots of 750 µL of both phases were sampled and measured with a 50% HPGe detector. To determine the distribution ratios (D), the 635.3 and 695.4 keV γ-rays from the decay of ^{196m}Tl and 632.9 and 875.4 keV γ-rays from the decay of ^{108}In were measured. The D values were calculated as the ratio of the decay-corrected net areas of the respective γ-ray peaks in the organic and aqueous phases.

RESULTS

The parameters strongly influencing the extraction (influence of oxidizing agent, different ionic liquids comparison, influence of HCl concentration and comparison of Tl and In extraction) were studied in details. It was found that in the presence of $NaClO_2$ as the oxidizing agent, thallium is effectively extracted into all the tested ionic liquids from 0.2–5M HCl. In absence of $NaClO_2$, thallium extraction strongly depends on the HCl concentration and no extraction of indium was observed (cf. Fig. 1). Using [C_6mim][NTf_2] and [Tbma][NTf_2], the thallium / indium separation factors SF(Tl/In) > $4x10^4$ can be achieved. Hence, the system with $NaClO_2$ oxidizing agent can be considered a candidate for the future studies of nihonium chemical properties.

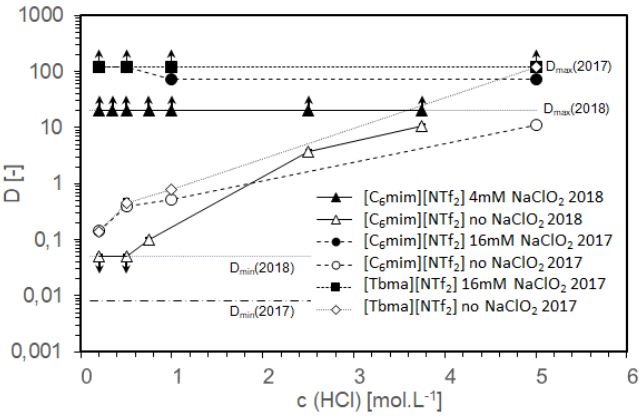

Fig. 1. The dependence of distribution ratio D of thallium extraction into various ionic liquids on the concentration of hydrochloric acid.

REFERENCES

[1] Aksenov, N.V. et al. (2017), Eur. Phys. J. 53: 158
[2] Eichler R. (2013), J. Phys.: Conf. Ser. 420 012003
[3] Čubová K. et al. (2018), J. Radioanal. Nucl. Chem. 318:2455–2461

This work was carried out within CANAM infrastructure project LM2015056 and within the Centre for advanced applied science, project number CZ.02.1.01/0.0/0.0/16_019/0000778, both supported by the Ministry of Education, Youth and Sports of the Czech Republic.

PERTECHNETATE SORPTION ON OXIDIZED AND REDUCED SURFACE OF ACTIVATED CARBON

Daňo, M.; Viglašová, E.[1]; Galamboš, M.[1]; Rajec, P.[1]

[1]Comenius University in Bratislava, Slovak Republic

INTRODUCTION

Activated carbon (AC) is pores space bounded by the carbon atoms [1]. It was shown that surface modified forms of carbon-based materials are promising sorbents for separation of various radionuclides . The mechanism of TcO_4^- sorption may differ according to the AC surface functional groups on its surface. It involves ion-exchange reaction between AC surface and TcO_4^- anions, and/or chemical bond or reduction of TcO_4^- on the surface. It has been found that the oxidation of AC, e.g. by nitric acid treatment, increases the weight distribution ratio for the extraction of radionuclides [2].

EXPERIMENTAL

Sample A was commercial sample produced by Polymer Institute of Academy Science, Slovakia. Surface area of sample A is 1014 $m^2 \cdot g^{-1}$. Sample B was an oxidized form of sample A, post-treated with aqueous solution of HNO_3 (68 %) in ratio 1:1 at 105 °C for 15 minutes. The surface area of sample B is 644 $m^2 \cdot g^{-1}$. Sample C was a reduced form of the sample A, obtained by treating it with 10 % aqueous solution of $Na_2S_2O_5$ at the boil for 15 min.

The aqueous solution of ~0.5 MBq/mL TcO_4^- (pH 2) was used for the sorption experiments. The batch sorption experiments of TcO_4^- on AC were carried out in the presence of competitive anions: CH_3COO^-, $HCOO^-$, NO_3^-, Cl^-, Br^-, ClO_4^- and SO_4^{2-}. Always 0.03 g of AC sample was mixed with 3 mL of the desired solution in a plastic test tube in laboratory extractor at constant mixing speed (250 rpm) for 1 h. Then, the phases were separated by centrifugation (10 min, 6000 rpm). The pH values after the sorption slightly increased (to pH~3) which corresponds to the OH^- release from the AC surface. Always 1 mL of supernatant aliquots was measured by NaI(Tl) and percentage of adsorption (R) was evaluated.

RESULTS

Sample A was prepared without any additives. The sorption of TcO_4^- was close to 100% at the lowest concentrations of anions. As shown in Fig. 1, percentage of sorption of TcO_4^- is the lowest at 0.1 M of ClO_4^- and reached 77%. Small changes of R occur in the presence of NO_3^- and $HCOO^-$. This is probably due to the fact, that these anions have the highest standard absolute molar enthalpies of hydration. Moreover, TcO_4^- and ClO_4^- have similar tetrahedral structure and therefore TcO_4^- anions could be replaced ClO_4^- in the active sites. The results obtained demonstrated that the sorption of TcO_4^- on AC is correlated with the standard absolute molar enthalpies of hydration (kJ mol^{-1}) of the competitive ions that follow the sequence: SO_4^{2-} (-1099) < $HCOO^-$ (-384) < CH_3COO^- (-374) < Cl^- (-359) < Br^- (-328) < NO_3^- (-316) < ClO_4^- (-205).

The influence of competitive anions on TcO_4^- sorption on sample B is shown in Fig. 2. The smallest sorbed amount of TcO_4^- for sample B is observed in the presence of NO_3^- followed by ClO_4^- with the largest standard absolute molar enthalpy. Sorption percentage of TcO_4^- in the presence of organic anions CH_3COO^- and $HCOO^-$ reached 76 and 70%, respectively.

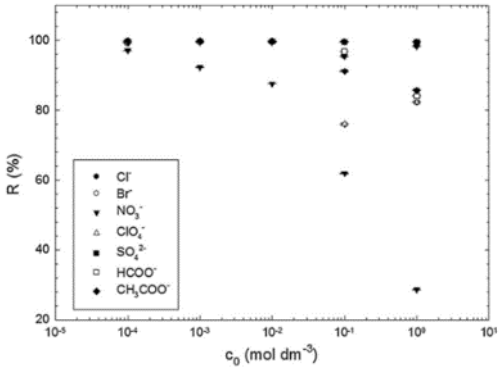

Fig. 1. Sample A, dependence of the percentage of TcO_4^- adsorption (R) on initial concentration of competitive anions (c_0).

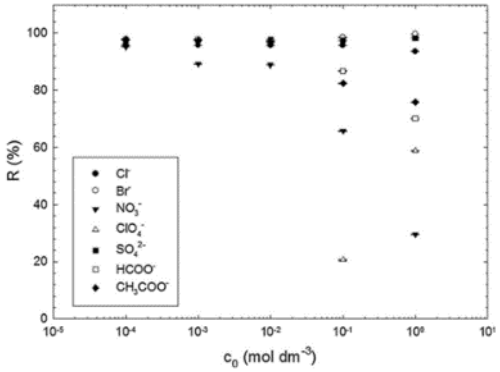

Fig. 2. Sample B, dependence of the percentage of TcO_4^- adsorption (R) on initial concentration of competitive anions (c_0).

The results of anion competition experiments in sample C are very similar to sample B. However, the lowest percentage of TcO_4^- sorption R was observed in the presence of NO_3^- and is equal to 42%. It seems that NO_3^- is suitable for desorption of TcO_4^- from the sample with reduced surface. From the point of view of anion competition results, oxidized and reduced forms of sample A are equally suitable for TcO_4^- sorption.

REFERENCES

[1] Marsh H., Rodríguez-Reinoso H. (2006) Activated carbon. Elsevier Science & Technology Books, Amsterdam

[2] Daňo M.; Viglašová E.; Galamboš M.; Rajec P.; Novák I. (2017) J. Radioanal. Nucl. Chem 314: 2219-2227.

This work was supported by the Slovak Research and Development Agency APVV Project No. SK-AT-2015-0003 and Agency of the Ministry of Education, Science, Research and Sport of the Slovak Republic and Slovak Academy of Sciences VEGA Project No. 1/0507/17.

SEPARATION OF THE MINOR ACTINIDES AMERICIUM(III) AND CURIUM(III) BY HYDROPHOBIC AND HYDROPHILIC BTPhen LIGANDS: EXPLOITING DIFFERENCES IN THEIR RATES OF EXTRACTION AND EFFECTIVE SEPARATIONS AT EQUILIBRIUM

Distler, P.; John, J.; Šťastná, K.; Afsar, A.[1]*;*
Harwood, L.M.[1]*; Hudson, M.J.*[1]*; Laventine, D.M.*[1]*; Lewis, F.W.*[2]

[1]University of Reading, Great Britain; [2]Northumbria University, Great Britain

INTRODUCTION

The extraction and complexation of the adjacent minor actinides Am(III) and Cm(III) by both hydrophobic and hydrophilic pre-organized 2,9-bis(1,2,4-triazin-3-yl)-1,10-phenanthroline (BTPhen) ligands has been studied in detail. These ligands are very prospective for the extremely challenging separation of the chemically similar minor actinides Am(III) and Cm(III) in future processes to close the nuclear fuel cycle. The structure of the $CyMe_4$-BTPhen is shown in Fig. 1.

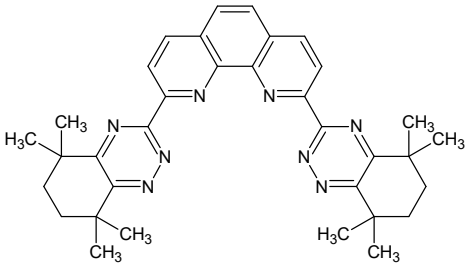

Fig. 1. Structure of $CyMe_4$-BTPhen.

EXPERIMENTAL

Hydrophobic ligands were dissolved in tested diluents for the extraction experiments. Aqueous phases with HNO_3 were spiked by ^{241}Am and ^{244}Cm tracers. In the case of hydrophilic complexation agents, organic phases contained 0.2 M TODGA dissolved in 5 % vol. 1 octanol in kerosene. Aqueous phase consisted of nitric acid solutions with hydrophilic sulfonated ligands and radionuclides mentioned above. Both phases were contacted for the appropriate time.

RESULTS

A kinetic effect was observed in the extraction of Am(III) and Cm(III) by hydrophobic ligand $CyMe_4$-BTPhen into three different diluents (octanol, octanol:toluene 40:60, cyclohexanone), leading to a more rapid extraction of Am(III) than Cm(III). Separation factors for Am(III) over Cm(III) ($SF_{Am/Cm}$) as high as 7.9 (in 1-octanol/toluene (40:60)) or around 5.0 (in cyclohexanone) are observed under these non-equilibrium (kinetic) extraction conditions. The second mentioned system is shown in Fig. 2.

This kinetic effect can be tuned through careful choice of the extraction variables (organic diluent, contact time, shaking speed, ligand concentration) and could thus potentially be exploited to carry out the extremely challenging but necessary separation of Am(III) from Cm(III) in a future closed nuclear fuel cycle.

In contrast, no such kinetic effect is observed with other BTPhen ligands containing linear alkyl groups, and these ligands do not separate Am(III) from Cm(III) effectively.

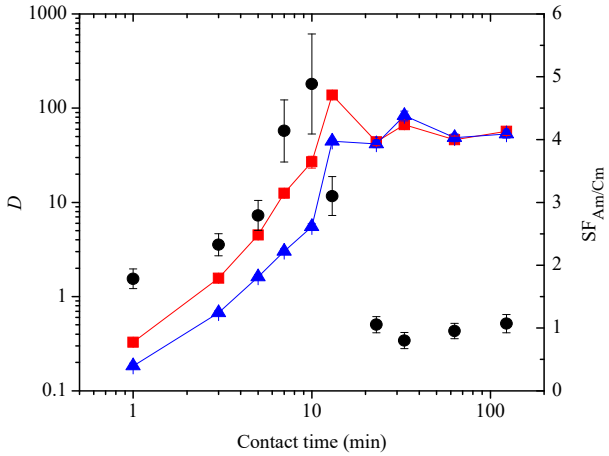

Fig. 2. Selective extraction of Am(III) over Cm(III) from 1 M nitric acid by solutions of $CyMe_4$-BTPhen in cyclohexanone (0.005 M) as a function of contact time (■ = D_{Am}, ▲ = D_{Cm}, • = $SF_{Am/Cm}$, mixing at 250 rpm, T = 20 ± 1 °C).

We attribute this kinetic separation to the slightly higher kinetic lability of the Am(III) aqua complex towards ligand substitution compared to the Cm(III) aqua complex, in analogy with the known trend in kinetic labilities of the corresponding trivalent lanthanide aqua complexes.

Next, we have shown that, under equilibrium conditions, hydrophilic tetrasulfonated BTPhen ligands can complex selectively Am(III) over Cm(III) in nitric acid and suppress its extraction by TODGA, leading to effective separations of Am(III) from Cm(III) ($SF_{Cm/Am}$ up to 4.6 observed).

Taken together with the separation factors reported in the literature, these results underline both hydrophobic and hydrophilic pre-organized BTPhen ligands as promising candidates for the difficult separation of Am(III) from Cm(III) in used nuclear fuel reprocessing, either under kinetic or thermodynamic (i.e. equilibrium) extraction conditions. The presented kinetic separation effects are described in details in [1].

REFERENCES

[1] Distler, P. et al. (2018) Sep. Sci. Technol. 53(2), 277-285.

This research has been supported by the Nuclear Fission Safety Program of the European Union for support under the ACSEPT (FP7-CP-2007-211267) and SACSESS (FP7-CP-2012-323282) contracts, and the Grant Agency of the Czech Technical University in Prague (grant No. SGS15/216/OHK4/3T/14).

SEPARATION OF TRIVALENT ACTINIDES AND LANTHANIDES BY USING SOLID-LIQUID EXTRACTION SYSTEMS

Distler, P.; John, J.; Afsar, A.[1]; Harwood, L.M.[1]; Cowell, J.[1]; Mohan, S.[1]; Davis, F.[1]

[1]University of Reading, Great Britain

INTRODUCTION

Previous work on the minor actinide-lanthanide separations has focused on solvent extraction processes (e.g. SANEX process). However, these processes come with other disadvantages, such as the requirement for substantial liquid storage and containment and generation of additional secondary waste. Although much progress has been made concerning the development of extractants for the liquid-liquid extraction processes that can partition minor actinides from lanthanides, far less effort has been emphasized on the alternative approaches such as e.g. solid-liquid extraction.

Replacing the current liquid-liquid extraction methods with a system based on a solid phase extractant could eliminate the large volumes of secondary organic waste generated during separation. To overcome the limitations of liquid-liquid extraction process, we previously demonstrated that when magnetic nanoparticles (MNPs) are combined with ligands such as $CyMe_4$-BTPhen, these functionalized MNPs could be used to extract the minor actinides and the radioactive material could then be collected magnetically in preference to centrifugation. As an example, the structure of $CyMe_4$-BTPhen covalently bound to silicagel with Fe_2O_3 MNPs is shown in Fig. 1. Within our studies [1-4], we tested the influence of extracting compounds, the surface and presence of MNPs on extraction properties of solid-liquid extraction systems.

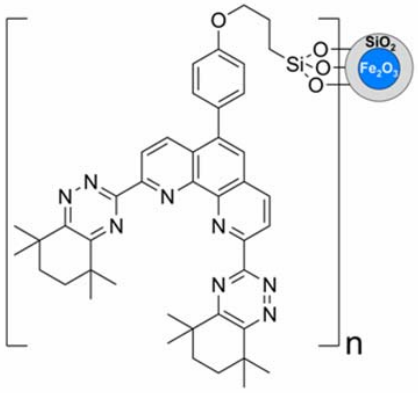

Fig. 1. $CyMe_4$-BTPhen covalently bound to the SiO_2-covered Fe_2O_3 MNPs.

EXPERIMENTAL

The aqueous solutions for the solid phase extraction experiments were prepared by spiking HNO_3/$HClO_4$/HI acid solutions (0.001 – 4 M) with ^{241}Am and ^{152}Eu and then contacting always 1 mL of spiked aqueous solution with a particular amount of solid extractant. The suspensions were sonicated for 10 min and shaken at 1800 rpm for 90 min, then the phases were separated by centrifugation.

RESULTS

Firstly, we reported a promising partitioning process for minor actinides, lanthanides and other fission products based on a column separation technique using novel BTBP/BTPhen immobilized silica gels. [1] The BTBP-functionalized SiO_2 gel can be used to remove problematic corrosion and fission products without extracting alkali or alkaline earth metal cations: while the BTPhen-functionalized SiO_2 gel extracts both minor actinides and lanthanides at low concentrations of HNO_3 yet exhibits very high selectivity for minor actinides over lanthanides at 4 M HNO_3 ($SF_{Am/Eu}$ = 140). We propose that this technology could pave the way for the design of an advanced partitioning process for PUREX raffinate consisting of an initial clean-up to remove d-block metals and a second stage to remove the minor actinides from the lanthanides.

Furthermore, both Am(III) and Eu(III) can be co-extracted at low concentrations of HNO_3 (0.1 M) if required. The uptake behaviour of Am(III) and Eu(III) by hydroxy-$CyMe_4$-BTPhen-SiO_2-Fe_2O_3 MNPs at different molarities of HNO_3 demonstrates that the extraction process is highly dependent on HNO_3 concentration and these results represent a substantial breakthrough in the development of solid-phase materials for the minor actinides-lanthanides separation. [2]

Next, a convenient route for immobilisation of $CyMe_4$-BTPhen ligands via a phenyl ether linkage onto the surface of zirconia-coated maghemite (γ-Fe_2O_3) magnetic nanoparticles was reported. These MNPs successfully co-extracted both Am(III) and Eu(III) from solutions up to 4 M HNO_3, with low selectivity ($SF_{Am/Eu}$ = 1.8) compared to that reported previously for SiO_2-coated MNPs ($SF_{Am/Eu}$ = > 1300). Based on FT-IR and elemental analysis data, the surface of the ZrO_2-MNPs appears to be less functionalized with $CyMe_4$-BTPhen ligands than the SiO_2-MNPs counterpart. Both ZrO_2 and SiO_2 provide an effective coating to the iron oxide core to enable chemical resistance to the harsh conditions in extraction processes, but since the SiO_2-MNPs can incur higher ligand loading, we conclude that SiO_2-MNPs should be favoured over ZrO_2-MNPs for future investigations to provide an effective extraction from SANEX-type processes.

REFERENCES

[1] Afsar, A. et al. (2017) Chem. Comm. 53, 4010-4013.
[2] Afsar, A. et al. (2017) Synlett 28, 2795-2799.
[3] Afsar, A. et al. (2018) Heterocycles 99. No pages.
[4] Afsar, A. et al. (2018) Tetrahedron 74(38), 5258-5262.

This research has been supported by the Nuclear Fission Safety Program of the European Union for support under the SACSESS (FP7-CP-2012-323282) contract, and the Grant Agency of the Czech Technical University in Prague (grant No. SGS15/216/OHK4/3T/14).

MODELLING OF THE Am(III) – Cm(III) KINETIC SEPARATION EFFECT OBSERVED DURING METAL ION EXTRACTION BY BIS-(1,2,4)-TRIAZINE LIGANDS

Distler, P.; Štamberg, K.; John, J.; Harwood, L.M.[1]; Lewis, F.W.[2]

[1]University of Reading, Great Britain; [2]Northumbria University, Great Britain

INTRODUCTION

The kinetic separation effect leading to a separation factor for Am(III) over Cm(III) as high as 7.9 by using $CyMe_4$-BTPhen ligands was observed in our recent study [1]. In an attempt to explain the observed tendencies, several kinetic models were tested.

EXPERIMENTAL

The aqueous solutions were prepared by spiking 0.5 M HNO_3 with stock solutions of ^{241}Am and ^{244}Cm tracers. Solutions of the 0.005 M hydrophobic $CyMe_4$-BTPhen ligand were prepared by dissolving the ligands in cyclohexanone. Prior to labelling, both phases were pre-equilibrated. Each organic phase (1 mL) was shaken separately with each of the aqueous phases (1 mL) for the desired time at a thermostatted temperature (22 ± 1 °C) using a GFL 3005 Orbital Shaker (250 min^{-1}). Each kinetic run consisted of 10 experimental points at different contact times: 1, 3, 5, 7, 10, 20, 30, 60, 90, and 120 minutes.

As regards the first step of the experimental data evaluation, the following kinetic models were tested and evaluated: mass transfer, film diffusion, diffusion in inert layer, diffusion in reacted layer, chemical reaction and gel diffusion; the rate-controlling processes being evident from their names. All of these models are given by ordinary first order differential equations where the numerical solution is relatively simple.

RESULTS

The mass transfer model had the best agreement between the experimental and theoretical values from all the tested models. The graphical evaluations of the Am(III) extraction, namely the experimental and calculated results, are depicted in Fig. 1.

The values of the overall mass-transfer coefficients confirmed that extraction of Am(III) by the $CyMe_4$-BTPhen is approximately twice as fast as the extraction of Cm(III) – the rate of extraction of americium is $8.67.10^{-3}$ min^{-1} while for curium it is only $4.73.10^{-3}$ min^{-1}.

The reason for this fact is not clear at this moment, although differences in the kinetic labilities of the Am(III) and Cm(III) aqua complexes toward ligand substitution, similar to those observed for the lanthanide series, have been suggested as one of the possible reasons.

Moreover, a dependence of Am/Cm separation coefficients $SF_{Am/Cm}$ on time was simulated and the obtained good fit of the calculated separation coefficients to the determined experimental values confirmed the validity of the theoretical model. The calculated and experimental data are shown in Fig. 2.

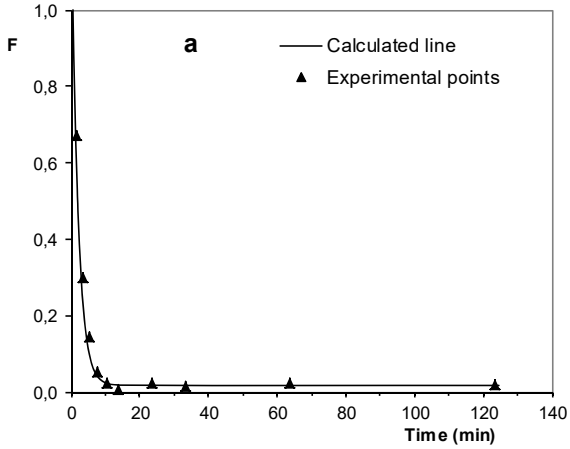

Fig. 1. Extraction kinetics of Am(III) for the liquid-liquid extraction systems based on CyMe4-BTPhen; F is a relative concentration of Am(III) in the aqueous phase (relatively to their respective initial concentrations).

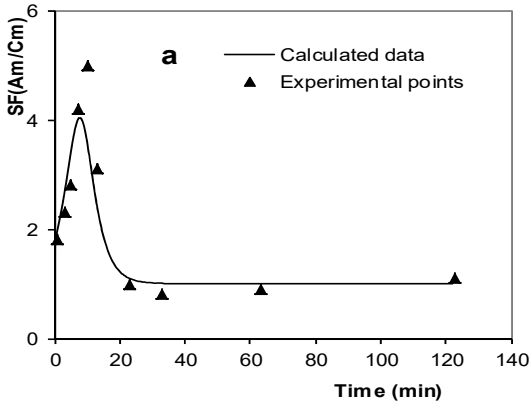

Fig. 2. The results of the simulation of the time-dependent separation factor, $SF_{Am/Cm}$ for the extraction systems based on $CyMe_4$-BTPhen.

This kinetic separation phenomenon and its explanation paves the way for potential new approaches to separation of metal ions with very similar properties, such as the adjacent minor actinides Am(III) and Cm(III).

In addition to a more detailed study of related systems, the next challenge is to engineer processes and devices that will be able to make practical use of this separation effect.

REFERENCES

[1] Lewis, F. W. et al. (2018) Solvent Extr. Ion Exc. 36(2), 115-135.

This research has been supported by the Seventh Framework Programme of the European Union – the SACSESS project, grant No. FP7-CP-2012-323282, and by the Grant Agency of the Czech Technical University in Prague, grant No. SGS15/216/OHK4/3T/14.

SEPARATION OF CURIUM FROM AMERICIUM USING COMPOSITE SORBENTS AND COMPLEXING AGENT SOLUTIONS

Šťastná, K.; Distler, P.; John, J.; Šebesta, F.

INTRODUCTION

TODGA-PAN or DGA resin composite sorbents and $(PhSO_3H)_2$-BTPhen in nitric acid solution were employed as a system for separation of curium from americium. The influence of aqueous phase composition (complexing agent and nitric acid concentrations) on weight distribution coefficients and Cm/Am separation factor was studied earlier in batch experiments with trace amounts of ^{241}Am and ^{244}Cm. [1] Based on the results obtained, column experiment was designed and conducted.

EXPERIMENTAL

For the extraction chromatography experiments, plastic column (4.7 mm diameter) was filled with 60 mg of TODGA-PAN or 190 mg of DGA resin to form 0.50 mL bed (29 mm height) and washed by 10 ml of 0.3 mol/L HNO_3. Trace amounts of ^{241}Am and ^{244}Cm were sorbed on the column top from 500 µL of 0.3 mol/L nitric acid at a flow rate of 0.6 ml/h. This low flow rate was selected to achieve the retention time of solution in the column comparable to the time needed to reach a sorption quasi-equilibrium in batch experiments (about 1 h) [1]. For the elution, 0.003 mol/L $(PhSO_3H)_2$-BTPhen (Fig. 1) solution in 0.3 mol/L HNO_3 was used at a flowrate of 0.6 mL/h. The eluting agent is shonw in Fig. 1.

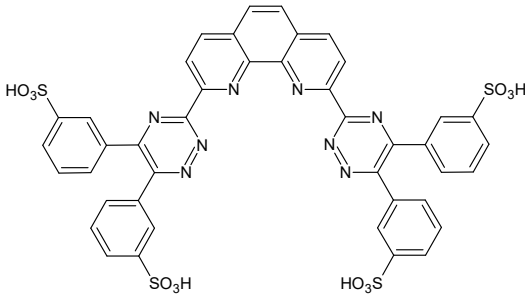

Fig. 1. Structure of $(PhSO_3H)_2$-BTPhen.

RESULTS

The reduced effluent volumes at the peak maximum, calculated from D_w values from batch experiment (25 ± 2 mL/g and 72 ± 2 mL/g for Am(III) and Cm(III), respectively) and sorbent weight in column had values of 4.8 mL for Am(III) and 13.7 mL for Cm (III). In Fig. 2, the chromatogram of Cm/Am separation on DGA resin, obtained in the column experiment described above, is shown. As can be seen, the predicted reduced effluent volumes are in good agreement with the elution volumes obtained in the column experiment. The D_w values corresponding to the measured experimental elution volumes are 27 and 72 mL/g; the values of *SF* calculated from the batch experiments data an column experiment being 2.9 ± 1 and 2.7, respectively.

When compared with the TODGA-PAN sorbent, the D_w and *SF* values for DGA resin are lower. Since the extractant is identical in both materials, this difference should be probably attributed to slower kinetics of Am and Cm uptake on DGA resin.

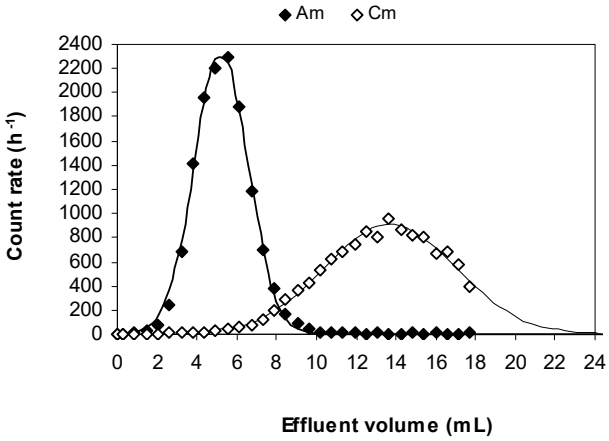

Fig. 2. Chromatogram of Cm/Am separation on a column with DGA resin – 0.003 mol/L $(PhSO_3H)_2$-BTPhen in 0.3 mol/L HNO_3 system (column: φ4.7 x 29 mm, 190 mg DGA Resin, bed volume 0.5 mL, flow rate 0.6 mL/h).

Contrary to TODGA-PAN system, tailing of the peaks (caused probably by sorption of An^{3+} on PAN matrix) did not occur for DGA resin and the resolution was better having a value of 0.65. The collected fraction containing 80 % of Cm(III) contained only 2 % of Am(III) contrary to the case of TODGA–PAN where this fraction contained 8 % of Am(III). Even the fraction containing 93 % of Cm(III) contained only 3 % of Am(III). The higher purity of fractions was also achieved by a bigger amount of DGA resin used to form the bed of the same volume and thus also higher amount of TODGA extractant in the column bed.

In conclusion, TODGA PAN composite sorbent as well as the DGA resin proved good performance for curium separation from americium when using $(PhSO_3H)_2$-BTPhen in HNO_3 solution as an eluting agent. The Cm/Am separation factor of 3.8 ± 0.1 found in batch experiments with TODGA-PAN could be reproduced also in column experiment. Further optimization of the parameters of the systems, such as column lengths, flow rates or $(PhSO_3H)_2$-BTPhen and HNO_3 concentrations, are expected to yield even better resolutions.

REFERENCES

[1] Šťastná, K. et al. (2015) J. Radioanal. Nucl. Chem. 304, 349-355.

This research has been supported by the Grant Agency of the Czech Technical University in Prague, grants No. SGS12/199/OHK4/3T/14 and No. SGS15/216/OHK4/3T/14.

SEPARATION OF RADIOACTIVE CONTAMINANTS FROM MOLYBDENUM SOLUTIONS ISSUING THE REPROCESSING OF CERMET Mo-BASED FUEL

Mareš, K.V.; Daňo, M.; Šebesta, F.; John, J.

INTRODUCTION

As described in the previous Annual Report [1], process for the reprocessing of CerMet Mo-based fuels for Accelerator-Driven Transmuters has been recently studied. The possibility to remove caesium and strontium as the main cationic impurities has been successfully demonstrated. The first aim of the present report has been to study the possibilities of technetium separation from the concentrated molybdate solutions. Finally, the separation of all these three contaminants in one step by a triple-bed column was tested.

EXPERIMENTAL

Model molybdenum solutions were prepared from diammonium dimolybdate (Alfa Aesar) and non-isotopic carrier NH_4ReO_4 (Sigma-Aldrich). In the case of Tc sorption studies the solution composition was 100 $g \cdot L^{-1}$ Mo, 10^{-4} $mol \cdot L^{-1}$ Re and pH = 9.1 (adjusted by ammonia). The solutions were spiked by $^{99}TcO_4^-$ (ÚJV Řež) or $^{99m}TcO_4^-$ from $^{99}Mo/^{99m}Tc$ generator (Drytec) for beta or gamma spectrometric measurements, respectively. During the simultaneous separation of all three contaminants, the model solution also contained caesium nitrate (Dorapis) spiked by ^{137}Cs (Institute for Research, Production and Use of Radioisotopes) as well as strontium nitrate (Lachema) spiked by ^{85}Sr (Perkin Elmer).

Determination of the sorption kinetics:

100 mg of solid extractants was mixed with 50 mL of molybdenum solution (V/m = 500 $mL \cdot g^{-1}$) in glass chemical reactor. The supernatant or filtrate (in the case of composite sorbent) was taken for the measurements.

Determination of the distribution coefficients:

16 mg of the sorbent was contacted with 4 mL of molybdenum solution (V/m = 250 $mL \cdot g^{-1}$) in 30mL PE bottles for 2 hrs using an orbital shaker at 250 rpm.

Column experiments:

a) Tc separation

Column made (bed volume, BV = 0.24 mL) from 1mL syringe (Terumo) fitted by PE frits was used. The column was filled with solid extractant based on Aliquat® 336 with polyacrylonitrile (PAN) binding matrix (solid extractant referred to A336-PAN) for Tc separation.

b) Simultaneous Cs, Sr and Tc separation

In the case of separation of all these three contaminants a column was prepared with three stacked beds (BV = 0.24 mL each) separated by PE frits made from 1mL syringe (Terumo). The three beds contained the KNiFC-PAN composite absorber for Cs separation, $Ba(Ca)SO_4$-PAN composite absorber for Sr separation that has been wetted prior to the experiment by sucking distilled water through the column and the A336-PAN solid extractant for Tc separation. The concentrations of all three contaminants (Cs, Sr and Tc) have been set to 10^{-4} $mol \cdot g^{-1}$ in the molybdenum solution that was passed through the column in upward direction by a peristaltic pump.

RESULTS

The sorption kinetics of Tc on A336-PAN is fast, the equilibrium was reached within 30 minutes. Influence of pH around the value 9.1 and of molybdenum concentration around 100 $g \cdot L^{-1}$ Mo were very low with no significant effect on the extraction process. The sorption isotherm was measured as well; the maximum sorption capacity obtained in batch experiments is 1.338 $mmol \cdot g^{-1}$ for Tc. Dynamic column tests for Tc separation were performed with the A336-PAN material, the breakthrough curve obtained is shown on Fig. 1. As can be seen, the 100% breakthrough was not achieved. It was possible to treat 22.3 BV of the solution of technetium with a rhenium non-isotopic carrier ($c_{Re} = 10^{-2}$ $mol \cdot L^{-1}$) with the breakthrough lower than 1 % (0.575 $mmol \cdot g^{-1}$) and 27.3 BV with the breakthrough lower than 10 % (0.688 $mmol \cdot g^{-1}$).

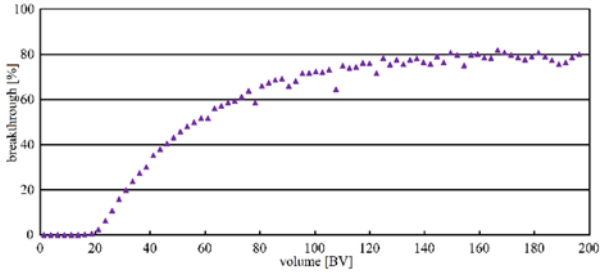

Fig. 1. Tc breakthrough curve through a column of A336-PAN solid extractant (BV = 0.24 mL, mass of A336-PAN = 92.3 mg, grain size < 0.3 mm, average flow rate = 5.93 $BV \cdot hr^{-1}$, concentration of non-isotopic Re carrier $c_{Re} = 10^{-2}$ $mol \cdot L^{-1}$, c_{Mo} = 100 $g \cdot L^{-1}$, initial pH = 9.1)

The dynamic column test for simultaneous Cs, Sr and Tc separation was performed by a triple-bed column, the results are shown in Fig. 2. During the experiment, 158 BV of the molybdenum solution was treated. The breakthrough of Cs observed after 120 BV was 1 %. No Sr or Tc breakthrough was observed.

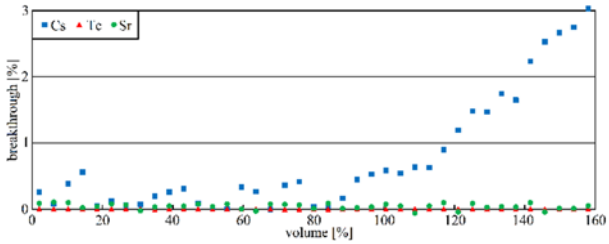

Fig. 2. Caesium, strontium and technetium breakthrough curve through a column of KNiFC-PAN, $Ba(Ca)SO_4$-PAN and A336-PAN (BV of each sorbent 0.24 mL, average flow rate = 4.10 $BV \cdot hr^{-1}$, concentration of caesium, strontium and non-isotopic rhenium carrier $c_{Re} = 10^{-4}$ $mol \cdot L^{-1}$, c_{Mo} = 100 $g \cdot L^{-1}$, initial pH = 9.1)

REFERENCES

[1] Mareš, K.V et al. (2014), Nuclear Chemistry, Annual Report 2013-2014, CTU, pp. 38

This study was supported by the EU 7th Framework Programme project ASGARD (EC-GA No. 295825, the Grant Agency of the Czech Technical University in Prague (grants No. SGS12/199/OHK4/3T/14 and SGS15/216/OHK4/3T/14), and by the Centre for Advanced Applied Science supported by the Ministry of Education, Youth and Sports of the Czech Republic, project No. CZ.02.1.01/0.0/0.0/16_019/0000778.

Radiation Chemistry

FORMATION OF HYDROXYL RADICALS IN DILUTED AQUEOUS SOLUTIONS EXPOSED TO ULTRAVIOLET RADIATION

Tomanová, K.; Přeček, M.[1]; Múčka, V.; Vyšín, L.[1]; Juha, L.[1,2]; Čuba, V.

[1]Institute of Physics, AS CR, Czech Republic; [2]Institute of Plasma Physics, AS CR, Czech Republic

INTRODUCTION

The border between chemical processes initiated by ionizing and non-ionizing (in particular UV) radiation in water or aqueous solutions is often blurred. During radiolysis, part of the absorbed energy is consumed to form stable products (H_2, H_2O_2) and many reactive intermediates that carry out numerous reactions [1]. It is well known that ·OH radicals play a prominent role among the intermediates. As the energy of radiation decreases, the probability of formation of ionized states decreases in favor of excited states. However, excited states of water molecules may dissociate to form ·OH and ·H radicals, and thus a short-wavelength UV radiation can initiate effects similar to those of ionizing radiation [2]. While there are reports available on ·OH radical formation under UV irradiation at wavelengths below 185 nm [3,4], similar data are lacking for wavelengths higher than 200 nm. However, our earlier study implied that there are strong indications that even the UV-C radiation, at a wavelength of 253.7 nm in particular, is able to produce the ·OH radicals in aqueous solutions [5]. Water molecules may constitute the main source of ·OH radicals in diluted aqueous solutions, obtained *via* photolysis:

$$H_2O \xrightarrow{h\nu} H_2O^* \rightarrow \cdot H + \cdot OH$$

Various detailed mechanisms of ·OH radical generation in aqueous solutions have been proposed in this study, including nonlinear processes, single photon excitation to the low-lying triplet states of water and subsequent intermolecular transfer of the excitation energy, and formation of van der Waals clusters that may decrease H–OH dissociation energy.

The aim of this study was to test the hypothesis on the possibility of creating the ·OH radicals in diluted aqueous solutions under the 253.7 nm irradiation.

EXPERIMENTAL

The following chemicals were used in the experiments: disodium hydrogenphosphate dihydrate $Na_2HPO_4 \cdot 2H_2O$, potassium dihydrogenphosphate KH_2PO_4, coumarin-3-carboxylic acid C3CA, and 7-hydroxycoumarin-3-carboxylic acid 7OH-C3CA. All chemicals were purchased from Sigma Aldrich and were used as received.

For UV irradiation, low pressure mercury UV lamps (TUV 25W–4P SE) emitting 253.7 nm photons with power input of 25 W were used. For UV irradiation, the 5ml solutions in PE tubes were placed between four such UV lamps. Total photon flow in this setup was determined to be $2.71 \cdot 10^{16}$ hν·s^{-1} (corresponding to the rate of deposited energy 4.2 J·kg^{-1}·s^{-1}). For gamma irradiation, samples in PE tubes were placed inside Gammacell 220 irradiator (^{60}Co) so that the dose rate was $\dot{D}$ (gammacell) = $9.7 \cdot 10^{-3}$ J·kg^{-1}·s^{-1} measured by Fricke dosimeter (1 J·kg^{-1} = 1 Gy).

RESULTS

Coumarin fluorescence dosimeter as a system reacting specifically with ·OH radicals in the presence of oxygen provided precise estimation of ·OH radical concentration in UV irradiated system and allowed us to calculate OH radical quantum yield. Rate of hydroxylated form of coumarin dosimeter (7OH-C3CA) production was determined as r(7OH-C3CA) = $1.6 \cdot 10^{-5}$ mmol·dm^{-3}·s^{-1} and was recalculated to the ‘‘dose rate’’ or the total efficiently absorbed energy measured by the coumarin dosimeter: $\dot{D}$ (coumarin) = $1.1 \cdot 10^{-3}$ J·kg^{-1}·s^{-1}. It corresponds to the amount of efficiently absorbed photons within 1 s, i.e. $h\nu_{\mathrm{eff}} = 7.02 \cdot 10^{12}$ $h\nu$ or 0.026 % of the total photon count. According to one set of published data [6], only 6% of ·OH radicals formed by irradiation corresponds to the detected 7OH-C3CA adduct, because various other hydroxylated products were formed as well. With this in mind we calculated the quantum yield of ·OH radicals as follows:

$$\Phi(\cdot OH) = \frac{[\cdot OH] \cdot V \cdot N_A}{h\nu_{\mathrm{eff}}} = 0.11$$

where V = 0.005 dm^3 is the irradiated volume and N_A is the Avogadro’s constant. This result was further specified by gamma irradiation of the coumarin dosimeter, where the radiation chemical yield of ·OH radicals is well known. The corrected quantum yield was calculated as $\Phi = 0.08$.

The resulting low quantum yield of ·OH radicals formed per single efficiently absorbed photon is in agreement with the assumption that photoexcitation of water under set conditions is an extremely rare process. However, at a given total photon fluence, the amount of photons spent on ·OH radical formation is rather significant (0.026 % of the total photon count). We propose that the hypothesis of a concerted action of two 4.9 eV photon excitation of water molecules into triplet states with subsequent dissociation to ·OH and ·H radicals could be considered as a possible mechanism of water photolysis in this study.

REFERENCES

[1] Le Caër, S. (2011) Water 3, 235-253.
[2] Gonzales, M. G. et al. (2004) J. Photochem. Photobiol. C 5, 225-246.
[3] Azrague, K. et al. (2005) Photochem. Photobiol. Sci. 4, 406-408.
[4] Kumar, A. et al. (2008) J. Phys. Chem. A 112, 5502-5508.
[5] Čuba, V. et al. (2012) Radiat. Phys. Chem. 81, 1411-1416.
[6] Louit, G. et al. (2005) Radiat. Phys. Chem. 72, 119-124.
[7] Tomanová, K. et al. (2017) Phys. Chem. Chem. Phys. 19, 29402-29408.

This research has been supported by the Czech Science Foundation, projects GA17-06479S and GA13-28721S.

* Full paper in [7].

DEGRADATION OF PHOSPHOLIPIDS UNDER DIFFERENT TYPES OF IRRADIATION AND VARYING OXYGEN SATURATION

Vyšín, L.[1]; Tomanová, K.; Pavelková, T.; Wagner, R.[2]; Davídková, M.[2]; Juha, L.[1,3]; Múčka, V.; Čuba, V.

[1]Institute of Physics, AS CR, Czech Republic; [2]Nuclear Physics Institute, AS CR, Czech Republic; [3]Institute of Plasma Physics, AS CR, Czech Republic

INTRODUCTION

According to the target theory, cell survival depends on the existence of a sensitive target within the cell which, when damaged, leads to the cell death. Cell membranes have been recognized as one of the vital targets for ionizing radiation. The cell membrane is the first target that stands in the interaction path or track of the ionizing radiation. When damaged or transformed, the result can be cell-signalling malfunction or finally a cell death [1].

Deleterious effects of ionizing radiation to the cell are often studied on very simple model systems. Phospholipid bilayers are important structural elements of many membranes of biological interest [2]. When exposed to a polar solvent, phospholipids tend to form closed structures called lipid vesicles or liposomes. It was shown that such phospholipid vesicles can serve as models of biological membranes [3].

Lipid hydroperoxides (LOOH) are formed by reaction with molecular oxygen, but direct path is spin-forbidden. The reaction proceeds either via an interaction with free radicals or the oxygen must be excited into a singlet state. The most important oxidative species formed by water radiolysis, the ·OH radical, can initiate chain reactions in the presence of molecular oxygen, resulting in the formation of lipid hydroperoxides.

EXPERIMENTAL

The DOPC 18:1 phospholipid (1,2-dioleoyl-sn-glycero-3-phosphocholine; Avanti Polar Lipids, Inc., USA) was used as a model membrane. The residual oxygen concentration in deoxygenated samples was determined using the DO_2 Meter 9500 (Jenway, UK). Proton irradiation (30 MeV protons) was carried out at the U-120 M isochronous cyclotron. Irradiation by gamma radiation was carried out using the Gammacell 220. To evaluate the amount of lipid hydroperoxides (LOOH) in the irradiated sample, the commercially available kit for lipid peroxides detection was used (Cayman Chemical Company, USA).

RESULTS

Phospholipids containing two single-unsaturated fatty acid chains in the form of small unilamellar vesicles were subjected to irradiation with various types of ionizing radiation. Figs. 1 and 2 show the dependence of radiation chemical yields on the dose of proton irradiation for various dose rates (Fig. 1) and of gamma irradiation for various levels of oxygen saturation (Fig. 2). It is obvious that the overall trends remain the same regardless of the type of radiation used. The radiation chemical yields *G* suggest that the reaction does not proceed via chain mechanism.

Fig. 1 shows that the radiation chemical yield decreases with increasing dose rate, which is most probably caused by the higher number of ·OH radical recombinations.

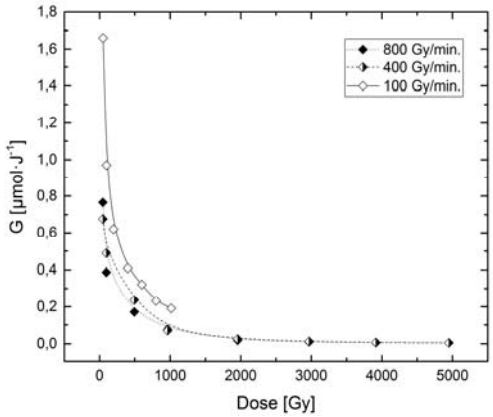

Fig. 1. Radiation chemical yields of lipid hydroperoxides as a function of absorbed dose. DOPC irradiated by accelerated protons with energy of 31 MeV at dose rates of 100, 400 and 800 Gy·min^{-1} [4].

Fig. 2 shows that the values of radiation chemical yields decrease with decreasing amount of oxygen dissolved in the irradiated solution. The presence of oxygen is crucial for the peroxidation process. None of the studied parameters affected the mechanism of the hydroperoxide formation.

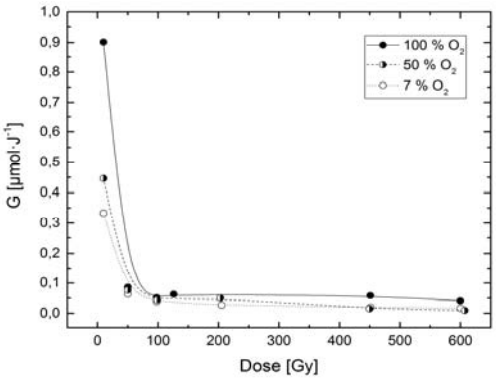

Fig. 2. Radiation chemical yields of lipid hydroperoxides as a function of absorbed dose for 7%, 50% and 100% oxygen saturation. DOPC irradiated by ^{60}Co γ-radiation at dose rate of 35 Gy·h^{-1} [4].

REFERENCES

[1] Catala A. (ed) (2012) Lipid peroxidation. InTech Open Access Publisher, Rijeka, Croatia, pp 261-278.

[2] Danielli, J. F.; Davson, H. (1935) J. Cell. Comp. Physiol. 5, 495-508.

[3] Chatterjee, S. N.; Agarwal, S. (1988) Free Radic. Biol. Med. 4, 51-72.

[4] Vyšín, L. et al. (2017) Radiat. Environ. Bioph. 56, 241-247.

This research has been supported by the Czech Science Foundation project no. GA13-28721S.

REDUCING THE RADIATION SENSITIVITY OF CELLS IRRADIATED BY UV RADIATION USING SCAVENGERS OF HYDROXYL RADICALS

Neužilová, B.; Múčka, V.

INTRODUCTION

Hydroxyl radicals formed by water radiolysis are toxic for living cells. The scavengers of ·OH radicals such as methanol and ethanol reduce radiation sensitivity of cells [1]. Using Fricke´s dosimeter it has already been demonstrated that UV radiation (254 nm) can produce OH radicals in the irradiated suspension [2]. The DNA of cells or other targets can be damaged due to ·OH production, in addition to the well-known photochemical dimerization of two spatially close pyrimidine bases, leading e.g. to thymine dimers. The aim of this work was to study the possible protection effect of both methanol and ethanol on yeast *Saccharomyces cerevisiae*, DBM 272 during UV irradiation by scavenging of ·OH radicals.

EXPERIMENTAL

Yeast *Saccharomyces cerevisiae* was taken from a stationary state of the 5-7 day old culture. The cells were introduced into isotonic salt solutions containing various concentrations of hydroxyl radical scavengers (ethanol or methanol). The suspension was irradiated with UV radiation (low-pressure mercury lamp, main wavelength 254 nm) in polypropylene tubes under vigorous stirring so that the nominal dose was 1 Gy at a nominal dose rate of 11.5 to 42.2 Gy h^{-1}. The doses were evaluated using iodide-iodate actinometer by multiplying the total photon flow in the mixed volume by the energy of 1 photon, divided by sample mass. After a suitable dilution, aliquots of the irradiated and non-irradiated cell suspensions were plated on the complete nutrient agar (Sabouard chloramphenicol). During 4-5 day incubation at 30° C, yeast colonies were formed, which were then counted. Every measurement was repeated three times and the mean value of the counted colonies was taken into account. The specific protection effect k was defined as a slope of dependence of the protection effect σ (defined as the ratio of natural logarithms of surviving fraction of cells irradiated both without and with scavenger) on the scavenging efficiency $Q = k_{OH} \times c_S$ where c_S and k_{OH} are concentrations of the scavenger and the rate constant of its reaction with ·OH radicals, respectively.

RESULTS

The dependence of σ-values on the scavenging efficiency Q was found to be linearly increasing for both alcohols and for all used dose rates. It means that both scavengers are effective in the protection of cells irradiated by ultraviolet radiation (Fig. 1). The specific protection effect k decreases with increasing dose rate in the range 11-42 Gy h^{-1} for both scavengers (Fig. 2). This may be caused by recombination processes ongoing at relatively high dose rates. The results give evidence that the scavenging of hydroxyl radicals (taking also other mechanisms for DNA damage or cell death into account) may be used for radiation protection also in UV-irradiated cultures similarly to the gamma radiation. This can help us to better understand the mechanisms of processes occurring in cells that protect against radiation.

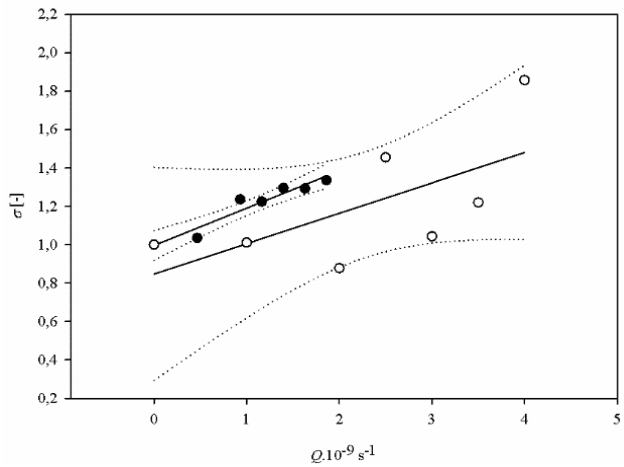

Fig. 1. Dependence of radiation protection effect σ on the scavenging efficiency Q for ethanol (circles) and methanol (filled circles) for a UV dose of 1 Gy at a dose rate of 15.8 Gy h^{-1}.

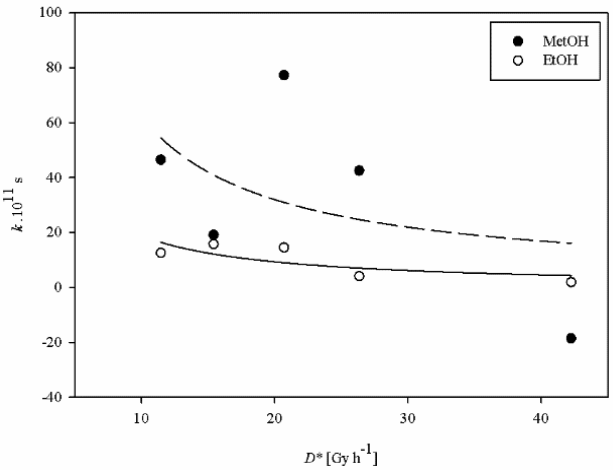

Fig. 2. Dependence of specific radiation protection effect k on the dose rate D^* of UV radiation for both alcoholic scavengers at the dose of 1 Gy.

REFERENCES

[1] Múčka, V. et al. (2013) Int. J. Radiat. Biol. 89, 1045-1052.

[2] Tomanová, K. et al. (2017) Phys. Chem. Chem. Phys. 19, 29402-29408.

This research has been supported by the Grant Agency of the Czech Technical University in Prague, project no. SGS17/195/OHK4/3T/14.

INFLUENCE OF THE DOSE RATE OF GAMMA IRRADIATION AND SOME OTHER CONDITIONS ON THE RADIATION PROTECTION OF MICROBIAL CELLS BY SCAVENGING OF OH RADICALS

Neužilová, B.; Ondrák, L.; Čuba, V.; Múčka, V.

INTRODUCTION

The efficient protection of living cells against ionizing radiation is of great importance, e.g., for minimization of the second cancer risk associated with the radiotherapy [1]. Many substances are supposed to protect irradiated cells by their reaction with free radicals [2-4]. The most active radicals (·OH radicals) may react with the sugar-phosphate part of DNA producing along with the breaks (SSB and DSB) also the so-called abasic sites (AS) with a similar efficacy [5]. Generally, all reactive oxygen species (ROS) can affect not only the radiation sensitivity itself but also its modification by scavengers of radicals. The main aim of the paper was to confirm the protective effects of the alcoholic scavengers of ·OH radicals on yeast and bacteria in a wide interval of irradiation conditions. Moreover, the influence of hypothermic conditions on the protecting effect was studied.

EXPERIMENTAL

The yeast *Saccharomyces cerevisiae* (haploid strain, type a, DBM 272) and *Escherichia coli* bacteria (DBM 3125) were used as representatives of eukaryotic and prokaryotic cells, respectively. Prior to irradiation, the yeast cells were cultivated on the nutrient agar layer to a stationary state for 3-5 days and the bacteria cells were used from a stationary state of the 24 h old culture. Methanol and ethanol were used as the scavengers of ·OH radicals. After preparation of the samples, the irradiation was performed in 10 mL polypropylene ampoules using the ^{60}Co gamma irradiator Gammacell 220. The doses and the dose rates ranged from 45 to 150 Gy and from 18 to 45 Gy h^{-1}, respectively. After cultivation of cells, 200 to 500 colonies were formed per dish. Each cultivation was independently repeated three times. Some samples (including the control samples) of bacteria were kept in isotonic salt solution at 0° C for 1 h both prior and after irradiation. After this treatment, they were processed in the standard way. The method of the evaluation of obtained results is described in [3,4].

RESULTS

The dependence of the σ-values on the scavenging efficiency Q for both yeast and bacteria is given in Fig. 1. It is obvious that the protective effect σ is higher than 1 and increases linearly with increasing scavenging efficiency Q for both yeast and bacteria inside the investigated Q-intervals from 0 to 1.86×10^9 s^{-1} for methanol and from 0 to 4×10^9 s^{-1} for ethanol. The same character of this dependence was found earlier for the yeast *Saccharomyces cerevisiae* irradiated with lower (5.6 Gy h^{-1}) or higher (70.0 Gy h^{-1}) dose rates [3]. On the ground of these measurements, we can generally conclude that the scavengers of ·OH radicals protect the living cells against the ionizing radiation. On the other hand, some other papers state a possibility to assume that the hypothermic treatment may decrease the radiation sensitivity of the cells [6]. It was shown that no effect was achieved after the cooling the bacterial culture at 0° C for 1 h prior and after the irradiation (Fig. 2).

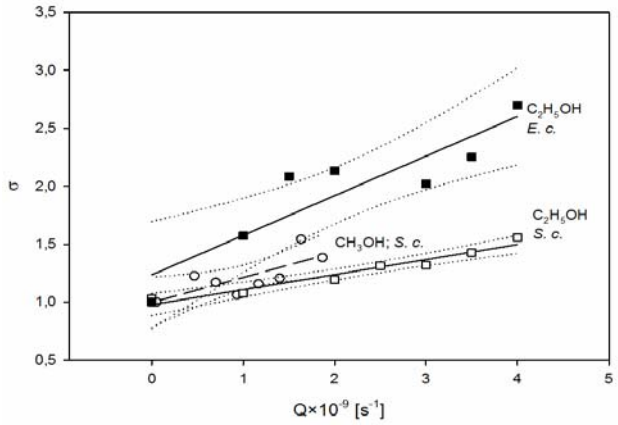

Fig. 1. Dependence of the σ-values for ethanol and methanol on its scavenging efficiency Q for yeast (*S. c.*) and bacteria (*E. c.*); dose 120 Gy, dose rate 38 Gy h^{-1} [7].

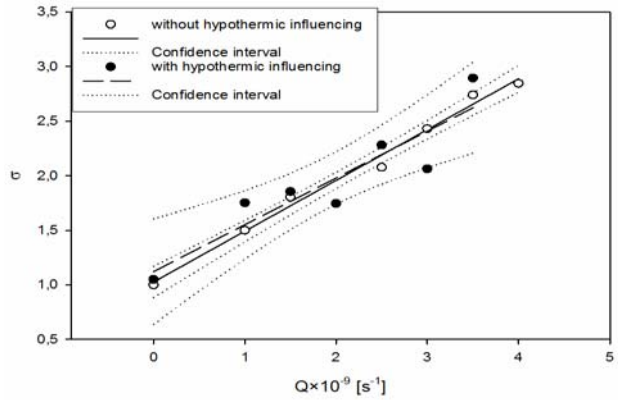

Fig. 2. Dependence of the σ-values of ethanol on its scavenging efficiency Q for bacteria (dose 45 Gy, dose rate 45 Gy h^{-1}) of gamma radiation both without and with the hypothermic treatment [7].

REFERENCES

[1] Imaoka, T. et al. (2016) Int. J. Radiat. Biol. 92, 289-301.
[2] Ewing, D. (1987) In: Farhatazis and Rodgers, M.A.J. (Eds.) Radiation Chemistry. Principles and applications. VCH Publishers, Inc., New York, pp. 501-526.
[3] Múčka, V. et al. (2013) Int. J. Radiat. Biol. 89, 1045-1052.
[4] Múčka, V. et al. (2015) J. Radioanal. Nucl. Chem. 304, 237-244.
[5] Shiina, T. et al. (2013) Radiat. Environ. Biophys. 52, 99-112.
[6] Dang, L. et al. (2012) Int. J. Radiat. Biol. 88, 507-514.
[7] Neužilová, B. et al. (2018) J. Radioanal. Nucl. Chem. 318, 2449-2453.

This research has been supported by the Ministry of Education, Youth and Sports of the Czech Republic, project no. CZ.02.0.1.01/0.0/0.0/16_019/0000778.
*Full paper in [7].

MONITORING OF SELECTED PARAMETERS AT IRRADIATION OF CELLS WITH IONIZING RADIATION

Ondrák, L.; Múčka, V.

INTRODUCTION

Ionizing radiation interacts with living cells directly or indirectly [1]. The direct effect is understood as interaction of radiation with targets in cells causing damage. Indirect effect corresponds to a situation when the cells are attacked by agents produced during radiolysis of water such as hydroxyl, peroxyl or hydroperoxyl free radicals, hydrated electrons etc. [2,3]. Because cells are composed of roughly 70 % water, large part of the damage is attributed to an indirect effect of ionizing radiation, mainly caused by hydroxyl free radicals originated in the immediate proximity to DNA molecule [3]. Therefore, hydroxyl radical scavengers can influence radiation sensitivity of living cells. Hydroxyl radicals can be scavenged by, for example, unsaturated organic molecules, molecules with thiol groups or flavonoids [4,5]. A widely used scavenger with the ability to easily penetrate the cell membrane is dimethyl sulfoxide. Since dimethyl sulfoxide is a very selective scavenger of hydroxyl free radicals with low acute chemical toxicity, it is used for quantification of indirect effect mostly attributed to hydroxyl radicals [6].

The aim of this paper was to study the influence of dimethylsulfoxide as a hydroxyl radical scavenger on the radiation sensitivity of the yeast *Saccharomyces cerevisiae*, DBM 272, during ^{60}Co gamma irradiation.

EXPERIMENTAL

Studied microorganism was yeast *Saccharomyces cerevisiae* (haploid strain, type a, DBM 272; UCT Prague, Czech Republic). *Saccharomyces cerevisiae* cells were cultivated on Sabouard chloramphenicol nutrient agar layer M 1067 (Himedia, India) at 32 °C for 5 days. The radiation protection was evaluated by counting of colonies grown up from surviving irradiated or non-irradiated cells. The applied dose rates and the doses ranged from 25.4 to 40 Gy/h and from 75 to 450 Gy, respectively. Dimethyl sulfoxide in concentration range 0-1.1 mol/L was used as scavenger of hydroxyl radicals.

The radiation protection σ of dimethylsulfoxide was defined as a ratio of natural logarithms of surviving fractions of the cells without (S_0) and with scavenger (S). The specific radiation protection k was defined as a slope of the dependence of radiation protection σ on a scavenging efficiency Q of dimethylsulfoxide. The Q-quantity is defined as a product of concentration c of dimethylsulfoxide and the reaction rate constant k_{OH} for the reaction of hydroxyl radical with dimethylsulfoxide.

RESULTS

The radiation protection σ and the specific radiation protection k were determined to be linearly growing functions of a dose rate of gamma radiation (Fig. 1) in the studied range of dose rates. Both of these quantities were found to be independent on the dose of gamma radiation (Fig. 2) in the studied range of doses.

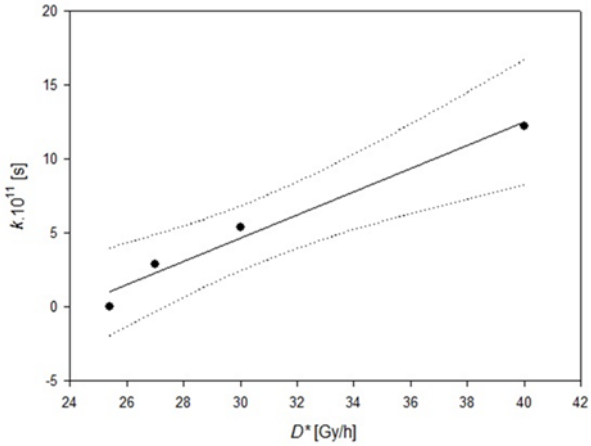

Fig. 1. Dependence of specific radiation protection k on the dose rate D^* of gamma radiation.

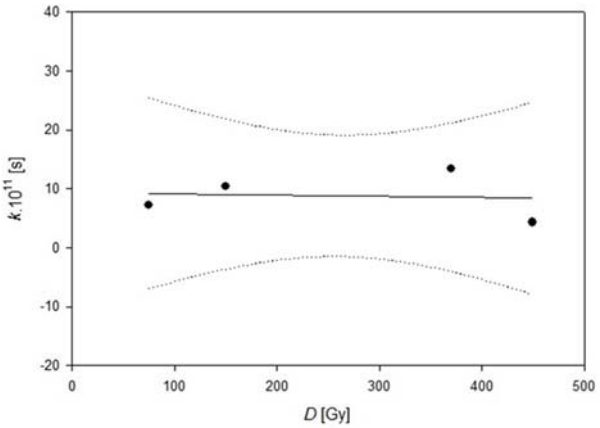

Fig. 2. Dependence of specific radiation protection k on the dose D of gamma radiation.

REFERENCES

[1] Hall, E. J.; Giaccia, A. J. (2006) Radiobiology for the Radiologist, Sixth Edition, Lippincott Williams & Wilkins, Philadeplhia, 546 p.
[2] Pouget, J. P.; Mather, S. J. (2001) Eur. J. Nucl. Med. Mol. Imaging 28, 541-561.
[3] von Sonntag, C. (2006) Free-Radical-Induced DNA Damage and Its Repair: A Chemical Perspective, Springer, 523 p.
[4] Citrina, D. et al. (2010) Oncologist 15, 360-371.
[5] Vrinda, B.; Devi, P. U. (2008) Mutat. Res. Genet. Toxicol. Environ. Mutagen. 498, 39-46.
[6] Chapman, J. D.et al. (1973) Radiat. Res. 56, 291-306.

This research has been supported by the Czech Technical University in Prague, project no. SGS17/195/OHK4/3T/14.

MODIFICATION OF EUKARYOTIC CELLS' RADIATION SENSITIVITY BY VARIOUS HYDROXYL RADICAL SCAVENGERS

Ondrák, L.; Múčka, V.

INTRODUCTION

Ionizing radiation interacts with living cells principally in two ways, directly and indirectly [1]. The direct effect is understood as interaction of radiation with targets (mostly DNA molecules) in the cells causing damage. In case of indirect effect, the cells are attacked by agents produced during radiolysis of water such as hydroxyl, peroxyl or hydroperoxyl free radicals, hydrated electrons etc. [2,3]. The way of cellular damage depends not only on the parameters of irradiation but also, for example, on the type of radiation or hydration of DNA molecule. Because cells are composed of roughly 70 % water, large part of the damage is attributed to an indirect effect of ionizing radiation [4] mainly caused by hydroxyl free radicals originated in the immediate proximity to DNA molecule [3]. Therefore, hydroxyl radical scavengers can influence radiation sensitivity of living cells.

The aim of this work was to study the influence of various scavengers on radiation sensitivity of yeast *Saccharomyces cerevisiae* under gamma irradiation of ^{60}Co at a dose rate of 40 Gy/h with a total absorbed dose of 150 Gy.

EXPERIMENTAL

The microorganism used for the study was yeast *Saccharomyces cerevisiae* (haploid strain, type a, DBM 272; UCT Prague, Czech Republic). *Saccharomyces cerevisiae* cells were cultivated on Sabouard chloramphenicol nutrient agar layer M 1067 (Himedia, India) at 32°C for 5 days. The radiation protection was evaluated by counting of colonies grown up from surviving irradiated or non-irradiated cells in the presence of various concentrations of scavengers (methanol, ethanol, *t*-butanol, isobutanol, pentan-1-ol, dimethyl sulfoxide, acetone, potassium formate and racemic D/L-alanine).

The radiation protection σ was defined as a ratio of natural logarithms of surviving fraction of the cells without (S_0) and with scavenger (S). The specific radiation protection k, i.e. radiation protection based on hydroxyl radical scavenging, was defined as a slope of the dependence of radiation protection σ on a scavenging efficiency Q. The scavenging efficiency Q is defined as a product of scavenger's concentration and the reaction rate constant k_{OH} of the reaction of hydroxyl radical with the scavenger.

RESULTS

It was found that the radiation protection σ of all scavengers linearly increases with increasing scavenging efficiency Q. It means that all scavengers under study act as radioprotectors. The specific radiation protection k hyperbolically decreases with increasing rate constant k_{OH} (Fig. 1) and it linearly rises with increasing concentration c_Q of scavengers at a constant scavenging efficiency Q (Fig. 2). Therefore, the radioprotection seems to be a rather complex process.

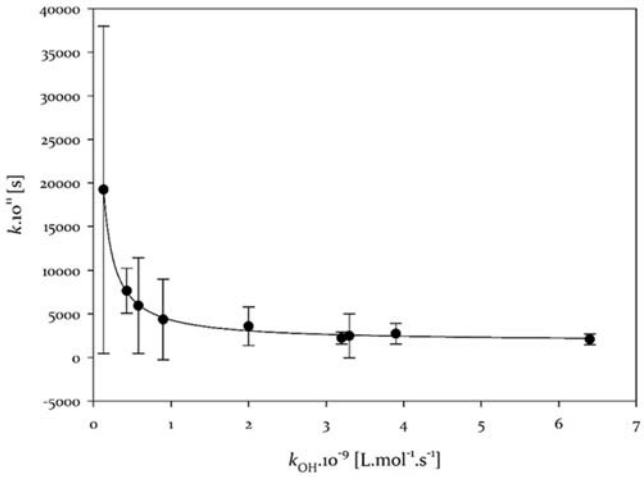

Fig. 1. Dependence of the specific radiation protection k on the reaction rate constant k_{OH} of the reaction of hydroxyl radical with the scavengers.

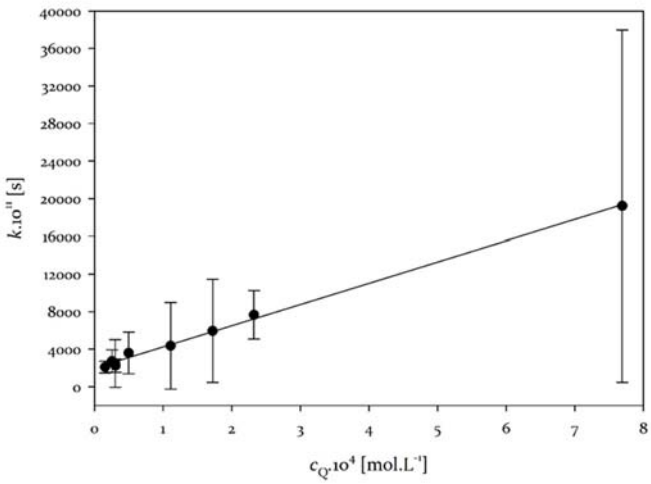

Fig. 2. Dependence of the specific radiation protection k on the concentration c_Q of scavenger at a constant scavenging efficiency Q.

REFERENCES

[1] Hall, E. J.; Giaccia, A. J. (2006) Radiobiology for the Radiologist, Sixth Edition, Lippincott Williams & Wilkins, Philadeplhia, 546 p.

[2] Pouget, J. P.; Mather, S. J. (2001) Eur. J. Nucl. Med. Mol. Imaging, 28, 541-561.

[3] von Sonntag, C. (2006) Free-Radical-Induced DNA Damage and Its Repair: A Chemical Perspective, Springer, 523 p.

[4] Saha, G. B. (2010) Physics and radiobiology of nuclear medicine, Springer Science & Business Media, 334 p.

This research has been supported by the Czech Technical University in Prague, project no. SGS17/195/OHK4/3T/14.

PHOTOINDUCED PREPARATION OF BAND-GAP- AND DEFECT-ENGINEERED GARNET POWDERS

Bárta, J.; Čuba, V.; Jarý, V.[1]; Beitlerová, A.[1]; Pánek, D.[2]; Parkman T.[2]; Nikl, M.[1]

[1]Institute of Physics, AS CR, Czech Republic; [2]Faculty of Biomedical Engineering, CTU in Prague

INTRODUCTION

Synthetic rare-earth garnets, cubic crystalline oxides with general formula $A_3B_2C_3O_{12}$ (A = Ln^{3+} or Y^{3+}; B,C = Al or Ga) are very important luminescent materials or ‚fast' scintillators with reasonably high light yields, using Pr^{3+} or Ce^{3+} as dopants. However, garnet single crystals are usually grown at very high temperatures, which induces a large amount of so-called anti-site defects (such as Lu_{Al} in $Lu_3Al_5O_{12}$: Lu^{3+} located at the B site) – shallow electron traps that decrease the efficiency of scintillation [1]. The effect of anti-site defects can be mitigated by tuning the garnet composition as garnets easily form solid solutions such as $Gd_3(Ga,Al)_5O_{12}$, with Ga lowering the conduction band minimum (band-gap engineering). However, this also increases the probability of thermal ionization from the Ce^{3+} excited state, which is located fairly high in the band gap, and subsequent loss of luminescence intensity.

Another approach to diminish the effect of electron traps is an alternative scintillation mechanism involving purposeful creation of Ce^{4+} (fast electron acceptor) ions by co-doping of garnets by alkali earth metals ions such as Mg^{2+} [2].

EXPERIMENTAL

Solutions containing 3 mmol dm^{-3} Gd^{3+} nitrate doped with 0.2% Ce, 5 mmol dm^{-3} of other trivalent metals nitrates (Ga^{3+}, Al^{3+}), and 0.1 mol dm^{-3} $HCOONH_4$ were irradiated in a water-cooled photochemical reactor (1.5 L) by medium-pressure mercury lamp UVH 1016-6 (power input 380 W) for 4 h. Fine gelatinous material formed during irradiation was filtered by microfiltration (Millipore HAWP filter 0.45 µm) and dried for several days at 40 °C, forming solid precursor. The addition of Mg^{2+} ions into GGAG:Ce,Mg was facilitated by partial substitution of Gd^{3+} ions in the solution prior to irradiation. The solid precursor was then calcined either in a Clasic 0415 vacuum furnace or in the Setaram Labsys Evo thermoanalyzer under air or Ar atmosphere up to 1500 °C.

X-ray powder diffraction using Rigaku MiniFlex 600 diffractometer was employed to check phase composition of the calcined powders and determine the lattice parameters of observed phases. Luminescence spectra of the samples were measured by a custom-made spectrofluorometer Horiba Jobin Yvon 5000 M under various excitation sources, along with photoluminescence decay curves.

RESULTS

An intense exothermic peak in the DTA curve coupled with crystallization of amorphous solid precursors was observed at ~950 °C; however, some samples calcined at 1200 °C still contained phase impurities such as $Gd_3(GaO_4)O_2$. In phase-pure samples prepared at ~ 1300 °C (see Fig. 1), the peaks of the garnet phase shifted with rising Ga content to lower angles, reflecting the increase in lattice parameter. This is caused by a larger size of Ga^{3+} with respect to Al^{3+}; linear increase of lattice parameters conforms to the Vegard's rule.

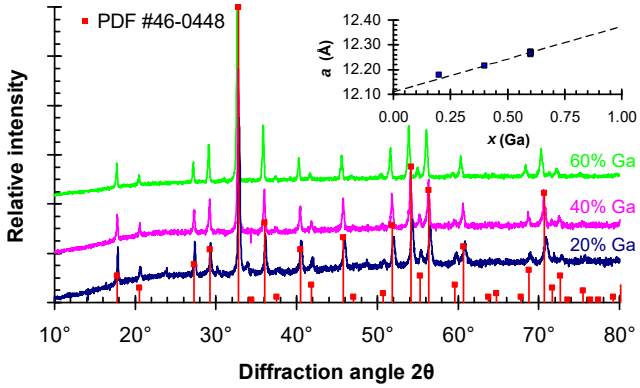

Fig. 1. Diffraction patterns of the prepared GGAG:Ce with different Ga content *x* on the B+C sites [3]. Inset: determined lattice parameters *a* of the GGAG phase compared to the Vegard's rule (dashed line).

Luminescence spectra of the samples are dominated by the Ce^{3+} 5*d* – 4*f* emission around 540 nm (see Fig. 2), which shifts to shorter wavelengths with increasing Ga content. Calcination in air and Mg^{2+} addition were found to have similar effects on the samples: decreasing luminescence intensity (loss of Ce^{3+} ions), smaller excitation peak at 340 nm (increasing Ce^{4+} absorption below ~350 nm) and shorter photoluminescence decay curves.

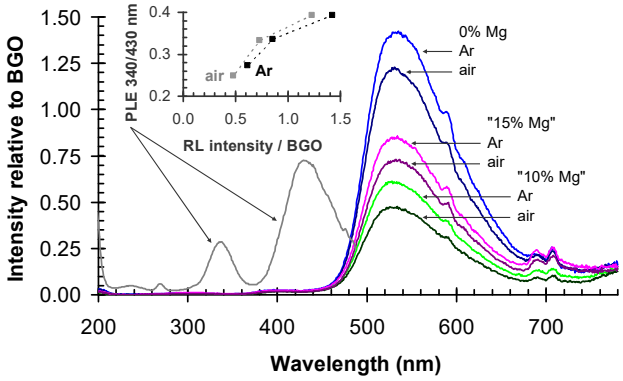

Fig. 2. Radioluminescence spectra of $Gd_3Ga_3Al_2O_{12}$:Ce samples co-doped with Mg ions and/or calcined in oxidizing atmosphere [3]. Inset: intensity ratios of excitation peaks (PLE) for the Ce^{3+} 4*f* - 5*d* transition.

REFERENCES

[1] Nikl, M. et al. (2005) Phys. Status Solidi B 242, R119-R121.

[2] Nikl, M. et al. (2014) Cryst. Growth Des. 14, 4827-4833.

[3] Bárta, J. et al. (2018) IEEE Trans. Nucl. Sci. 65, 2184-2190.

This work was supported by the Czech Science Foundation grant GA17-06479S, the Czech Technical University project SGS17/195/OHK4/3T/14 and the Technology Agency of the Czech Republic project TG02010033.

SOL-GEL PREPARATION OF HIGHLY LUMINESCENT Ce-DOPED YSO/LSO MICROCRYSTALS

Popovich, K.; Šípková, M.; Čuba, V.; Procházková, L.; Bárta, J.; Nikl, M.[1]

[1]Institute of Physics, AS CR, Czech Republic

INTRODUCTION

Due to their properties, rare-earth-doped yttrium and lutetium oxyorthosilicates (Y_2SiO_5, YSO; Lu_2SiO_5, LSO) are used in a wide range of applications, such as LEDs manufacture [1], medical and high energy physics [2] and many others [3]. These materials are usually available as bulk single crystals grown by very expensive Czochralski method [4].

Sol-gel technique is extensively used for the preparation of pure materials under room temperature for diverse applications. This method is based on hydrolysis and polycondensation of alkoxides (in this case silicon alkoxide), leading to formation of colloidal particles.

In this work, we present results of the preparation of YSO/LSO microcrystals with good luminescent properties via sol-gel route, having their prospective fast-timing application in mind.

EXPERIMENTAL

Precursor for YSO/LSO was prepared using the sol-gel method at room temperature. Firstly, $Y(NO_3)_3$ or $Lu(NO_3)_3 \cdot xH_2O$ and $Ce(NO_3)_3 \cdot 6H_2O$ were dissolved in distilled water. Separately, ethanolic solution containing TEOS (tetraethylorthosilicate) was prepared. Both solutions were then mixed and an aqueous solution of NH_3 was added dropwise to the reaction mixture. The suspension was stirred and subsequently dried in air. The prepared precursor was powdered and thermally treated up to 1300 °C.

The size of YSO:Ce microcrystals was reduced by grinding in a vibration ball mill and fractionalization process.

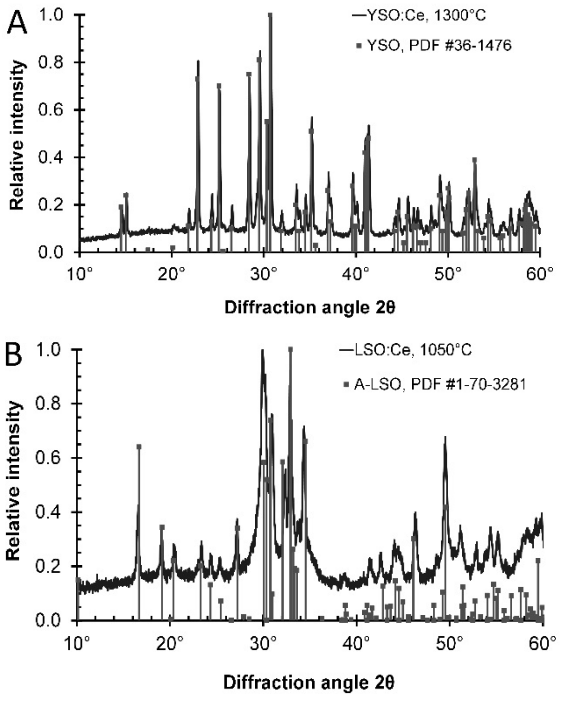

Fig. 1. Diffractograms of YSO:Ce (A) and LSO:Ce (B) compared to records from the ICDD PDF-2 database.

RESULTS

X-ray diffraction analysis (Fig. 1) shows that the diffraction patterns are in good agreement with the ICDD PDF-2 database records of YSO, A-LSO and B-LSO. Along with B-LSO, a separate phase of Lu_2O_3 was also observed.

Room temperature radioluminescence spectra of the samples (Fig. 2, 3) show a typical broad emission band in the range of 350-600 nm caused by $5d - 4f$ transition of Ce^{3+} ions. Both YSO:Ce and LSO:Ce samples show higher emission intensity than the powder BGO ($Bi_4Ge_3O_{12}$) reference scintillator. Spectral analysis of the small particles fraction of YSO:Ce indicates that their emission intensity was not significantly influenced by the size reduction process.

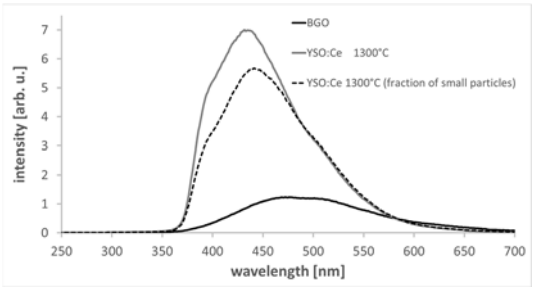

Fig. 2. Room temperature radioluminescence spectra of the YSO:Ce^{3+} sample.

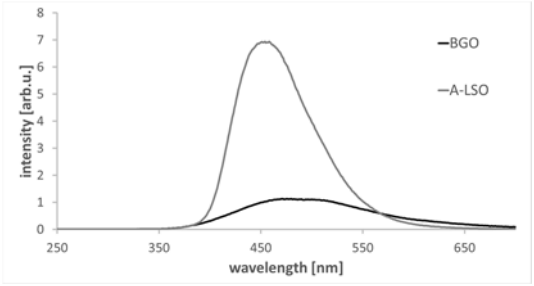

Fig. 3. Room temperature radioluminescence spectra of the LSO:Ce^{3+} sample.

REFERENCES

[1] Chiriu, D. et al. (2016) Mater. Chem. Phys. 171, 201-207.
[2] Fan, L. et al. (2016) Chem. Phys. Lett. 644, 41-44.
[3] Ren, G. et al. (2004) Nucl. Instr. Meth. Phys. Res. A 531, 560-565.
[4] Melcher, C. L. et al. (1992) IEEE Trans. Nucl. Sci. 39, 502-505.
[5] Popovich, K. et al. (2019) Radiat. Meas. 122, 84-90.

This work was supported by the Czech Science Foundation [GA17-0647S], Grant Agency of the CTU in Prague, [SGS17/195/OHK4/3T/14], the Ministry of the Interior of the Czech Republic [VI20172020106]; and the Ministry of Education of Youth and Sports of the Czech Republic [CZ.02.1.01/0.0/0.0/16_019/0000778].

*Full paper in [5].

NANOHYBRID SYSTEMS BASED ON LuAG:Pr^{3+} NANOPARTICLES FOR PDTX

Popovich, K.; Tomanová, K.; Čuba, V.; Procházková, L.; Pelikánová, I.T.; Jakubec, I.[1]; Mihóková, E.[2]; Nikl, M.[2]

[1]Institute of Inorganic Chemistry, AS CR, Czech Republic; [2]Institute of Physics, AS CR, Czech Republic

INTRODUCTION

X-ray induced photodynamic therapy (PDTX) is a modern method for cancer treatment, which uses tumor-destroying agents based on scintillating nanoparticles (NP) conjugated with photosensitizer (PS) molecules. The agent accumulates preferentially in the target cells; X-ray irradiation leads to the excitation of NP and emission of secondary radiation, which is subsequently absorbed by PS molecules. Their deexcitation via non-radiative energy transfer (ET) results in the production of very cytotoxic singlet oxygen [1].

In this work, we present a concept of preparation of LuAG:Pr^{3+}@SiO_2-PpIX nanocomposite for application in PDTX. Core for nanocomposite was prepared by photo-induced method; subsequently, surface of nanoparticles was coated by amorphous SiO_2 shell via sol-gel method. Finally, LuAG:Pr^{3+}@SiO_2 NPs were conjugated with a PS molecule. By methods of optical spectroscopy, we demonstrated the presence of non-radiative energy transfer between the core and PS outer layer.

EXPERIMENTAL

Preparation procedure of the nanocomposite material includes three main steps:

synthesis of the core (LuAG:Pr^{3+}) by photo-induced method [2];

encapsulation in amorphous silica shell using modified sol-gel process described by Liu et al. [3];

conjugation of the silica-coated nanoparticle with a PS molecule (protoporphyrin IX) [4].

As a result, three-layer nanocomposite is formed (Fig. 1).

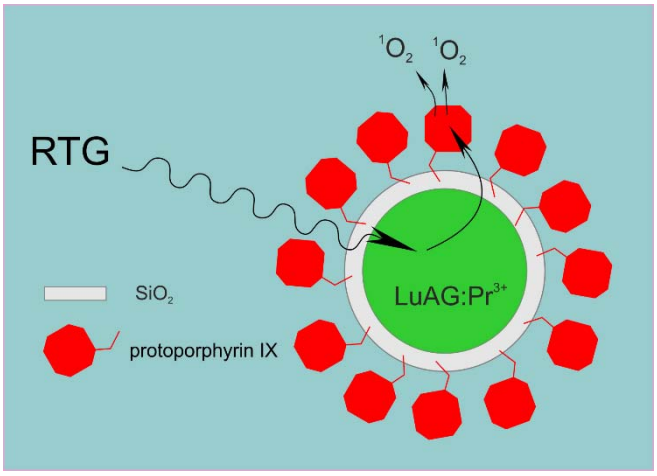

Fig. 1. Schematic illustration of the PDTX nanocomposite and principle of singlet oxygen production.

RESULTS

Radioluminescence emission (RL) spectra of LuAG:Pr^{3+}, LuAG:Pr^{3+}@SiO_2 and LuAG:Pr^{3+}@SiO_2-PpIX samples (Fig. 2) manifest emission bands associated with $5d$ – $4f$ and $4f$ – $4f$ transitions of Pr^{3+} in UV and visible spectral region, respectively. The shape and intensity of the spectra were not influenced by SiO_2 surface modification, but a dramatic decrease of luminescence intensity in the LuAG:Pr^{3+}@SiO_2-PpIX spectrum confirms non-radiative ET from the NP core to PpIX outer layer, as a prerequisite for $^1O_2$ generation.

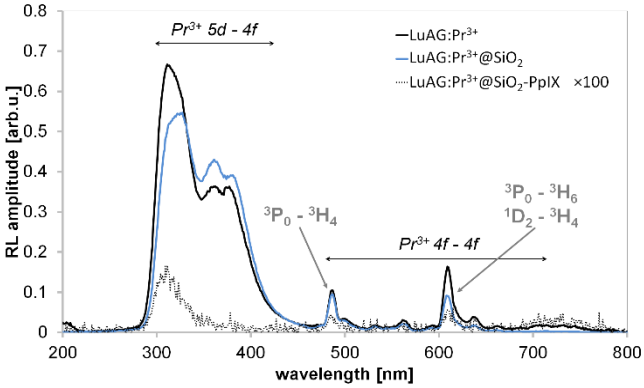

Fig. 2. Room temperature RL spectra of the LuAG:Pr^{3+}, LuAG:Pr^{3+}@SiO_2 and LuAG:Pr^{3+}@SiO_2-PpIX.

In the photoluminescence (PL) emission spectra of the LuAG:Pr^{3+}@SiO_2-PpIX sample (Fig. 3), it was observed that excitation of Pr^{3+} results in red PpIX emission. ET was also confirmed by excitation of the sample at the PpIX Soret band at 410 nm.

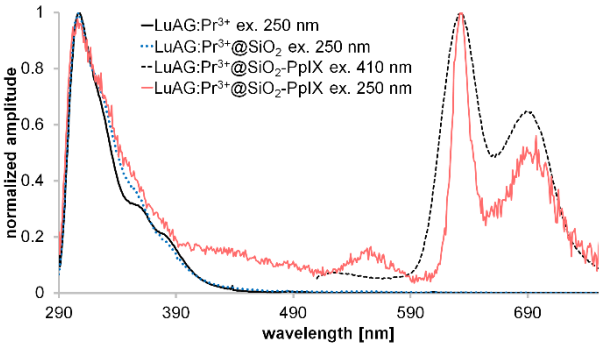

Fig. 3. Room temperature PL emission spectra under excitation at 250 nm (LuAG:Pr^{3+}@SiO_2 and LuAG:Pr^{3+}@SiO_2-PpIX samples) and 410 nm (LuAG:Pr^{3+}@SiO_2-PpIX sample).

REFERENCES

[1] Bulin, A.-L. et al. (2013) J. Phys. Chem. C 117, 21583-21589.

[2] Bárta, J. et al. (2012) J. Mater. Chem. 22, 16590-16597.

[3] Liu, Q. et al. (1998) Chem. Mater. 10, 3936-3940.

[4] Nowostawska, M. et al. (2011) J. Nanobiotechnol. 9, 13.

[5] Popovich, K. et al. (2018) J. Photochem. Photobiol. 179, 149-155.

This work was supported by the Czech Science Foundation grant no. GA17-0647S and by the Grant Agency of the CTU in Prague project no. SGS17/195/OHK4/3T/14.

*Full paper in [5].

RADIATION-INDUCED PREPARATION OF ZnO:Ga-BASED SCINTILLATORS WITH BAND GAP MODULATION

Procházková, L.; Čuba, V.; Beitlerová, A.[1]; Jarý, V.[1]; Omelkov, S.[2]; Nikl, M.[1]

[1]Institute of Physics, AS CR, Czech Republic; [2]Institute of Physics, University of Tartu, Estonia

INTRODUCTION

Zinc oxide is known for its outstanding optoelectronic features: wide direct band gap (3.4 eV), extremely large exciton binding energy (60 meV), sub-nanosecond luminescence lifetime and low afterglow. Pure ZnO naturally has a strong defect-related emission in visible spectral range and may exhibit weak exciton-related emission in UV.

The principle of band gap modulation in (Zn,Cd/Mg)O:Ga is to shift the bottom edge of the conduction band by affecting the energy levels of 2p levels of Zn^{2+} and composition of the conduction band minimum by admixture of specific isovalent ions such as Cd^{2+} or Mg^{2+} and their energy levels.

While the exceptional properties together with high radiation stability predetermine the scintillators based on ZnO:Ga as perspective materials for high-energy physics (HEP) detectors and time-of-flight detectors e.g. in positron emission tomography (TOF-PET), band gap modulation allows to change the emission band position of the scintillating nanoparticle and increased overlap with the absorption band of a photosensitizer used for $^1O_2$ production.

EXPERIMENTAL

Preparation of Zn(Mg,Cd)O:Ga scintillators was based on our previous work [1] via photochemical synthesis. Irradiation of solutions was performed using low pressure mercury lamps (total power: 100 W). Formed solid phase was decomposed at 250 °C in air, followed by two-step heat treatment at 950 or 1000 °C in air and additional treatment at 800 °C under the Ar/H_2 (10:1) atmosphere.

For phase purity confirmation, X-ray diffraction (XRD; Rigaku MiniFlex 600) was used. X-ray fluorescence (XRF) spectra were recorded by Niton XL3t 900 GOLDD analyzer. In the case of CdO presence, the weight ratio between wurtzite ZnO and cubic rock-salt CdO phase was estimated via RIR method. Luminescence properties were evaluated by measuring photo- and radioluminescence (PL, RL) emission spectra using Horiba Jobin Yvon 5000M spectrofluorometer equipped with nanoLED 339 nm and Seifert X-ray tube as the excitation source. Detection part consists of a single grating monochromator and TBX-04 photomultiplier tube (IBH Scotland).

RESULTS

UV-irradiation led to the formation of mixed zinc cadmium peroxide crystalline phase with no separation of the phases, in the whole range of Cd concentrations. After heat treatment at 250 °C, only wurtzite phase of (Zn,Cd)O was observed. The precipitation of Cd^{2+} ions in the form of $(Zn,Cd)O_2$ is not quantitative, but correlates with the Cd content in the irradiated solutions. XRF elemental analysis shows that the Cd concentration in the solid phase is significantly lower. We used the XRF in combination with XRD and Vegard's law (using calculated lattice parameters) to estimate the real Cd content incorporated in the ZnO structure (Fig. 1). A shift of diffraction peaks (Fig. 2) together with a strong band gap modulation (Fig. 3) provides firm evidence of the incorporation of Cd or Mg into the ZnO structure. Significant blue or red shift of emission maxima was obtained with 13 mol % of Cd or Mg ions, without any emission in the visible spectral range. It was shown that the UV emission can be shifted between 376 and 425 nm.

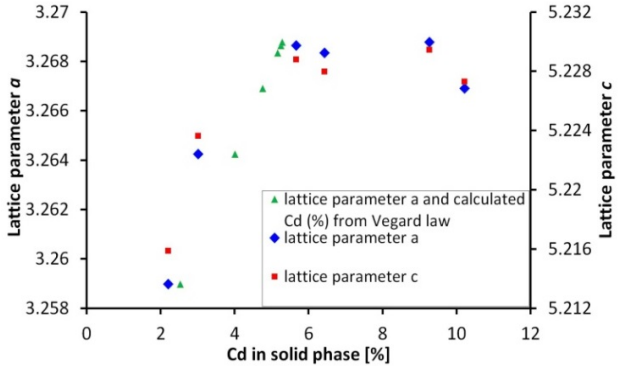

Fig. 1. Plot of lattice parameters *a* and *c* versus Cd concentration estimated from XRD and XRF or Cd concentration calculated from Vegard's law [2].

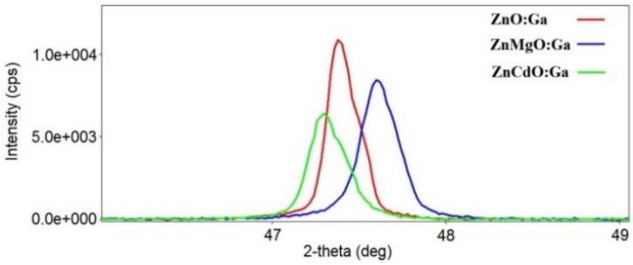

Fig. 2. Diffraction peaks (1 0 2) with a noticeable shift for (Zn,Cd)O:Ga, ZnO:Ga and (Zn,Mg)O:Ga [2].

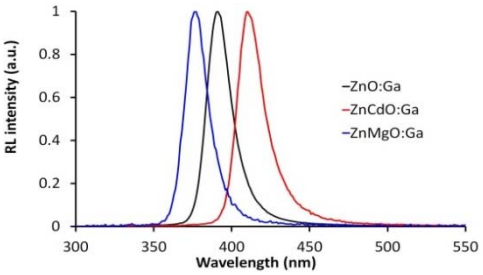

Fig. 3. RL emission manifesting red ($Zn_{0.87}Cd_{0.13}O$:Ga) and blue (ZnMgO:Ga) shift [2].

REFERENCES

[1] Procházková, L. et al. (2015) Opt. Mater. 47, 67-71.
[2] Procházková, L. et al. (2018) Opt. Express 26, 29482-29494.

This research has been supported by the Czech Science Foundation grant GA13-09876S and by the Czech Technical University in Prague grant SGS14/207/OHK4/3T/14.

NANOPLATINUM PREPARATION BY IRRADIATION METHODS IN MICELLAR SYSTEMS

Silber, R.; Beck, P.; Čamra, M.[1]

[1]Tesla V.T. Mikroel, Czech Republic

INTRODUCTION

Metal nanoparticles such as nanoplatinum, both pure and in bimetallic particles, are synthesized and studied for their many and varied applications. In recent years, many methods have been developed to prepare particles with specific sizes, morphologies and composition, which have a very wide range of potential applications [1]. The preparation of platinum nanoparticles using irradiation of aqueous solutions by ionizing radiation offers the possibility to control the size and yield of formed nanoparticles by applied dose of radiation or dose rate. The main products of water radiolysis are ·H and OH radicals; the latter have to be scavenged by some additives to prevent oxidation reactions. In this work, solutions of Pt(IV) and nonionic surfactant Triton X-100, which also serves as ·OH radical scavengers, were irradiated by accelerated electron beam.

EXPERIMENTAL

The solution for nanoplatinum radiation synthesis was prepared according to the following procedure: aqueous solution of the Triton X-100 surfactant was prepared at the desired concentration (2 wt. %) by adding the liquid Triton X-100 to water and continuous mixing for about 1 hour until a homogenous solution was formed. Solid $PtCl_4$ was then dissolved in the vigorously stirred solution. Samples were stored in the dark to shield them from the effects of UV light present in natural sunlight. The solutions were irradiated by a pulsed radiofrequency linear electron accelerator LINAC 4-1200 (mean electron energy 4 MeV) at doses 2 to 24 kGy.

UV/Vis absorption spectra were recorded on Genesys 20 and double-beam Varian Cary 100 spectrophotometers, powder X-ray diffraction analysis was measured using Rigaku MiniFlex 600.

RESULTS

UV/VIS optical absorption spectra for 0.01 mol.L^{-1} $PtCl_4$ samples irradiated with various doses are shown in Fig. 1.

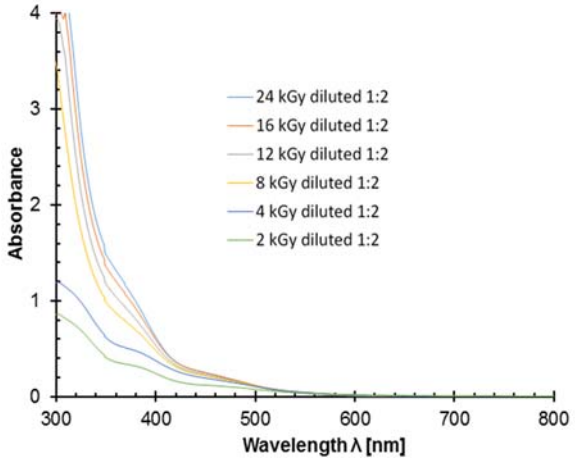

Fig. 1. UV/VIS spectra for solutions containing 10 mM $PtCl_4$ and 2 wt. % Triton X-100 irradiated by doses between 2 and 24 kGy.

The increasing absorbance corresponds to the gradual formation of Pt nanoparticles. The surface plasmon peak at ~ 215 nm is masked by a very strong absorbance of the Triton X-100 surfactant in this region. TEM micrograph shown in Fig. 2 corroborates with results of photon cross correlation spectrometry and indicates that platinum nanoparticles occur in nanometre-sized units. Some larger particles were also observed, probably due to the aggregation of nanoparticles into larger units.

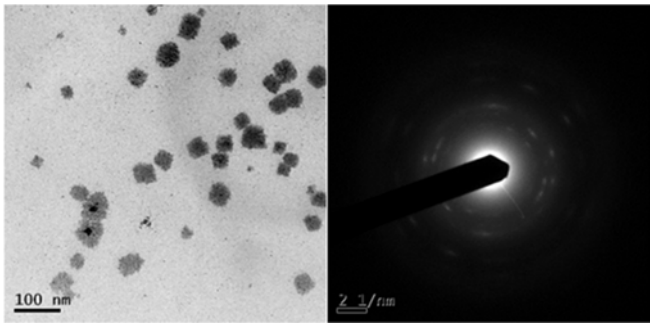

Fig. 2. TEM micrograph and electron diffraction pattern of the nanoplatinum prepared by irradiation of solution containing 0.1 mol.L^{-1} $PtCl_4$ and 2 wt. % of Triton X-100 by electron beam (absorbed dose 6 kGy).

Due to small size of Pt particles, filtration or other separation methods were unsuitable. Therefore, irradiated solution was soaked into PVDF filtration membrane, which was not soluble in Triton X-100, and dried. In Fig. 3, the diffractogram of such membrane with dried sample is shown and compared to virgin membrane. The difference diffraction pattern shows broad peaks consistent with cubic platinum.

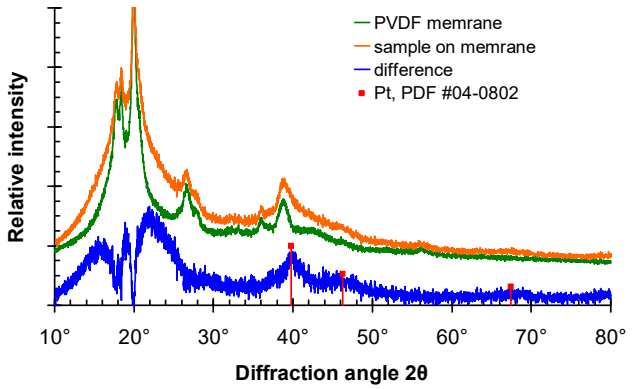

Fig. 3. Diffractogram of PVDF filtration membrane soaked with solution containing 2 mM $PtCl_4$ and 2 wt. % of Triton X-100 irradiated with a dose of 8 kGy.

REFERENCES

[1] Chen, A.; Holt-Hindle, P. (2010) Chem. Rev. 110, 3767-3804.

This research has been supported by the Ministry of Industry and Trade of the Czech Republic, grant no. FV30139.

SORPTION PROPERTIES OF SELECTED OXIDIC NANOPARTICLES FOR THE TREATMENT OF SPENT DECONTAMINATION SOLUTIONS BASED ON CITRIC ACID

Fišera, O.[1]; Kareš, J.[1]; Procházková, L.; Popovich, K.; Bárta, J.; Čuba, V.

[1]Division of the Chemical, Biological, Radiological and Nuclear Protection, Military Research Institute, Czech Republic

INTRODUCTION

Spent decontamination solutions used by units dealing with Chemical, Biological, Radiological and Nuclear (CBRN) response are treated as hazardous radioactive liquid waste. The main active components of decontamination solutions are usually complexing or chelating agents (citric acid, oxalic acid, EDTA, NTA, etc.) and surfactants. The large volume of the liquid waste might be reduced when using effective sorption materials. Prospective sorption materials should be sufficiently chemically and radiation stable and feature high specific surface area.

Nanoparticles of metal oxides with high specific surface area were tested for the separation of selected radionuclides (^{241}Am, ^{60}Co, ^{137}Cs and ^{90}Sr) from simulated spent decontamination solutions containing citric acid. The following materials, prepared via photoinduced synthesis, were tested: NiO, NiO/TiO_2 and ZnO:Cu. Buffer solutions with a concentration of citric anions equal to 0.01 mol l^{-1} were used in the tests. Sorption properties were investigated in pH range 2–12. Additionally, the influence of surfactants on the sorption was studied.

EXPERIMENTAL

Sorption properties of the sorbents were studied according to the following procedure: 40 mg of solid phase was contacted with 10 ml of simulated decontamination solution as liquid phase (V/m = 250 ml g^{-1}) in a 50 ml polyethylene bottle for 2 hours. The mixture was shaken on linear laboratory shaker IKA 260 HS (IKA, USA) at 150 rpm. Aliquots of 7 ml were introduced into test-tubes and centrifuged on CompactStar CS4 (VWR, USA) for 5 minutes at 3400 RCF (6000 rpm).

Efficiency of phase separation was checked during experiments. Transmittance of the centrifuged solutions was also measured and subsequently, 4 ml aliquot of the centrifuged solution was taken for measurement. 4 ml samples of simulated decontamination solutions before the contact of phases were used as activity standards.

Activity measurements of standards (A_0) and samples (A) were performed on a HPGe detector equipped with multichannel analyzer Inspector 2000 (Canberra, USA) for ^{241}Am, ^{137}Cs and ^{60}Co. Activity of ^{90}Sr was measured via Cherenkov radiation on a liquid scintillation counter Triathler (Hidex, Finland).

Kinetics of sorption was also studied for ^{241}Am at pH = 8.3 under conditions described above, but with a variable time of contact in the shaker. Effects of surfactants and other active components were also studied, with the composition of solutions corresponding to those in use by the units dealing with CBRN response [1].

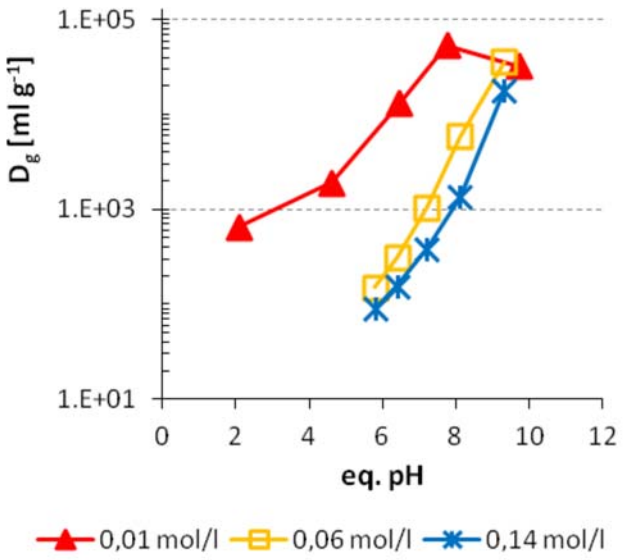

Fig. 1. The effect of citrate concentration on the sorption of ^{90}Sr by NiO/TiO_2; aqueous phase: 0.01 mol l^{-1} citrate buffer, carrier concentration approx. 1 × 10^{-8} mol l^{-1}, V/m = 250 ml g^{-1}, $D_{g,min}$ = 10 ml g^{-1} [2].

RESULTS

Of all nanosorbents under study, NiO/TiO_2 nanocomposite proved to be the most prospective. High retention over 85 % was achieved for all radionuclides with nanosorbent NiO/TiO_2 in the presence of citrate at a concentration of 0.01 mol l^{-1}. Increasing citrate concentration strongly decreased distribution factors (Fig. 1). For ^{241}Am and ^{90}Sr, the retention was approx. 99 %. Sorption of radionuclides was strongly affected by the presence of surfactants and also by a higher concentration of complexing agents. Kinetics of uptake was very fast as expected due to the form of nanoparticles. A further study should be concentrated on the elimination or suppression of surfactants influence; for that, photocatalytic properties of materials tested could be possibly utilized. Final procedure for treatment of spent decontamination solutions based on citric acid will be tested with real-life solutions originated from radiological emergency response exercise.

REFERENCES

[2] Decontamination of radioactive substances. Combat Fire Regulations - Tactical Procedures. (in Czech) http://www.hzscr.cz/soubor/l9-dekontaminace-ral-pdf.aspx. Accessed 17 Mar 2017.

[3] Fišera, O. et al. (2018) J. Radioanal. Nucl. Chem. 318, 2443-2448.

* Full paper in [2].

AFTERGLOW AND QUANTUM TUNNELING IN Ce-DOPED LUTETIUM ALUMINUM GARNET

Mihóková, E.[1]; Babin, V.[1]; Pejchal, J.[1]; Čuba, V.; Bárta, J.; Popovich, K.; Schulman, L. S.[2]; Yoshikawa, A.[3]; Nikl, M.[1]

[1]Institute of Physics, AS CR, Czech Republic; [2]Physics Department, Clarkson University, USA; [3]Institute for Materials Research & NICHe, Tohoku University, Japan

INTRODUCTION

A tunneling process can significantly affect the dynamics of a luminescence center excited state and consequently also the performance of luminescence materials. Its effectiveness strongly depends on the distance between the luminescence center and the host trap. Quantum tunneling was suggested to be a cause of "anomalous fading". This phenomenon was observed some time ago in the luminescence decay of various materials used in thermally and optically stimulated luminescence dating [1]. Calculations based on tunneling between recombination centers and traps at randomly distributed distances provide an inverse power-law decay of luminescence over many orders of magnitude [2]. An alternative explanation of anomalous fading can be given by models of localized or semilocalized transitions regarding hole-electron pairs in irradiated materials.

In the present work, the quantum tunneling was studied by a modified afterglow measurement. We monitored the afterglow signal and searched for an inverse power-law decay, but unlike the usual afterglow measurement, the excitation by ionizing radiation was not used. Rather, using a continuous light source, we selectively excited directly into the $4f$-$5d_1$ Ce^{3+} absorption band.

EXPERIMENTAL

LuAG:Ce pellet was fabricated from a photochemically synthesized solid precursor nanopowder calcined at 900 °C by pressing in a manual laboratory press and subsequent sintration at 1450 °C in mild vacuum. Photoluminescence emission (PL) and excitation (PLE) spectra were excited with a deuterium steady-state lamp and detected by a custom made Horiba Jobin Yvon 5000M spectrofluorometer. The afterglow measurement was performed in the same setup. The sample was irradiated by a deuterium steady-state lamp for about 15 minutes with excitation monochromator set at 447 nm and a filter to block the light from second order diffraction. After the excitation cut-off, the spectrally unresolved decay signal was monitored by a TBX-04 photon counting detector (IBH Scotland). The measurement was performed at various temperatures in an interval within the temperature range 77-400 K. The temperature of the sample was controlled by a Janis cryostat.

Thermally stimulated luminescence (TSL) measurements in the 77-700 K temperature range were performed with a heating rate of 6 K/min after irradiation at 77 K. The temperature was controlled by a Janis cryostat. X-ray irradiation was realized with a Seifert X-ray tube operated at 40 kV and 15 mA. The TSL signal was detected by a TBX-04 detector (IBH, Scotland) coupled to a monochromator (Horiba Jobin Yvon). TSL curves were registered by a monochromator at zero order.

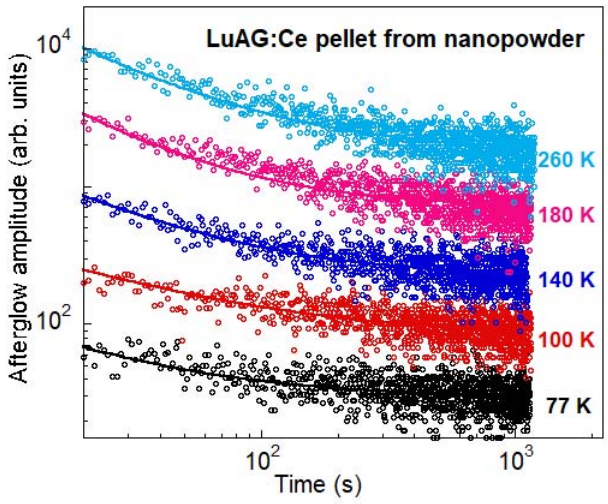

Fig. 1. Afterglow of the LuAG:Ce pellet prepared from nanopowder. Empty symbols represent experimental data, solid lines are power-law fits to the data [3].

RESULTS

In the delayed recombination decay measurement, the quantum tunneling is manifested by a constant non-zero slow decay intensity within a certain temperature range. In the afterglow measurement (such as that presented in this work) the quantum tunneling is manifested by a slow decay that can be fitted by the inverse power-law formula with an exponent close to one.

Similar to LuAG:Ce single crystals, the afterglow of LuAG:Ce pellet prepared from nanopowder (Fig. 1) could be fitted a power-law exponent close to 1 up to a temperature of about 250 K. The power-law exponents of the fits presented in Fig. 1 are, in order of increasing temperatures, $m = 1.01$, 1.09, 0.98, 0.81, and 0.88, respectively.

Thus, it was confirmed that at temperatures up to 200-250 K, the quantum tunneling is the process responsible for the afterglow signal.

REFERENCES

[1] Visocekas, R. et al. (1976) Phys. Status Solidi A 35, 315-327.

[2] Huntley, D. J. (2006) J. Phys.: Condens. Matter 18, 1359-1365.

[3] Mihóková, E. et al. (2018) IEEE Trans. Nucl. Sci. 65, 2085-2089.

* A brief summary of research fully reported in [3].

MATERIAL CHARACTERIZATION OF GARNET CRYSTALS FORMED BY MICRO-PULLING-DOWN METHOD

Pejchal, J.[1]; Bárta, J.; Guguschev, C.[2]; Buryi, M.[1]; Babin, V.[1]; Nikl, M.[1]

[1] Institute of Physics, AS CR, Czech Republic; [2] Leibniz-Institut für Kristallzüchtung, Germany

INTRODUCTION

Single crystals of oxides used for scintillator materials are often grown from the melt at very high temperatures using Czochralski technique, which usually takes more than one week. Additionally, the melt is always in equilibrium with the growing crystal, leading to high segregation coefficients for dopants. These disadvantages may be avoided with a micro-pulling-down method (μ-PD), which has been used at the Institute of Physics, AS CR since 2015. In this method, radiofrequency heating is employed to heat iridium crucible with a shaping die on its bottom and an afterheater (Fig. 1). The melt from the crucible flows through a capillary in the die and comes into contact with a single-crystalline seed that is constantly pulled down. Due to a relatively high growth speed (~0.1 mm/min), segregation coefficient is less pronounced and crystal growth is finished within 1 day. Structural and elemental characterization of some crystals was done at the Department of Nuclear Chemistry [1,2].

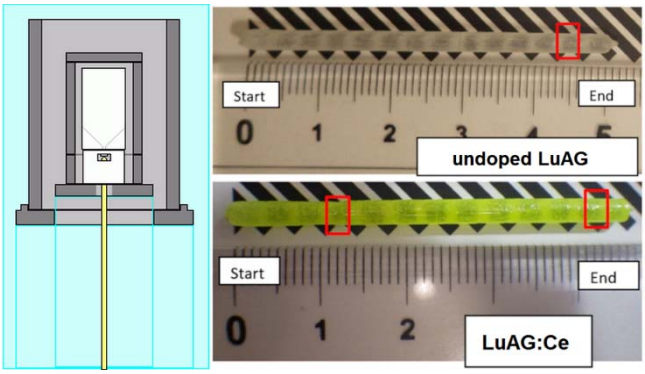

Fig. 1. Schematic representation of the hot zone for μ-PD crystal growth (left; white: Ir, gray: ceramics, blue: fused silica) and grown $Lu_3Al_5O_{12}$ crystals (right).

EXPERIMENTAL

Various LuAG and LuGAG ($Lu_3Ga_3Al_2O_{12}$) single crystals were grown using Akita Seiko T-MPD-OX μ-PD apparatus with iridium crucibles (3 mm circular die) from a mixture of constituent oxides. Argon atmosphere was used for LuAG, whereas a mixture of Ar with ~1% O_2 was employed for LuGAG growth to suppress Ga_2O_3 decomposition and evaporation. Selected parts of the crystal rods were then cut and characterized by X-ray fluorescence analysis (Niton XL3t 900 GOLDD; evolution of elemental composition during the growth) and, after grinding into a powder in agate mortar, by X-ray diffraction (Rigaku MiniFlex 600; phase purity assessment, determination of lattice parameters).

RESULTS

In the LuAG-based single crystals, only a single garnet phase consistent with $Lu_3Al_5O_{12}$ was found [1], but in some non-stoichiometric samples, admixtures such as Al_2O_3 or $Lu_4Al_2O_9$ were also detected [2]. The Al/Lu ratio slightly increased along the growing crystals, probably because of the tendency of LuAG to form Lu-rich garnet phase, whereas dopant concentrations remained almost constant. In the LuGAG crystals, Ar+O_2 atmosphere was found to be necessary, even though it degrades the iridium crucible (IrO_2 forms, which decomposes and deposits Ir elsewhere). When no oxygen was added to the argon, Ga content sharply decreased along the growing crystal and a separate Lu_2O_3 phase appeared near the end part due to imbalance of Lu and Al+Ga in the melt (see Fig. 2). In the Ar+1% O_2 atmosphere, this behaviour was significantly suppressed.

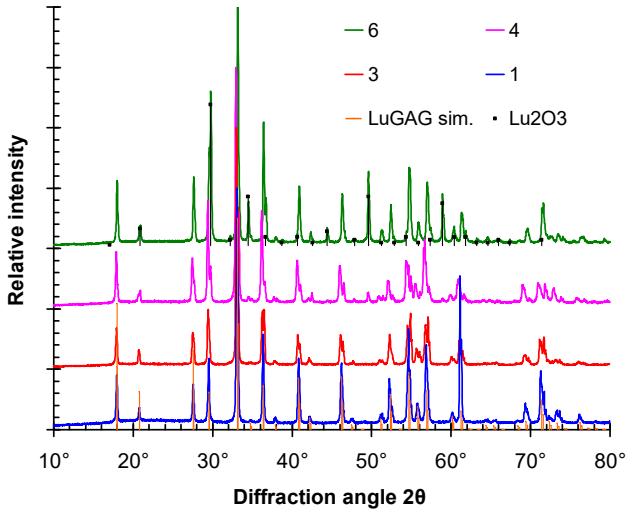

Fig. 2. Diffraction patterns of powdered LuGAG crystal parts (numbers increase from Start to End) grown in a pure Ar atmosphere [2].

In most powdered LuGAG crystal parts, the presence of several distinct garnet phases was detected (see Fig. 3) and the Energy Dispersive Laue Mapping (EDLM) of the cut crystals revealed that the rods are not single-crystalline, but composed of many different grains and sub-grains. Micro-XRF measurements revealed that Ga content increases toward the surface of the crystal rod. The main cause might be different behaviour during the radial flow from the capillary to the whole surface area of the die.

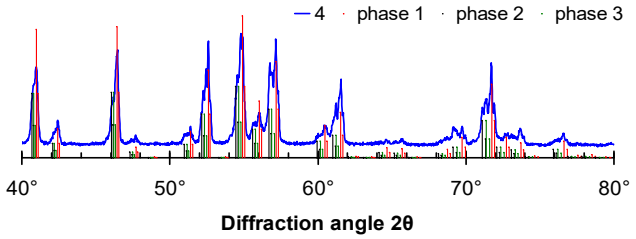

Fig. 3. Detail of a LuGAG diffraction pattern indicating the presence of several slightly different garnet phases.

REFERENCES

[1] Pejchal, J. et al. (2017) J. Lumin. 181, 277-285.
[2] Pejchal, J. et al. (2018) Opt. Mater. 86, 213-232.

* Compilation based on papers [1] and [2].

CIRCADIAN LIGHT SOURCE BASED ON $K_XNa_{1-X}LuS_2:Eu^{2+}$ PHOSPHOR

Jarý, V.[1]; Havlák, L.[1]; Bárta, J.; Rejman, M.[1]; Bystřický, A.[1]; Dujardin, C.[2]; Ledoux, G.[2]; Nikl, M.[1]

[1]Institute of Physics, AS CR, Czech Republic, [2]Institut Lumière Matière, Université Lyon 1, France

INTRODUCTION

A relatively unexplored family of luminescence materials based on ternary sulphides $ALnS_2$ (A = alkali metals; Ln = lanthanides, Y, Sc) has been recently studied in a fruitful cooperation between Department of Nuclear Chemistry and Institute of Physics, AS CR. Doping of $KLuS_2$ host with Eu was found to result into stable Eu^{2+} centers with broad emission bands in the green spectral region [1]. Using other A and Ln elements, this emission band could be shifted to any part of the visible spectrum. Synthesis from the mixture of K and Na carbonates yielded mixed $(K,Na)LuS_2$ crystals with $NaLuS_2$-like red emission, $KLuS_2$-like green emission or intermediate states, which could be excited differently in the blue or near UV spectral region [2]. This opened the possibility to use this material in circadian light sources, when excited by blue and UV LED diodes. The colour of the resulting light, composed of transmitted excitation light and emitted light can be tuned from reddish hues to white in accordance with the human circadian rhythm [3].

EXPERIMENTAL

Thin platelets of rhombohedral $(K,Na)LuS_2$ were prepared at 1000 °C in a tube furnace from the melt of alkali metal carbonates and Eu-doped Lu_2O_3 within H_2S atmosphere. The formed crystals were obtained by washing of the reaction product with water and manually separated into two fractions: of bigger platelets (up to 3×3×0.2 mm) and smaller platelets. K/Na ratio was estimated using XRF analysis (Niton XL3t 900 GOLDD) and independently from the lattice parameter *c* by X-ray diffraction analysis (Rigaku MiniFlex 600). The platelets were placed into a self-made circadian light source (composed of three 1 W nearUV LEDs at 380 nm and one 3 W blue LED at 460 nm) and the overall emission spectrum was recorded using Ocean Optics QE65000 spectrometer with CCD detector. Quantification of the resulting colour properties was made using CIE 1931 chromacity diagram, Colour Rendering Index (CRI) and Colour Quality Scale (CQS) metrics.

RESULTS

A wide range of $(K,Na)LuS_2$:Eu samples was investigated, with melt composition having huge effect on the crystal properties. Smaller and bigger crystals from each batch were also found to have different compositions (K/Na ratio). The spectrum of the circadian source depended not only on the sample chosen, but also on independently controlled LED power settings (see Fig. 1), requiring a very large amount of measurements. Some recorded spectra converted into a colour perceived by average human eye are shown in Fig. 2 as white dots connected by a line indicating each sample (samples description in [3]). Changing power settings thus allows for a good tuneability of light colour. The best ability of the light source to truthfully show the perceived colour of any object was obtained in the $K_{0.65}Na_{0.35}LuS_2:Eu^{2+}$ sample (1s in Fig. 2), for which the maximum values of CQS = 82.5 and CRI = 87.2 were calculated from spectra measured at various power settings of both LED types. Overall, the $(K,Na)LuS_2$:Eu luminophores render green and yellow objects much better (higher CQS) than orange or blue-green colour due to the emission spectra shape (Fig. 1).

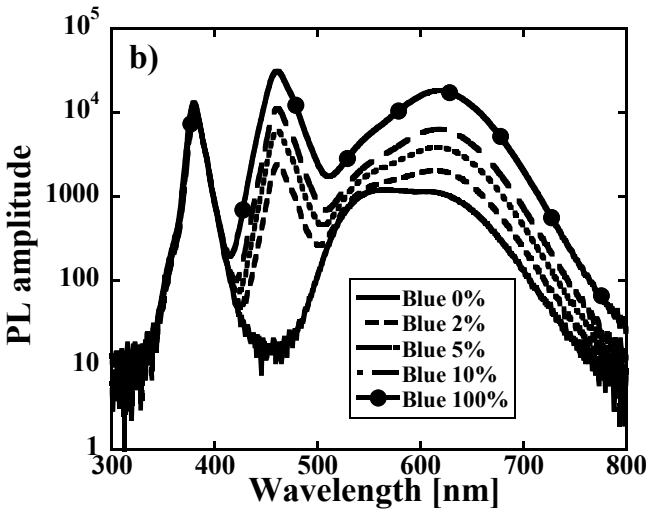

Fig. 1. Overall emission spectra of the circadian light source with a $K_{0.8}Na_{0.2}LuS_2:Eu^{2+}$ sample (fraction of big crystals), fixed nearUV LED power (10 %) and varying blue LED power [2].

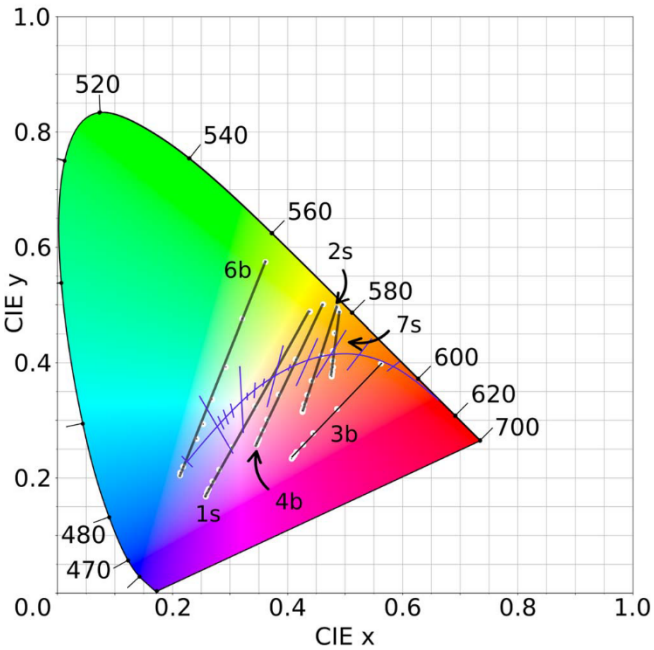

Fig. 2. CIE chromacity diagram illustrating the regions of tuneability for the most promising $(K,Na)LuS_2:Eu^{2+}$ phosphors (lines) with Black Body Locus (curve) [2].

REFERENCES

[1] Jarý, V. et al. (2013) Chem. Phys. Lett. 574, 61-65.
[2] Havlák, L. et al. (2016) Mater. Design 106, 363-370.
[3] Jarý, V. et al. (2018) ECS J. Solid State Sci. Technol. 7, R3182-R3188.

* Full paper in [3].

Radiopharmaceutical Chemistry

PREPARATION AND LABELLING OF SUPERPARAMAGNETIC IRON OXIDE NANOPARTICLES

Valová, V.; Sobkuliaková, Z.; Kukleva, E.; Mokhodoeva, O.[1]; Vlk, M.; Kozempel, J

[1] *Vernadsky Institute of Geochemistry, Russian Academy of Sciences, 19 Kosygin Str., 119991 Moscow, Russian Federation*

INTRODUCTION

Superparamagnetic iron oxide nanoparticles (*SPIONs*) are widely studied as contrast agents and radionuclide carriers in nuclear medicine and radiology thanks to their low toxicity, biocompatibility and paramagnetic properties. Further, *SPIONs* might be vectorised by an external magnetic field to a target tissue [1]. The scope of our work was the synthesis and characterization of *SPIONs* and their labelling with: ^{18}F as a representative of PET radionuclides, and with ^{90}Y, ^{186}Re, ^{223}Ra as representatives of therapeutical radionuclides

EXPERIMENTAL

SPIONs were prepared by co-precipitation method [2]. The pH-range during the synthesis of *SPIONs* was between 8-14 with maintaining molar ratio of Fe^{3+}/Fe^{2+} 2:1 under the inert atmosphere. The structure and composition of the synthesised nanoparticles was checked by TEM (Fig. 1), FT-IR, Raman spectrometry and XRPD. The size distributions of the nanoparticles in aqueous dispersions was determined by dynamic light scattering DLS (66 – 254 nm) and the stability was determined by the zeta potential measurement.

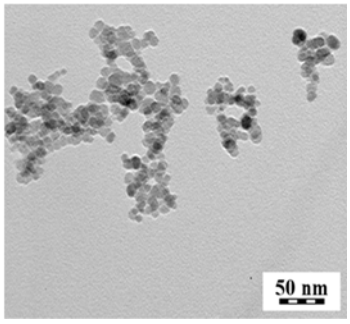

Fig. 1. TEM image of Fe_3O_4.

Isotope of ^{68}Ga was obtained from the commercial generator. Radium-223 was gained inhouse, from an ^{227}Ac/^{227}Th/^{223}Ra generator. The ^{18}F, ^{90}Y and ^{186}Re were obtained commercially in the corresponding chemical forms.

RESULTS

The exact amount of nanoparticles (5 mg for ^{223}Ra and 2 mg for other radionuclides) was dispersed in a saline. Then the radionuclide was added and the reaction mixture was incubated for 30 minutes. For labbeling with ^{18}F, ^{90}Y, ^{186}Re and ^{223}Ra non-stabilized nanoparticles were used, but for ^{68}Ga SPIONs stabilised by sodium citrate and TEOS and then functionalized with *t*-Boc-L-histidine and DOTAGA were used. These nanoparticles were dispersed in corresponding buffer (pH = 4 - 6) and reaction mixture was heated at 90°C for 20 minutes.

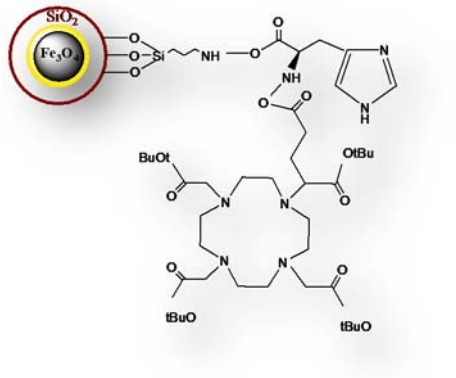

Fig. 2. Stabilized SPION functionalized with DOTAGA.

Tab. 1. Labelling conditions and labelling yields for ^{68}Ga.

Buffer	pH	A [MBq]	Yield %
Acetate	5	28	96
Acetate	5,5	9	96
HEPES	5,4	20	97
BRB	4	19	74
BRB	5	22	85
BRB	6	10	90

Tab. 2. Radiochemical yields for other radionuclides.

Radionuclide	^{18}F	^{90}Y	^{186}Re	^{223}Ra
Yields %	72	90	90	98

REFERENCES

[1] Wahajuddin M., et. al. (2012) Int. J. Nanomed. 7
[2] Mokhodoeva O., et. al. (2016) J. Nanoparticle Res. 301, 1-12

This work was supported partially by Health Research Agency of the Czech Republic, grant no.: 16-30544A, CTU in Prague grant SGS16/251/OHK4/3T/14, and Technology Agency of the Czech Republic, grant no.: TJ01000334.

LABELLED SUPERPARAMAGNETIC IRON OXIDE NANOCARRIERS FOR MULTISTAGE SPECT DIAGNOSTIC

Sobkuliaková Z.; Valová, V.; Kukleva, E. ; Sakmár, M. ; Mokhodoeva, O.[1]; Vlk, M. ; Kozempel, J.

[1]Vernadsky Institute of Geochemistry, Russian Academy of Sciences, 19 Kosygin Str., 119991 Moscow, Russian Federation

INTRODUCTION

Nanotechnology has given scientists new tools for the development of advanced materials for the detection and diagnosis of disease. Iron oxide nanoparticles (SPIONs) in particular have been extensively investigated as novel magnetic resonance imaging (MRI) contrast agents due to a combination of favorable superparamagnetic properties, biodegradability and surface properties of easy modification for improved *in vivo* kinetics and multifunctionality. *SPIONs* have become a promising tool in the magnetic resonance imaging, magnetic drug targeting, hyperthermia anti-cancer strategy, and enzyme immobilization. The aim of our work was the synthesis and characterization of *SPIONs* and their labelling with ^{99m}Tc useful for multistage-SPECT diagnostics. [1, 2]

EXPERIMENTAL

SPIONs were prepared by co-precipitation method and then stabilised with 0.1 M sodium citrate, the pH range during the synthesis was between 8-14 with maintaining molar ratio of Fe^{3+}/Fe^{2+} 2:1. The reaction mixture was held under inert condition.

The structure and composition of the synthesised nanoparticles were confirmed by FTIR and XRPD. The size of non-stabilised nanoparticles is 9±7nm and the size of stabilised NPs is 5±3nm. The size was also determined by dynamic light scattering (DLS). The stability of the nanoparticle dispersion was determined by the measurement of Z-potential. The transmission electron microscopy images (TEM - Fig.1) were created for the determination of the size.

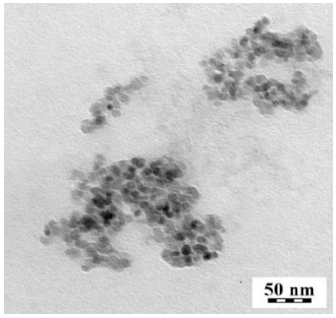

Fig. 1. TEM image of stabilized Fe_3O_4.

RESULTS

Labelled *SPIONs* were synthesized by contacting suspension of 1-5 mg *SPIONs* with ^{99}Mo/^{99m}Tc generator eluate containing $Na^{99m}TcO_4$ (200-250 MBq). Commercial MDP and HDP kits were labelled with 200 – 250 MBq $Na^{99m}TcO_4$. *SPIONs* labelled with ^{99m}Tc ($T_{1/2}$ = 6 h) - Tab.1 - had excellent yields (> 90%). Labelled *SPION*s after the incubation were separated using a magnet.

In vitro stability of ^{99m}Tc-NPs were studied in physiological saline (S), bovine serum (BS) and albumin (A) - Tab.2, Fig.2.

Tab. 1. Radiochemical yields ^{99m}Tc-NPs (non-stabilised)

Sample	Initial A [MBq]	Yield [%]
ZS 2-0	130	99
ZS 2-BS	553	94
ZS 2-A	696	92
ZS 2-S	620	92

Tab. 2. *In vitro* stability in physiological saline (S), bovine serum (BS) and albumin (A)

Sample	Initial A [MBq]	Released A [MBq]				
		2h	7h	12h	17h	25h
ZS 1-BS	105	4	5	3	2	4
ZS 1-A	130	4	8	4	5	2
ZS 2-A	170	9	6	5	3	1

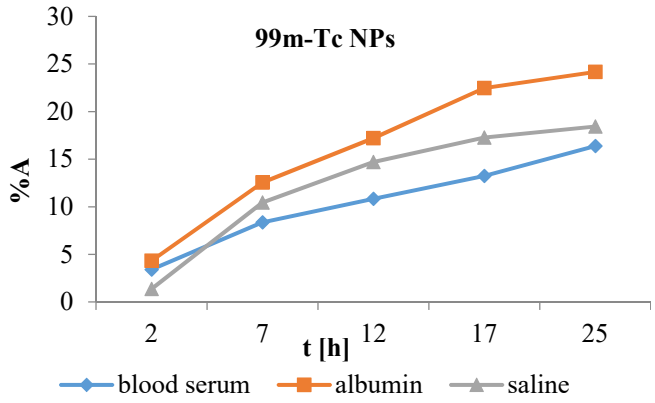

Fig. 2. *In vitro* stability of non-stabilized ^{99m}Tc-NPs in physiological saline (S), bovine serum (BS) and albumin (A).

REFERENCES

[1] Mokhodoeva O., et. al. (2016) J. Nanoparticle Res. 301, 1-12

Madru R., et. Al. (2012) J. Nucl. Med. 53, 459-463

[2] Stephen Z.R., (2011) Mater. Today 14, 330-338

This work has been supported by the Health Research Agency of the Czech Republic under contract No. 16-30544A, and CTU in Prague grant SGS16/251/OHK4/3T/14.

HYDROXYAPATITE NANOPARTICLES AS THERANOSTIC VECTORS FOR RADIOPHARMACY

Kozempel, J.; Vlk, M.; Kukleva, E.; Sakmár, M.; Suchánková, P.

INTRODUCTION

The main inorganic component of human hard tissues is hydroxyapatite (HAp) with a chemical formula $Ca_{10}(PO_4)_6(OH)_2$. Hydroxyapatite in its synthetic form is frequently used as a drug-delivery system for bone therapy applications because of its biocompatibility, bioactivity, and osteotropic properties. Nanoparticles of HAp might be used as carriers for various radionuclides. In this study, HAp was labelled with several diagnostic and therapeutic nuclides (^{18}F, ^{68}Ga, ^{99m}Tc and ^{223}Ra) and *in vitro* stabilities of ready-made particles were tested in saline, bovine serum, bovine plasma and 5% albumin solution.

EXPERIMENTAL

Hydroxyapatite NPs were prepared by the precipitation of $Ca(NO_3)_2$ with $(NH_4)_2HPO_4$. The pH was set up to 11 with 0.1 M NaOH before the reaction. Reaction mixture was stirred overnight. The prepared NPs were separated from reaction mixture by centrifugation (3500 rpm for 5 minutes) and washed with deionized water. Spectral analyses confirmed the Hap-NPs structure and shape.

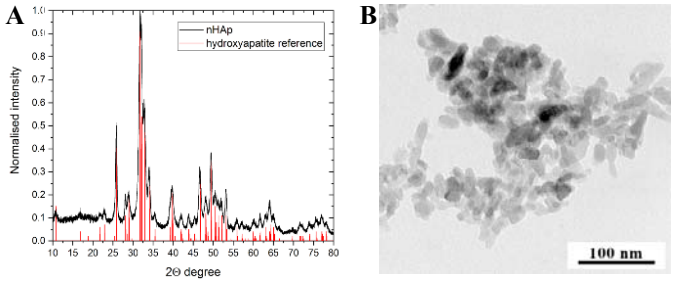

Fig. 1. A-XRPD spectrum of hydroxyapatite **B**-hydroxyapatite photo from TEM.

The labelling was performed by contacting corresponding radionuclide with NPs at particular pH. Isotopes of ^{68}Ga and ^{99m}Tc were obtained from commercial generators. ^{223}Ra was gained inhouse, from an $^{227}Ac/^{227}Th/^{223}Ra$ generator. The ^{18}F was a commercial sample from ÚJV Řež (Czech Rep.). The exact amount of nanoparticles (5 mg) was dispersed in a given solution (see Tab.1). Then the radionuclide was added and the reaction mixture was incubated for a certain period of time (Tab.1). Finally, the sample was centrifuged and washed with saline.

Tab. 1. Labelling conditions and labelling yields

Radionuclide	Half-life	Incubation conditions	Reaction medium	Yield %
^{223}Ra	11.4 d	1 h, lab. t.	saline	96
^{99m}Tc	6.01 h	1 h lab. t	saline, $SnCl_2$	95
^{18}F	108 min	15 min., lab. t.	saline	84
^{68}Ga	68 min	30 min, 70 °C	buffer (pH=5)	95

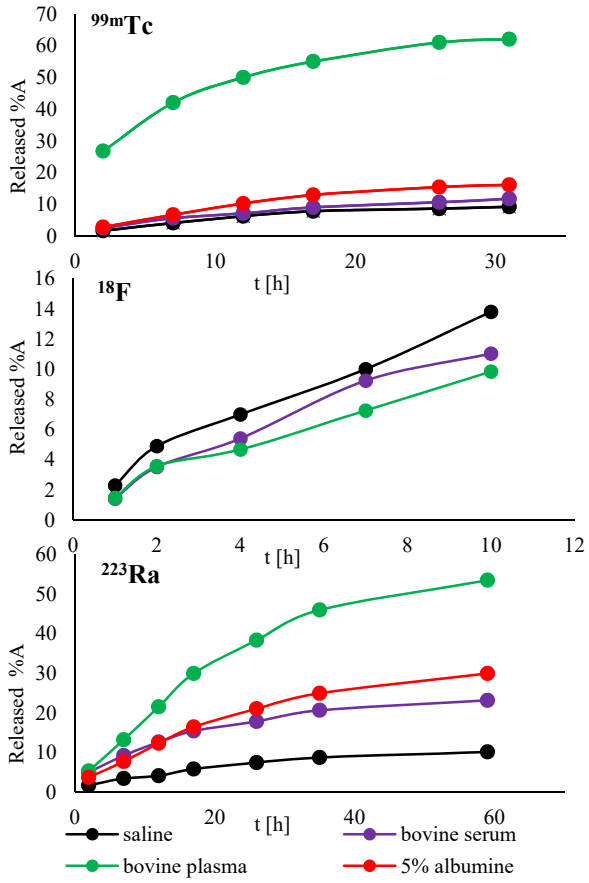

Fig. 2. Released cumulative activity for: ^{99m}Tc-HAp; ^{223}Ra-HAp; ^{18}F-Hap.

RESULTS

Prepared HAp nanoparticles were labelled by the diagnostic radionuclides ^{18}F, ^{68}Ga, ^{99m}Tc and therapeutic radionuclide ^{223}Ra. Labelling yields are summarized in Tab.1. *In vitro* stabilities were determined in saline, bovine plasma, bovine serum and 5% solution of albumin and the released activities are show in Fig.2. In the case of ^{68}Ga major release of activity was observed. The sufficient *in vivo* stability without fast aggregation of the HAp-NPs is required for the theranostic application. Therefore, the modification of HAp surface with various organic substances will be studied in future experiments.

REFERENCES

[1] Kozempel, J., et al. (2014), J. Radioanal. Nucl. Chem. 304, 443-447
[2] Okada, M., et al. (2016), Sci. Technol. Adv. Mater.13

This research has been supported by Health Research Agency of the Czech Republic, grant No.: NV16-30544A, Technology Agency of the Czech Republic, grant No.: TJ01000334 and the Ministry of Education Youth and Sports of the Czech Republic and the EU, grant No.:CAPCZ.02.1.01/0.0/0.0/15_003/0000464

SURFACE MODIFICATION OF HYDROXYAPATITE NANOPARTICLES

Sakmár, M.; Suchánková, P.; Kukleva, E.; Kozempel, J.; Vlk, M.

INTRODUCTION

Hydroxyapatite (HAp), the prime constituent of tooth and bone minerals, has been used extensively as an artificial bone substitute in different medical applications, due to its biocompatibility, bioactivity, osteoconductivity, nontoxicity, non-inflammatory behavior, and non-immunogenicity It might be used as a drug carrier in diagnostics and cancer treatment. The sufficient *in vivo* stability without fast aggregation of the HAp-NPs is required for the theranostic application. Therefore, the modification of HAp surface with various organic substances has been the subject of many studies that have given novel functions and stabilization of this material. The aim of this work was to study various phosphonic acids as potential HAp stabilizers and technetium-99m chelators.

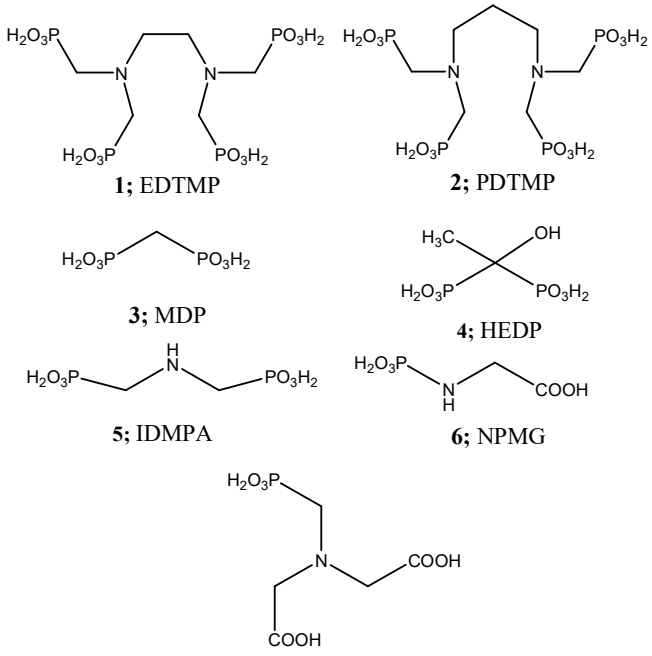

Fig. 1. Structures of used acids.

EXPERIMENTAL

Hydroxyapatite nanoparticles were prepared by precipitation of $Ca(NO_3)_2$ with $(NH_4)_2HPO_4$ at pH = 11. The precipitate was washed, lyophilized and crushed. Stabilized samples were prepared from already-made HAp-NPs by ultrasound dispergation in corresponding phosphonic acid solution (0.2 M). For experiments, the following phosphonic acids were used: ethylenediamine tetra(methylene phosphonic acid) (**1;** EDTMP), prophylendiamine tetra(methylene phosphonic acid) (**2;** PDTMP), medronic *acid (**3;** MDP), etidronic acid (**4;** HEDP),* Iminodi(methylphosphonic) acid (**5;**IDMPA), *N*-(phosphonomethyl)glicine (**6;** NPMG), *N*-(phosphono-methyl)iminodiacetic acid (**7;** NPMIDA). The hydrodynamic size distributions and zeta potentials of studied stabilized particles were determined using dynamic light scattering (Zetasizer, Malvern, UK).

Prepared samples were labelled with technetium-99m eluted from $^{99}Mo/^{99m}Tc$ generator (DRYTEC, GE Healthcare). The labelling was performed by two different methods. In the first procedure, technecium-99m was added to ready-made nanoparticles stabilized by phosphonic acids. The second approach used for labelling the nanoparticles already labelled phosphonic acids. In both ways, the reaction mixture was incubated for 1h, then the sample was centrifuged and washed with saline. The labelling yields for both ways is shown in Tab.1.

Tab. 1. Hydrodynamic size (d), zeta potential (ζ) and labelling yields for corresponding acid and both labelling methods.

Acid	d [nm]	ζ [mV]	Yield[1] %	Yield[2] %
EDTMP	78	-51,8	38	8
PDTMP	82	-48,8	65	33
MDP	69	-47,7	32	1
HEDP	66	-45,9	51	3
NPMIDA	59	-55,8	39	10
IDMPA	98	-50,3	48	32
NPMG	110	-33,8	28	7

RESULTS

Surface modification of HAp nanoparticles was tested using various phosphonic acids. For the prepared composite compounds, hydrodynamic sizes and zeta potentials were measured by dynamic light scattering and finally nanoparticles were labelled with ^{99m}Tc using two different methods. The results obtained in this work are a good basis for the surface modifications of HAp nanoparticles. The prepared particles have been stable in the aqueous solution over a long period of time, but for future experiments it is necessary to optimize the labelling method.

REFERENCES

[1] Othamani. M., et al. (2013) Appl. Surf. Sci. 274, 151-157
[2] Okada, M., et al. (2016) Sci. Technol. Adv. Mater.13
[3] Han, Y., et al (2008) J. Mater. Sci. Mater. Med. 19, 2993-3003

This work was supported by Ministry of the Interior of the Czech Republic, grant no. VI20172020106 and the EU & Ministry of Education Youth and Sports of the Czech Republic grant No.: CZ.02.1.01/0.0/0.0/15_003/0000464.

NEW SORBENT FOR $^{68}Ge/^{68}Ga$ RADIONUCLIDE GENERATOR

Fialová, K.; Adámek K.; Šebesta, F.; Vlk. M.; Kozempel, J.; Kukleva, E.

INTRODUCTION

$^{68}Ge/^{68}Ga$ radionuclide generator becomes one of the most important sources of radionuclides for positron emission tomography (PET). Commercially available generators usually use inorganic ion exchangers, such as titanium and tin oxides, as a stationary phase [1, 2]. This study is focused on the preparation of the new sorbent for the separation of ^{68}Ge and ^{68}Ga. For this purpose cerium(IV) oxide and zirconium(IV) hydroxide were studied as perspective materials and two composite sorbents with polyacrylonitrile (PAN) matrix were prepared and tested.

EXPERIMENTAL

Cerium(IV) oxide, CeO_2, was prepared by calcination of cerium(III) nitrate at 400 °C for 1 hour, zirconium(IV) hydroxide, $Zr(OH)_4$, was purchased from MEL Chemicals. Both materials were characterized by X-ray powder diffraction, thermogravimetric analysis, measurement of specific surfaces, transmission and scanning electron microscopy, FT-IR and Raman spectrometry.

Sorption qualities of both materials were examined by measurement of equilibrium distribution coefficients of ^{68}Ge and ^{68}Ga in the presence of diluted hydrochloric acid (concentrations: 1 mol/l; 0.1 mol/l; 0.01 mol/l; 0.001 mol/l). Galium-68 was gained from commercial $^{68}Ge/^{68}Ga$ generator IGG–100 (EZAG, Deutschland) and Germanium-68 was purchased from Eckert & Ziegler Isotope Products. The incubation time was 2 hours.

Composite sorbents, CeO_2-PAN and $Zr(OH)_4$-PAN, were prepared by granulation of CeO_2 resp. $Zr(OH)_4$ into the polyacrylonitrile matrix [3].

RESULTS

The results of specific surfaces measurement and the sizes of crystallites gained from X-ray powder diffraction before and after thermogravimetric analysis (TGA) are for both materials summarized in Tab. 1. It can be seen that these characteristics are similar for both materials.

Tab. 1. Specific surfaces, S, and size of crystallites before and after TGA, d and d_{TGA}, for both tested materials.

Sample	S m^2/g	d nm	d_{TGA} nm
CeO_2	2.74	142	1.40
$Zr(OH)_4$	2.64	153	1.80

The dependences of equilibrium distribution coefficients, D_w of ^{68}Ge and ^{68}Ga on the concentration of hydrochloric acid are depicted in Fig. 1 and Fig. 2, respectively. It is notable that the values of equilibrium distribution coefficients rise with the concentration of the acid in the case of both materials and both radionuclides.

To evaluate the optimal concentration of acid for the separation of two examined radionuclides, it was necessary to determine the separation factor, α of these radionuclides for tested concentrations. Considering the separation factor, α of ^{68}Ge and ^{68}Ga for individual acid concentrations, the optimal medium for separation of these radionuclides is 0.1mol/l hydrochloric acid ($\alpha = 26\,857$ for cerium(IV) oxide and $\alpha = 4\,949$ for zirconium(IV) hydroxide) (Tab. 2).

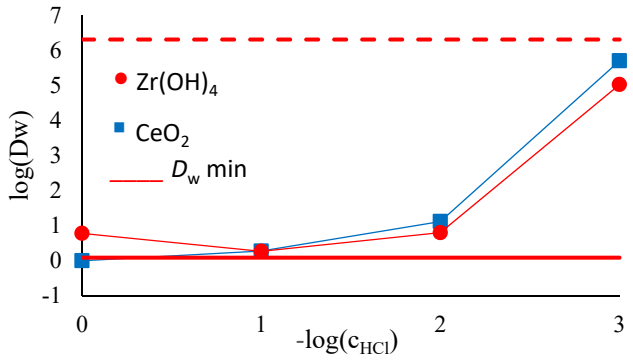

Fig. 1. Dependence of equilibrium distribution coefficients, D_w, of ^{68}Ga on the concentration of hydrochloric acid, c_{HCl}.

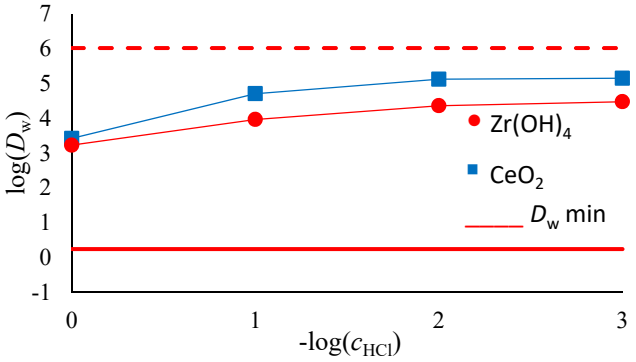

Fig. 2. Dependence of equilibrium distribution coefficients, D_w, of ^{68}Ge on the concentration of hydrochloric acid, c_{HCl}.

Tab. 2. Separation factor, α, for both materials and tested concentrations of hydrochloric acid, c.

c mol/l	α_{CeO2} -	$\alpha_{Zr(OH)4}$ -
1	-	279
0.1	26857	4949
0.01	10036	3602
0.001	0.28	0.28

In the future study it will be necessary to evaluate prepared composites in column experiments.

REFERENCES

[1] Razbash, A. et al. (2005) Czech. J. Phys. 56, D623-D628).

[2] Obninsk 68Ge/68Ga Generator Product Information. Eckert & Ziegler, Eurotope GmbH, 7131-0006 /Rev.08 / 05.2013.

[3] Šebesta, F. (1997) J. Radioanal. Nucl. Chem. 220, p. 77 – 88.

This research has been supported by Technology Agency of The Czech Republic, grant no. TJ01000334.

PROGRESS IN TARGETED ALPHA-PARTICLE THERAPY. WHAT WE LEARNED ABOUT RECOILS RELEASE FROM IN VIVO GENERATORS

Kozempel. J.; Mokhodoeva, O.[1]; Vlk, M.

[1] Vernadsky Institute of Geochemistry and Analytical Chemistry, Moscow, Russia

INTRODUCTION

The basic advantage of TAT over commonly used β^- emitting radionuclides therapy lies in the irradiation of fewer cancer cells, micrometastases or tumors by an emission of a single alpha particle or by a cascade of alpha particles from close vicinity. The 2+ charged α particles with high linear-energy transfer (LET) lose the maximum of their energy close to the Bragg peak at the end of their track. The range in tissues is about 50–100 μm depending on the alpha-particle energy. The energy deposition then occurs in a very small tissue volume and with high relative biological effectiveness (RBE) [1].

In the case of *in vivo* generator the nuclear recoil effect causes the release of radioactive daughter nuclei from the original radiopharmaceutical preparations. It may lead to unwanted irradiation of healthy tissues. Dosimetric studies should separately evaluate in detail the contributions of a radiolabelled targeted vector, its labelled metabolites, liberated mother nuclide as well as daughter recoils.

Several different approaches were developed regarding the carriers for TAT. Small molecules, particularly those labelled with single α emitters, brought the advantage of fast kinetics even though their in vivo stability was not always good. Additional approaches to mitigate radiotoxic effects were studied, e.g., to protect kidneys [2]. Immunoactive molecules like antibodies, antibody fragments, nanobodies or receptor-specific peptides represent another group of highly selective targeting vectors [3]. A relatively novel concept of at least partially recoil-resistant carriers for TAT was developed. It employs nanoconstructs composed of various nanoparticulate materials that allow further surface chemistry, including antibody targeting.

GENERAL RADIOPHARMACEUTICAL ISSUES

Due to the momentum conservation law, part of the decay energy is transferred to a daughter nucleus. The comparison of LET and ion ranges of α particles and ^{219}Rn recoils originating from ^{223}Ra decay is shown in Fig. 1.

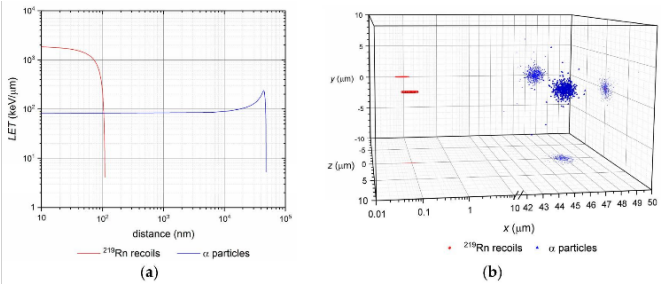

Fig. 1. (a) Log/log plot of linear-energy transfer (LET) of α particles and ^{219}Rn ions vs. their path (distance) in water up to the rest; (b) Semi-log 3D plot of final at rest positions of α particles and ^{219}Rn ions with their xy, xz and yz plane projections. The recoil, in fact, travels in opposite direction to the emitted α particle (common decay-event origin at x,y,z = 0,0,0).

Recoils spread mitigation by time—the spread of daughter radioactive ions takes time, so their spread in the organism would also depend on their half-life.

Recoils spread mitigation by nanoconstruct size/material—daughter-recoiling nuclide consumes some of its energy while getting through the nanoconstruct.

Recoils spread mitigation by the nanoconstructs number/depot—even though the recoil ion may escape a nanoconstruct, the probability of its back-implantation or its implantation into surrounding nanoconstruct units is relatively high.

Efficient and specifically targeted carriers need to be developed in order to realize the potential and favourable properties of α emitters. A variety of conventional and novel drug-delivery systems have been investigated for these purposes: biological macromolecules (antibodies, antibody fragments), small molecule compounds (peptides, affibodies) and nanocarriers/nanoconstructs.

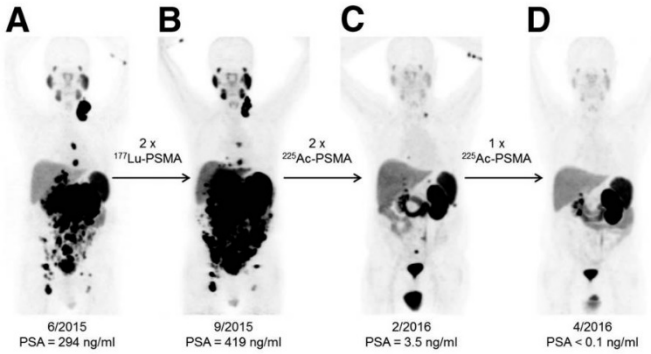

Fig. 2. ^{68}Ga-PSMA-11 positron emission tomography (PET)/computed tomography (CT) scans of a patient comparing the initial tumor spread (A); restaging after 2 cycles of β− emitting ^{177}Lu-PSMA-617 reveals progression (B). In contrast, restaging after second (C) and third (D) cycles of α emitting ^{225}Ac-PSMA-617 shows impressive response. This research was originally published in JNM [4].

REFERENCES

[1] Song, H. et al. (2012) Antibodies 1, 124–148
[2] Jaggi, J.S. et al (2006) Int. J. Radiat. Oncol. Biol. Phys. 64, 1503–1512
[3] Dekempeneer, Y. et al. (2016) Expert Opin. Biol. Ther. 16, 1035–1047
[4] Kratochwil, C. et al. (2016) J. Nucl. Med. 57, 1941–1944.

This research has been supported by the Health Research Agency of the Czech Republic, grant No.: NV16-30544A, the Russian Foundation for Basic Research, and Moscow city government according to the research project No.: 15-33-70004 «mol_a_mos», the Technology Agency of the Czech Republic, grant No.: TJ01000334 and the EU & Ministry of Education Youth and Sports of the Czech Republic grant No.: CZ.02.1.01/0.0/0.0/15_003/0000464.

SYNTHESIS OF DIGLYCOLAMIDE EXTRACTION AGENTS ANCHORED TO POLYACRYLONITRILE MATRIX

Fialová, K.; Vlk, M.; Kozempel, J.; Šebesta, F.; Dračínský, M.[1]

[1] Ústav organické chemie a biochemie Akademie věd České republiky

INTRODUCTION

Diglycolamides (DGA) are extraction agents used in many fields, including nuclear medicine. They are most commonly used as solid extractants impregnated on a chromatographic matrix [1]. The main issue of impregnated extractants is leakage of the active agent. The anchoring of diglycolamide to the matrix would solve the problem. In this study, polyacrylonitrile (PAN) was chosen as a convenient material as it was already widely studied as matrix in the form of beads for separation chemistry and its chemical structure enables anchoring of diglycolamide [2]. The synthesis is based on partial surface reduction of nitrile groups of PAN beads to primary amine and subsequent solid-state synthesis of diglycolamide.

EXPERIMENTAL

PAN matrix was reduced under various conditions which are summarized in Tab. 1. Eight samples of modified PAN matrix were prepared. The content of amine groups in the prepared samples was determined using acid-base titration.

Tab. 1. Reduction conditions and amine content c_{amine} for prepared samples.

sample	reduction conditions	c_{amine} µmol/g
I	$LiAlH_4$/THF:MeOH = 2:1, Ar, r. t., 2 h	157
II	$LiAlH_4$/THF:MeOH = 2:1, Ar, r. t., 6 h	257
III	$LiAlH_4$/THF:MeOH = 2:1, Ar, r. t., 12 h	285
IV	$LiAlH_4$/THF:MeOH = 2:1, Ar, r. t., 24 h	55
V	$NaBH_4$, $CoCl_2 \cdot xH_2O$/MeOH, Ar, r. t., 2 h	114
VI	$NaBH_4$, $NiCl_2 \cdot xH_2O$, MeOH, Ar, r. t., 2 h	588
VII	$NaBH_4$, $LaCl_3 \cdot xH_2O$/MeOH, Ar, r. t., 2 h	602
VIII	H_2,[Ru(cod)(methylallyl)$_2$]/PPh_3, tBuOK/toluene, 80 °C 6 h	252

Subsequently, the solid extractant, DODGA-PAN, was prepared by reaction of modified PAN matrix with highest content of amine (sample III) and monoamide precursor with coupling agent, T3P®, in the presence of pyridine at room temperature for 24 hours. The structure of final extractant is shown in Fig. 1

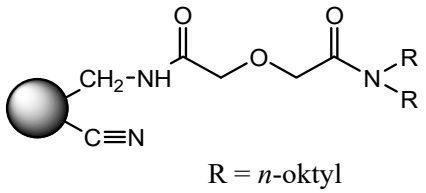

R = *n*-oktyl

Fig. 1. Structure of the solid extractant DODGA-PAN.

Prepared solid extractant was characterized by FT-IR and NMR spectrometry, scanning electron microscopy and measurement of specific surfaces, and tested by the basic sorption experiments with $^{152+154}EuCl_3$ solution in HCl (2500 cps/ml) and V/m = 100 ml/g.

RESULTS

The contents of amine groups in prepared samples of modified PAN matrix is given in Tab. 1. Regarding the fact that samples VI and VII required wash-out with nitric acid which could dissolve PAN matrix, the most convenient reduction route is the reduction by complex metal hydride $LiAlH_4$ with reaction time of 12 hours (sample III).

The results of sorption experiments with prepared extractant were compared with the results obtained for nonmodified PAN matrix and solid extractant, 1% TODGA-PAN, consisting of PAN matrix impregnated with 1 % of *N,N,N',N'*-tetraoctyldiglycolamide. The results for all sorbents are depicted in Fig. 2 as the dependence of equilibrium distribution coefficient on the concentration of hydrochloric acid.

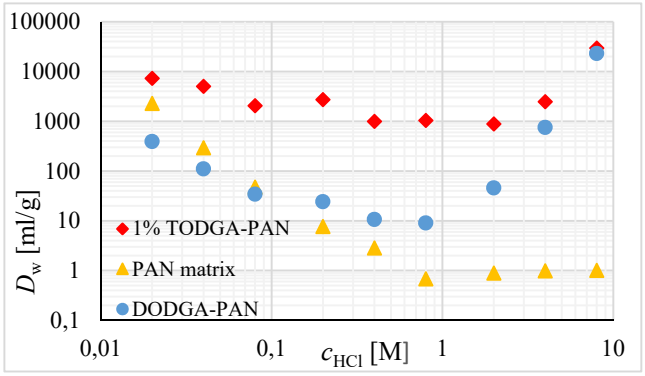

Fig. 2. Dependence of equilibrium distribution coefficient D_w on concentration of hydrochloric acid c_{HCl}.

It can be seen that prepared solid extractant DODGA-PAN has shown similar sorption behaviour towards Eu^{3+} as 1% TODGA-PAN, especially in higher acid concentrations. Sorption behaviour at lower acid concentrations is, on the other hand, caused by PAN matrix.

REFERENCES

[1] ALGETA AS. Isotope production method. Inventors: Karlson, J.R.; Børretzen, P. European patent application. EP2564397 A1. 29.4.2011.

[2] Šebesta, F. et al. (1995) Evaluation of Polyacrylonitrile (PAN) as a Binding Polymer for Absorbers Used to Treat Liquid Radioactive Wastes. *SAND95-2729*.

This research has been supported by Ministry of the Interior of the Czech Republic, grant no. VI20172020106 and the EU & Ministry of Education Youth and Sports of the Czech Republic grant No.: CZ.02.1.01/0.0/0.0/15_003/0000464.

TITANIUM DIOXIDE - PERSPECTIVE NANOCARRIER MATERIAL FOR MEDICINAL NUCLIDES DELIVERY

Suchánková, P.; Kukleva, E.; Nykl, P.; Sakmár, M.; Vlk, M.; Nespesna, L.[1]; Kozempel, J.

[1] UJV Řež, a.s. – Husinec Řež, Czech Republic

INTRODUCTION

This study is focused on a potential targeted diagnostics and therapy system, which could transfer medicinal radionuclides into the targeted tissue. Titanium dioxide nanoparticles (TiO_2-NPs) were chosen especially due to their versatility, high specific surface, chemical stability and sorption abilities (used as inorganic sorbent in some $^{68}Ge/^{68}Ga$ generators). Due to increasing attention given to alpha emitters in therapy, ^{223}Ra was chosen. [1] On th contrary, ^{99m}Tc was selected as a diagnostic radionuclide because of its availability on departments of nuclear medicine. The most important requirement on carriers used in targeted therapy or diagnostics are the stable binding of the mother radionuclide and daughter recoils retention. [2]

EXPERIMENTAL

TiO_2-NPs were prepared by the hydrolysis of the tetra-n-butyl orthotitanate. The ^{223}Ra stock was prepared from $^{227}Ac/^{227}Th/^{223}Ra$ generator prepared at our laboratory. [1] The stock ^{99m}Tc solution was gained from commercial generator DRYTEC™.

Two labelling strategies were chosen. The first one, surface, with ready-made nanoparticles. Dispersed TiO_2-NPs were incubated one hour with both radionuclides. The second one, volume, was about direct incorporation of radionuclides into NPs structure during NPs preparation. Tetra-n-butyl orthotitanate in 2-propanol was added into excess of solution of radionuclides. Yields were determined.

Also *in vitro* stability tests of the labelled TiO_2-NPs were performed in saline, bovine blood plasma, serum and albumine solutions (1 and 5%). The released activity was measured 2 – 7 – 12 – 17 – 26 – 35 – 59 hours after labelling. The total released activities were similar in all matrixes and were less than 5 % (Fig. 1 and 2).

RESULTS

The ability of titanium dioxide nanoparticles to retain radium and technetium was experimentally proven. The stability of labelled TiO_2-NPs in all matrixes was >95 % with less than 5 % total activity released (Fig. 1. and 2.). In spite of interesting results it is necessary to prepare another in vivo experiments for the verification of results.

CONCLUSIONS

The labelling yields were comparable in both strategies. So the ability of titanium dioxide to retain ^{223}Ra and ^{99m}Tc was proven. The stability of ^{223}Ra-TiO_2 was higher than 95 % in all matrixes with total released activity less than 5%. The stability of ^{99m}Tc-TiO_2 was higher than 80 % in all matrices except bovine blood plasma, where the total released activity was 65 %. Retention of $^{223}Ra.$-TiO_2 in tumor was approximately 80 %.

Tab. 1. Labelling yields for both strategies. (S – surface labelling; V – volume labelling; N = 6).

Radionuclide	Note	Yield [%]	Note	Yeild [%]
^{223}Ra	S	98.6±0.5	V	99.1±0.3
^{99m}Tc		98.4±0.5		97.6±0.7

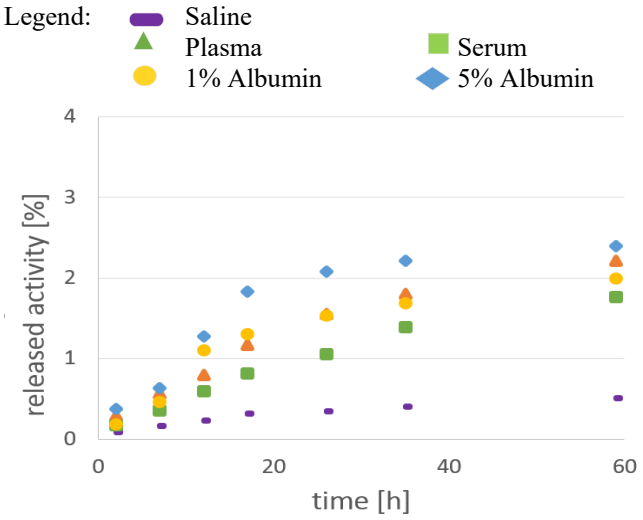

Fig. 1. Released activity during *in vitro* stability tests with ^{223}Ra-TiO_2 volume labelled.

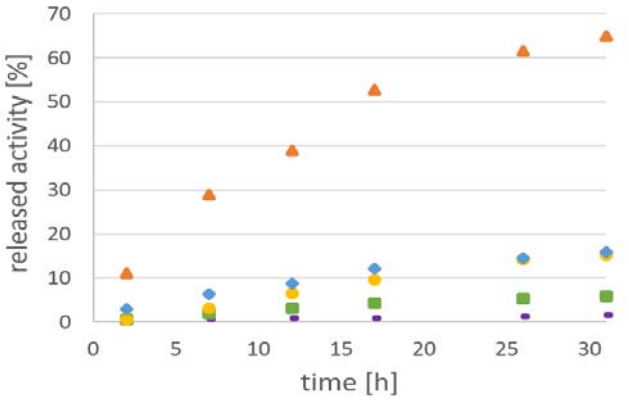

Fig. 2. Released activity during in vitro stability tests with ^{99m}Tc-TiO_2 volume labelled.

REFERENCES

[1] Guseva L.I., et al., (2004) Radiochemistry, 46, 58–62.
[2] Bilewicz, A. et al., (2013) Theranostics Imaging and Therapy

This research has been supported by the Technology Agency of the Czech Republic (TA03010027) and the Czech Technical University (SGS15/094/OHK4/1T/14).

DOTA DECORATED HYDROXYAPATITE NANOPARTICLES LABELLED WITH ^{68}Ga

Kukleva, E.; Vlk, M.; Kozempel, J.; Suchánková, P.

INTRODUCTION

Hydroxyapatite nanoparticles (HAp-NPs) are widely used in medicine because of their biocompatibility and stability in various media [1] with high specific surface area (117 m^2/g). The HAp-NPs also belong to promising drug carrier systems for medicinal radionuclides such as ^{68}Ga as the part of multipurpose theranostic system [2]. Diagnosis and therapy of some diseases is expected to be very accurate and beneficial.

EXPERIMENTAL

Commercial ^{68}Ge/^{68}Ga radionuclide generator (Eckert-Ziegler, Germany) was used to get ^{68}Ga without further purification. DOTA was used as a chelating agent due to its high affinity to various structures and 3+ ions.

The labelling was performed with ready-made HAp-NPs (5 mg) dispersed in 0.5 M Britton-Robinson buffer solution (5-6 ml) to cover the studied pH range (5 - 9). Elution of $^{68}GaCl_3$ was performed with 0.1 M HCl without further purification. Labelling was carried out with pristine NPs and NPs decorated with selected ligands: DOTA, NOTA, TETA and TRAP (0.05 mg). Incubation and labelling was performed during 10 minutes in preheated media at 80 ^{0}C.

Labelling kinetics were studied in shortened incubation time intervals. Labelled nanoparticles' stability was studied *in vitro* in biological matrices such as physiological saline, bovine serum and bovine plasma. Tests were performed during 4 hours (approx. 4 half-lives of ^{68}Ga)

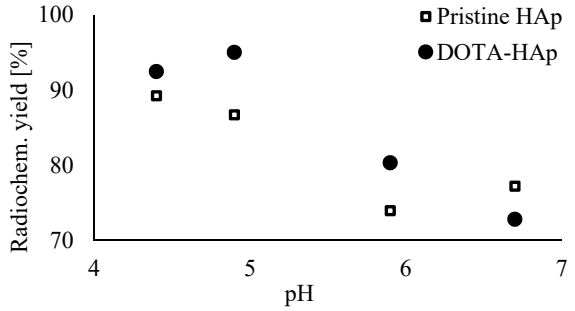

Fig. 1. Labelling yield vs. pH.

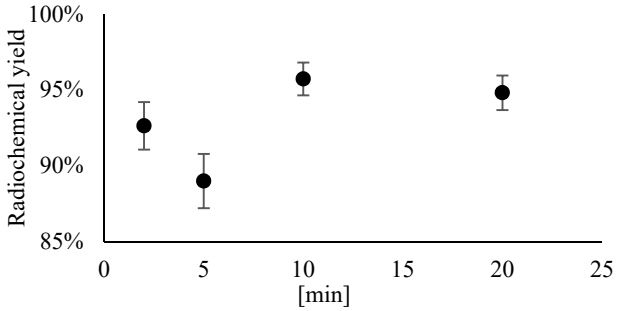

Fig. 2. Labelling kinetics of ^{68}Ga-DOTA-HAp-NPs.

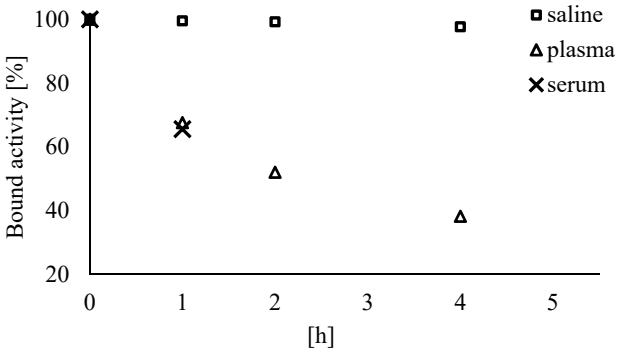

Fig. 3. In vitro stability of [^{68}Ga]-DOTA-HAp-NPs.

RESULTS

Labelling strategy when ligand was firstly labelled with ^{68}Ga and then added to HAp-NPs dispersion does not provide any sufficient results. Experiments with pristine HAp-NPs have shown ^{68}Ga uptake with maximal yield of about 85 % at pH = 5 (30 min incubation) (Fig. 1.). Best result was obtained in a procedure when the ^{68}Ga was added to the NPs dispersion in the DOTA ligand solution heated to 70 ºC and incubated for 30 min. at pH = 5 resulting in 95 % yield (Fig. 1.). Further experiments have shown that uptake kinetics is quite fast (over 90% yield within 5 minutes) (Fig. 2.). *In vitro* stability experiments have shown good stability of ^{68}Ga-DOTA-HAp-NPs nanoconstruct in a physiological saline (more than 95 % of activity remained bound to the NPs in 4 hours), but very poor results were obtained in bovine plasma and serum. Therefore, further experiments are needed to block the ^{68}Ga release (Fig. 3.)

Labelling yields for other ligands was not sufficient. Labelling with TETA showed that TETA does not affect labelling (same results as for pristine HAp).

Stability in bovine serum and plasma is not satisfactory during the whole tested period, but it is sufficient for 1 hour needed for PET scan.

REFERENCES

[1] E. M. Rivera-Munoz, in Biomedical Engineering – Frontiers and Challenges, (Ed: R. Fazel), Rijeka, Croatia, 2011, pp. 75-98.

[2] I. Velikyan, Theranostics. 2014; 4, 1.

This research has been supported by the Czech Health Research Control under project No. AZV ČR - 16-30544A and by Technology Agency of the Czech Republic under project No. TJ01000334.

Electroscope made by Günther & Tegetmeyer (NTM)

Electroscope
– device for the qualitative measurement of electrostatic charge

X-ray Tubes (FNSPE)

X-ray tube
– vacuum tube producing characteristic X-rays and bremsstrahlung

Diffusion Cloud Chamber (NTM)

Cloud chamber
– allows to visualize charged particle paths in air containing supersaturated vapors of e.g. alcohol

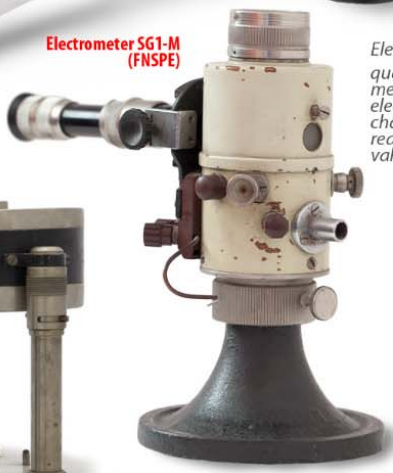

Electrometer SG1-M (FNSPE)

Electrometer –
quantitatively measures electrostatic charge and allows to read the measured value on a scale

Electrometer designed by Dr. F. Běhounek (NTM)

Photomultiplier
– a special tube for transforming the incident photons into an electrical signal

Photomultipliers (FNSPE)

Inorganic Scintillators NaI(Tl) (FNSPE)

Multichannel analyzer
– an electronic device to analyze the input pulses by height and register them in the corresponding channels

Multichannel Analyzer Intertechnique (FNSPE)

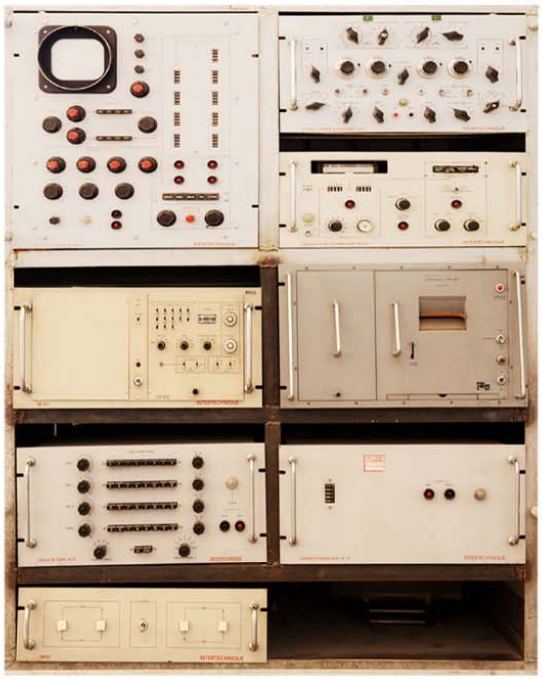

Scintillator
– a material that converts ionizing radiation into visible light

Ionization Chambers Victoreen (FNSPE)

Ionization chamber
– a detector that measures the charge from the number of ion pairs created within a gas caused by incident radiation

Radiometer NNC 253 T (NTM)

Radiometer
– measures the dose rate of ionizing radiation

Pen Dosimeters (NTM)

Dosimeter of ionizing radiation
– a device for measuring the dose or other dosimetric quantity of ionizing radiation

Detector of ionizing radiation
– a device that records and measures ionizing radiation

Electrometer UNIVEL (NTM)

Proportional Detectors (FNSPE)

The exhibits come from the physics collection of the National Technical Museum in Prague and the Faculty of Nuclear Sciences and Physical Engineering, CTU in Prague

PUBLICATIONS

BOOKS

Daňo, M. - Galamboš, M. - Frišták. V.: **Nuclear Radiation Laws - Measurement - Calculations - Statistics.** Bratislava: Univerzita Komenského Bratislava, 2017. ISBN 978-80-223-4085-4. (in Slovak).

BOOK CHAPTERS

Kozempel, J.: **Radon Nuclides and Radon Generators.** In: ADROVIC, F., ed. Radon. Rijeka: InTech, 2017. pp. 7-23. ISBN 978-953-51-3656-9.

PAPERS

Afsar, A. - Cowell, J. - Distler, P. - Harwood, L. M. - John, J. - Westwood, J.: **Synthesis of Novel BTPhen-Functionalized Silica-Coated Magnetic Nanoparticles for Separating Trivalent Actinides and Lanthanides. Synlett. 2017, vol. 28, no. 20, pp. 2795-2799. ISSN 0936-5214.**

Afsar, A. - Distler, P. - Harwood, L. M. - John J. - Westwood, J.: **Extraction of Minor Actinides, Lanthanides and Other Fission Products by Silica-Immobilized BTBP/BTPhen Ligands.** Chemical Communications. 2017, vol. 53, no. 1, pp. 4010-4013. ISSN 1359-7345.

Afsar, A. - Westwood, J. - Distler, P. - Harwood, L. M. - Mohan, S. - John, J. - Davis, F. J.: **Separation of Am(III), Cm(III) and Eu(III) by Electro-Spun Polystyrene-Immobilized CyMe4-BTPhen.** Tetrahedron. 2018, vol. 74, no. 38, pp. 5258-5262. ISSN 0040-4020.

Baborová, L. - Vopálka, D. - Červinka, R.: **Sorption of Sr and Cs onto Czech Natural Bentonite: Experiments and Modelling.** Journal of Radioanalytical and Nuclear Chemistry. 2018, vol. 318, no. 3, pp. 2257-2262. ISSN 0236-5731.

Baimukhanova, A. - Chakrova, E. T. - Karaivanov, D. V. - Kozempel, J. - Roesch, F. - Filosofov, D. V.: **Production of Positron-emmitting Radionuclide ^{68}Ga: Radiochemistry Scheme of a ^{68}Ge → ^{68}Ga Radionuclide Generator.** Chemical Bulletin of Kazakh National University. 2018, vol. 2018, no. 2, pp. 20-26. ISSN 1563-0331. (in Russian).

Baimukhanova, A. - Radchenko, V. - Kozempel, J. - Marinova, A. - Brown, V. - Karandashev, V. -Karaivanov, D. -Schaffer, P. - Filosofov, D.: **Utilization of (p, 4n) Reaction for ^{86}Zr Production with Medium Energy Protons and Development of a ^{86}Zr → ^{86}Y Radionuclide Generator.** Journal of Radioanalytical and Nuclear Chemistry. 2018, vol. 316, no. 1, pp. 191-199. ISSN 0236-5731.

Bárta, J. - Čuba, V. - Jarý, V. - Beitlerová, A. - Pánek, D. - Parkman, T. - Nikl, M.: **Photoinduced Preparation of Bandgap-Engineered Garnet Powders.** IEEE Transactions on Nuclear Science. 2018, vol. 65, no. 8, pp. 2184-2190. ISSN 0018-9499.

Bláha, P. - Koshlan N. A. - Koshlan, I. V. - Petrova, D. V. - Bogdanova, Y. V. - Govorun, R.D. - Múčka, V. -Krasavin, E. A.: **Delayed Effects of Accelerated Heavy Ions on the Induction of HPRT Mutations in V79 Hamster Cells.** Mutation Research - Fundamental and Molecular Mechanisms of Mutagenesis. 2017, vol. 803-805, pp. 35-41. ISSN 0027-5107.

Čubová, K. - Semelova, M. - Nemec, M. - John, J. - Milacic, J. - Omtvedt, J. P. - Stursa, J.: **Extraction of Thallium and Indium Isotopes as the Homologues of Nihonium into the Ionic Liquids.** Journal of Radioanalytical and Nuclear Chemistry. 2018, vol. 318, no. 3, pp. 2455-2461. ISSN 0236-5731.

Daňo, M. - Viglašová, E. - Galamboš, M. - Rajec, P. - Novák, I.: **Sorption Behaviour of Pertechnetate on Oxidized and Reduced Surface of Activated Carbon.** Journal of Radioanalytical and Nuclear Chemistry. 2017, vol. 314, no. 3, pp. 2219-2227. ISSN 0236-5731.

Distler, P. - Štamberg, K. - John, J. - Harwood, L. M. - Lewis, F. W.: **Modelling of the Am(III) - Cm(III) Kinetic Separation Effect Observed During Metal Ion Extraction by bis-(1,2,4)-triazine Ligands.** Separation Science and Technology. 2018, vol. 53, no. 2, pp. 277-285. ISSN 0149-6395.

Fibrich, M. - Šulc, J. - Zavadilová, A. - Jelínková, H.: **Nonlinear Mirror Mode-Locked Pr:YAlO3 Laser.** Laser Physics. 2017, vol. 27, no. 5. ISSN 1054-660X.

Fišera, O. - Kareš, J. - Procházková, L. - Popovich, K. - Bárta, J. - Čuba, V.: **Sorption Properties of Selected Oxidic Nanoparticles for the Treatment of Spent Decontamination Solutions Based on Citric Acid.** Journal of Radioanalytical and Nuclear Chemistry. 2018, vol. 318, no. 3, pp. 2443-2448. ISSN 0236-5731.

Hofmanová, E. - Červinka, R.: **Do We Really Understand Radionuclide Diffusion through Compacted Bentonite, after More than 30 Years of Study?** Bezpečnost jaderné energie. 2017, vol. 25, no. 63, pp. 23-27. ISSN 1210-7085. (in Czech).

Jarý, V. - Havlák, L. - Bárta, J. - Rejman, M. - Bystřický, A. - Dujardin, Ch. - Ledoux, G. - Nikl, M.: **Circadian Light Source Based on $K_xNa_{1-x}LuS_2:Eu^{2+}$ Phosphor.** ECS Journal of Solid State Science and Technology. 2018, vol. 7, no. 1, pp. R3182-R3188. ISSN 2162-8769.

Kolatorova Sosvorova, L. -Chlupacova, T. - Vitku, J. - Vlk, M. - Heracek, J. - Starka, L. - Saman, D. - Simkova, M. - Hampl, R.: **Determination of Selected Bisphenols, Parabens and Estrogens in Human Plasma Using LC-MS/MS.** Talanta. 2017, vol. 174, pp. 21-28.

Kozempel, J. - Mokhodoeva, O. - Vlk, M.: **Progress in Targeted Alpha-Particle Therapy. What We Learned about Recoils Release from In Vivo Generators.** Molecules. 2018, vol. 23, no. 3, ISSN 1420-3049.

Kreyling, W. G. - Holzwarth, U. - Haberl, N. - Kozempel, J. - Hirn, S. - Wenk, A. - Schleh, C. - Schäffler, M. - Lipka, J. - Semmler-Behnke M. - Gibson N.: **Quantitative Biokinetics of Titanium Dioxide Nanoparticles After Intravenous Injection in Rats (Part 1).** Nanotoxicology. 2017, vol 11, no. 4, pp. 434-442. ISSN 1743-5390.

Kreyling, W. G.- Holzwarth, U. - Schleh, C. - Kozempel, J. - Wenk, A. - Haberl, N. - Hirn, S. - Schäffler, M. - Lipka, J. - Semmler-Behnke M. - Gibson N.: **Quantitative Biokinetics of Titanium Dioxide Nanoparticles After Oral Application in Rats (Part 2).** Nanotoxicology. 2017, vol. 11, no. 4, pp. 443-453. ISSN 1743-5390.

Kreyling, W. G.- Holzwarth, U. - Haberl, N. - Kozempel, J. - Wenk, A. - Hirn, S. - Schleh, C. - Schäffler, M. - Lipka, J. - Semmler-Behnke M. - Gibson N.: **Quantitative Biokinetics of Titanium Dioxide Nanoparticles After Intratracheal Instillation in Rats (Part 3).** Nanotoxicology. 2017, vol. 11, no. 4, pp. 454-464. ISSN 1743-5390.

Lewis , F. W. - Harwood, L. M. - Hudson, M. J. - Afsar, A. - Laventine, D. M. - Šťastná, K. - John J. - Distler, P.: **Separation of the Minor Actinides Americium(III) and Curium(III) by Hydrophobic and Hydrophilic BTPhen Ligands: Exploiting Differences in their Rates of Extraction and Effective Separations at Equilibrium.** Solvent Extraction and Ion Exchange. 2018, vol. 36, no. 2, pp.115-135. ISSN 0736-6299.

Mihóková, E.- Babin, V. - Pejchal, J. - Čuba, V. - Bárta, J. - Popovich, K. - Schulman, L. S. - Yoshikawa, A. - Nikl, M.: **Afterglow and Quantum Tunneling in Ce-Doped Lutetium Aluminum Garnet.** IEEE Transactions on Nuclear Science. 2018, vol. 65, no. 8, pp. 2085-2089. ISSN 0018-9499.

Mrázek, J. - Kašík, I. - Procházková, L. - Čuba, V. - Girman, V. - Puchý, V. - Blanc, W. - Peterka, P. - Aubrecht, J. - Cajzl, J. - Podrazký, O.: **YAG Ceramic Nanocrystals Implementation into MCVD Technology of Active Optical Fibers.** Applied Sciences. 2018, vol. 8, no. 8, ISSN 2076-3417.

Múčka, V. - Červenák, J. - Reimitz, D. - Čuba, V. - Bláha, P. - Neužilová, B.: **Effects of Irradiation Conditions on the Radiation Sensitivity of Microorganisms in the Presence of OH-Radical Scavengers.** International Journal of Radiation Biology. 2018, vol. 94, no. 12, pp. 1142-1150. ISSN 0955-3002.

Neužilová, B. - Ondrák, L. - Čuba, V. - Múčka, V.: **Influence of the Dose Rate of Gamma Irradiation and Some Other Conditions on the Radiation Protection of Microbial Cells by Scavenging of OH Radicals.** Journal of Radioanalytical and Nuclear Chemistry. 2018, vol. 318, no. 3, pp. 2449-2453. ISSN 0236-5731.

Pejchal, J. - Barta, J. - Babin, V. - Beitlerova, A. - Prusa, P. - Kucerkova, R. - Panek, D. - Parkman, T. - Guguschev, C. - Havlak, L. - Zemenova, P. - Kamada, K. - Yoshikawa, A.: **Influence of Mg-Codoping, Non-Stoichiometry and Ga-Admixture on LuAG:Ce Scintillation Properties.** Optical Materials. 2018, vol. 86, pp. 213-232. ISSN 0925-3467.

Pejchal, J. - Buryi, M. - Babin, V. - Prusa, P. - Beitlerova, A. - Barta, J. - Havlak, L. - Kamada, K. - Yoshikawa, A. - Laguta, V. - Nikl, M.: **Luminescence and Scintillation Properties of Mg-Codoped LuAG:Pr Single Crystals Annealed in Air.** Journal of Luminescence. 2017, vol 181, pp. 277-285. ISSN 0022-2313.

Podrojková, N. - Oriňak, A. - Oriňaková, R. - Procházková, L. - Čuba, V. - Patera, J. - Smith, R. M.: **Effect of Different Crystalline Phase of ZnO/Cu Nanocatalysts on Cellulose Pyrolysis Conversion to Specific Chemical Compounds.** Cellulose. 2018, vol. 25, no. 10, pp. 5623-5642. ISSN 0969-0239.

Popovich, K. - Tomanová, K. - Čuba, V. - Procházková, L. - Pelikánová, I. T. - Jakubec, I. - Mihóková, E. - Nikl, M.: **LuAG:Pr^{3+}- Porphyrin Based Nanohybrid System for Singlet Oxygen Production: Toward the Next Generation of PDTX Drugs.** Journal of Photochemistry and Photobiology B: Biology. 2018, vol. 179, pp. 149-155. ISSN 1011-1344.

Procházková, L. - Čuba, V. - Beitlerová, A. - Jarý, V. - Omelkov, S. - Nikl, M.: **Ultrafast Zn(Cd,Mg)O:Ga Nanoscintillators with Luminescence Tunable by Band Gap Modulation.** Optics Express. 2018, vol. 26, no. 22, pp. 29482-29494. ISSN 1094-4087.

Rosa, T. G. - dos Santos, S. N. - Pinto, T. A. - Ghisleni, D. D. M. - Barja-Fidalgo, T. Ch. - Ricci-Junior, E. - Al-Qahtani, M. - Kozempel, J. - Bernardes, E. S. - Oliveira, R. S.: **Microradiopharmaceutical for Metastatic Melanoma.** PHARMACEUTICAL RESEARCH. 2017, vol. 34, no. 12, pp. 2922-2930. ISSN 0724-8741.

Rosendorf, T. - Hofmanová, E. - Vopálka, D. - Vetešník, A. - Červinka, R.: **Comparative Study of HTO Diffusion on Individual and Coupled Systems of Compacted Bentonite and Fresh Ordinary Portland Cement Paste.** Applied Geochemistry. 2018, vol. 97, pp. 102-108. ISSN 0883-2927.

Smrček, S. - Kozempel, J. - Vlk, M. - Nykl, P. - Psondrova, S. - Krmelova, T.: **Environmental Aspects of Radiopharmaceuticals: Extraction and Translocation of Ra-223 in Plants.** International Journal of Environmental Engineering. 2017, vol. 4, no. 1, pp. 50-53. ISSN 2374-1724.

Suchánková, P. - Červenák, J. - Kozempel, J. - Vlk, M.: **Targeted Alpha Therapy and its Role in a Modern Nuclear Medicine.** Nukleární medicína. 2018, vol. 2018, no. 7, pp. 7-12. ISSN 1805-1146. (in Czech).

Špendlíková, I. - Němec, M. - Steier, P. - Keçeli, G.: **Sorption of Uranium on Freshly Prepared Hydrous Titanium Oxide and its Utilization in Determination of ^{236}U Using Accelerator Mass Spectrometry.** Journal of Radioanalytical and Nuclear Chemistry. 2017, vol. 311, no. 1, pp. 447-453. ISSN 0236-5731.

Šťastná, K. - Distler, P. - John, J. - Šebesta, F.: **Separation of Curium from Americium Using composite sorbents and Complexing Agent Solutions: Part 2.** Journal of Radioanalytical and Nuclear Chemistry. 2017, vol. 312, no. 3, pp. 685-689. ISSN 0236-5731.

Tomanová, K. - Přeček, M. - Múčka, V. - Vyšín, L. - Juha, L. - Čuba, V.: **At the Crossroad of Photochemistry and Radiation Chemistry: Formation of Hydroxyl Radicals in Diluted Aqueous Solutions Exposed to Ultraviolet Radiation.** Physical Chemistry Chemical Physics. 2017, vol. 19, no. 43, pp. 29402-29408. ISSN 1463-9076.

Vencovský, V. - Vetešník, A.: **Analysis of Level Dependence of 2f(1) - f(2) Component of Otoacoustic Emissions Using Nonlinear 2D Cochlear Model.** Acta Acustica united with Acustica. 2018, vol. 104, no. 5, pp. 891-894. ISSN 1610-1928.

Viglašová, E. - Daňo, M. - Galamboš, M. - Krajňák, A. - Rosskopfová, O. - Rajec, P.: **Investigation of Cu(II) Adsorption on Slovak Bentonites and Illite/Smectite for Agricultural Applications.** Journal of Radioanalytical and Nuclear Chemistry. 2017, vol. 314, no. 3, pp. 2425-2435. ISSN 0236-5731.

Vyšín, L. - Burian, T. - Ukraintsev, E. - Davídková, M. - Grisham, M. E. - Heinbuch, S. - Rocca, J. J. - Juha L.: **Dose-Rate Effects in Breaking DNA Strands by Short Pulses of Extreme Ultraviolet Radiation.** Radiation Research. 2018, vol. 189, no. 5, pp. 466-476. ISSN 0033-7587.

Vyšín, L. - Davídková, M. - Wachulak, P. - Fiedorowicz, H. - Bartnik, A. - Krůs, M. - Kozlová, M. - Skála, J. - Dostál, J. - Dudžák, R. - Juha, L.: **Biological Action in and out of the Water Window.** Acta Physica Polonica A. 2018, vol. 133, no. 2, pp. 236-238. ISSN 1898-794X.

Vyšín, L.- Tomanová, K. - Pavelková, T. - Wagner, R. - Davídková, M. - Múčka, V. - Čuba, V.: **Degradation of Phospholipids under Different Types of irradiation and Varying Oxygen Saturation.** Radiation and Environmental Biophysics. 2017, vol. 56, no. 3, pp. 241-247. ISSN 0301-634X.

Westwood, J. - Harwood, L. M. - Afsar, A. - Cowell, J. - Distler, P. - John, J.: **Synthesis and Screening of a Novel (dppz)-BTPhen Ligands for the Separation of Americium from Europium.** Letters in Organic Chemistry. 2018, vol. 15, no. 5, pp. 340-344. ISSN 1570-1786.

CONFERENCE CONTRIBUTIONS

Babain, V. - Alyapyshev, M. - Voronaev, I.G. - Tkachenko, L. - Kenf, E.V. - Mindová, M. - Distler, P. - John, J.: **Fluorinated Carbonates as New Diluents for Extraction of f-Elements.** In: Czech Chemical Society, Symposium Series 2. 18th Radiochemical Conference, Mariánské Lázně. Praha: Česká společnost chemická, 2018, vol. 16, p. 135. ISSN 2336-7202.

Baborová, L. - Vopálka, **D.: Time Development of Cs and Sr Concentration Profiles In Compacted Bentonite.** In: The 7th International Conference on Clays in Natural and Engineered Barriers for Radioactive Waste Confinement. Clay Conference 2017, Davos, Basel: Congrex Switzerland Ltd., 2017, pp. 602-603.

Baborová, L. - Vopálka, D.: **Sorption of Sr and Cs onto Czech Natural Bentonite - Experiments and Modelling.** In: Czech Chemical Society, Symposium Series 2. 18th Radiochemical Conference, Mariánské Lázně. Praha: Česká společnost chemická, 2018, vol. 16, p. 198. ISSN 2336-7202.

Baimukhanova, A. - Chakrova, E. - Roesch, F. - Kozempel, J. - Filosofov, D.: **Production of Positron Emitter Radionuclide ^{68}Ga via Generator ^{68}Ge → ^{68}Ga.** In: Czech Chemical Society, Symposium Series 2. 18th Radiochemical Conference, Mariánské Lázně. Praha: Česká společnost chemická, 2018, vol. 16, p. 248. ISSN 2336-7202.

Bárta, J. - Jarý, V. - Beitlerova, A. - Čuba, V. - Nikl, M.: **Photo-Induced Preparation of Band-Gap-Engineered Garnet Powders.** In: SCINT 2017 - Abstracts: Poster Session 2. SCINT 2017 - 14th Int. Conference on Scintillating Materials and their Applications, Chamonix. Genéve: CERN, 2017.

Bárta, J. - Kuzár, M. - Müllerová, E. - Procházková, L. - Čuba, V. - Nikl, M.: **Photochemical Synthesis and Characterization of Multi-Component Garnet Powders.** In: Lumdetr 2018 Book of Abstracts. Praha: České vysoké učení technické v Praze, Fakulta jaderná a fyzikálně inženýrská, 2018, p. 125. ISBN 978-80-01-06479-5.

Bárta, J. - Tomanová, K. - Procházková, L. - Vaněček, V. - Kuzár, M. - Nikl, M. - Čuba, V.: **Photochemical Synthesis of Nanoparticles in Aqueous Solutions.** In: ANGEL 2018 - Book of Abstracts. Lyon: University Claude Bernard Lyon 1, 2018, p. 39.

Bartl, P. - Omtvedt, J. P. - John, J. - Němec, M. - Sochor,J. - Štursa, J.: **Microfluidic Studies of SHE Homologues in New Facility at NPI REZ.** In: Czech Chemical Society, Symposium Series 2. 18th Radiochemical Conference, Mariánské Lázně. Praha: Česká společnost chemická, 2018, vol. 16, p. 268. ISSN 2336-7202.

Červenák, J. - Čepa, A. - Ráliš, J. - Tomeš, M. - Kozempel, J. - Vlk, M. - Seifert, D. - Lebeda, O.: **Labelling of Peptides by ^{68}Ga a ^{64}Cu radionuclides.** In: 54. Dny Nukleární Medicíny. Špindlerův Mlýn. . Praha: Česká lékařská společnost J. E. Purkyně, 2017, p. 6. ISSN 1805-1146. (in Czech).

Distler, P. - Afsar, A. - Šťastná, K. - Westwood, J. - Lewis, F. W. - Štamberg, K. - John, J. - Harwood, L.: **Partitioning of Minor An(III) and Ln(III) by the 1,2,4-Triazine Extracting Compounds.** In: Czech Chemical Society, Symposium Series 2. 18th Radiochemical Conference, Mariánské Lázně. Praha: Česká společnost chemická, 2018, vol. 16, p. 56. ISSN 2336-7202.

Fenclová, K. - Němec, M. - Prášek, T. - John, J. - Daňo, M. - Bilous, M.: **Accelerator Mass Spectrometry - New Possibilities for Selected Actinides Determination.** In: Czech Chemical Society Symposium Series 5. 70. Sjezd českých a slovenských chemických společností. Praha: Česká společnost chemická, 2018, vol. 16. ISSN 2336-7202. (in Czech).

Fialová, K. - Vlk, M. - Kozempel, J.: **Separation of ^{223}Ra in nuclear medicine.** In: Osmančíková, P. - Hanušová, T. eds.: Kutnohorský experiment - Studentská konference radiologické fyziky 2017. Kutná Hora. Praha: ČVUT, Fakulta jaderná a fyzikálně inženýrská, KDAIZ, 2017, p. 14. (in Czech).

Fialová, K. - Vlk, M. - Kozempel, J.: **Synthesis of Diglycolamide Extraction Agents Anchored to Polyacrylonitrile Matrix.** In: Zborník recenzovaných príspevkov - Študentská vedecká konferencia PriF UK 2017. Bratislava. Bratislava: Univerzita Komenského, Přírodovědecká fakulta, 2017, pp. 910-915. ISBN 978-80-223-4310-7. (in Czech).

Fialová, K. - Vlk, M. - Kozempel, J. - Šebesta, F. - Dračínský, M.: **Synthesis of Diglycolamide Extraction Agents Anchored to Polyacrylonitrile Matrix.** In: Czech Chemical Society, Symposium Series 2. 18th Radiochemical Conference, Mariánské Lázně. Praha: Česká společnost chemická, 2018, vol. 16, pp. 136-137. ISSN 2336-7202.

Hupka, I. - Pokorný, M. - Zavadilová, A.: **Speciation and Luminescence Properties of Eu(III) and U(VI) in Solutions Using Complexing Agents.** In: Czech Chemical Society, Symposium Series 2. 18th Radiochemical Conference, Mariánské Lázně. Praha: Česká společnost chemická, 2018, vol. 16, p. 118. ISSN 2336-7202.

Hupka, I. - Zavadilová, A.: **Determination of low concentrations of uranium by Laser-induced Fluorescence with Use of Complexing Agents.** In: Bulletin spektroskopické společnosti Jana Marka Marci. Praha: Spektroskopická společnost Jana Marka Marci, 2018, p. 179. (in Slovak)

Jarý, V. - Havlák, L. - Bárta, J. - Rejman, M. - Nikl, M.**: Eu^{2+}-Doped $ARES_2$ Sulfides - Novel Multifunctional Optical Materials.** In: Lumdetr 2018 Book of Abstracts. Praha: České vysoké učení technické v Praze, Fakulta jaderná a fyzikálně inženýrská, 2018, p. 98. ISBN 978-80-01-06479-5.

Kittnerová, J. - Drtinová, B. - Vopálka, D.: **A Comparative Study of Radium and Strontium Uptake by Cementitious Materials.** In: Czech Chemical Society, Symposium Series 2. 18th Radiochemical Conference, Mariánské Lázně. Praha: Česká společnost chemická, 2018, vol. 16, p. 133. ISSN 2336-7202.

Kittnerova, J. - Lange, S. - Drtinová, B. - Deissmann, G. - Bosbach, D. - Vopálka, D.: **Impact of Carbonation on the Uptake of Radium by Cementitious Materials.** In: NUWCEM 2018 Book of Abstracts. Paris: CEA, 2018.

Kozempel, J. - Vlk, M. - Kukleva, E. - Sakmár, M. - Suchánková, P.: **Hydroxyapatite Nanoparticles as Theranostic Vectors for Radiopharmacy.** In: Symposium Scientific Programme and Collection of Abstracts. 13th International Symposium on the Synthesis and Application of Isotopically Labelled Compounds, Praha. Praha: Česká společnost chemická, 2018, p. 105. ISBN 978-80-86238-89-0.

Kozempel, J. - Vlk, M. - Mičolová, P. - Kukleva, E. - Nykl, P. - Sakmár, M.: **Nanocarriers of ^{223}Ra for TAT.** In: 10th International Symposium on Targeted Alpha Therapy. Kanazawa. Ispra: European Commission - Joint Research Centre, 2017. p. 49.

Kozempel, J. - Vlk, M. - Suchánková, P. - Kukleva, E. - Nykl, P. - Sakmár, M.: **^{223}Ra Nanocarriers for Targeted Alpha Therapy.** In: 54. Dny Nukleární Medicíny. Špindlerův Mlýn. Praha: Česká lékařská společnost J. E. Purkyně, 2017, p. 11. ISSN 1805-1146. (in Czech).

Kukleva, E. - Mičolová, P. - Kozempel, J. - Vlk, M. - Sakmár, M.: **Hydroxyapatite Nanoparticles labelled by ^{68}Ga and ^{18}F.** In: XXXIX. Pracovní dny Radiofarmaceutické sekce České společnosti nukleární medicíny. Kroměříž, Praha: ČLS JEP, 2017. (in Czech).

Kukleva, E. - Mičolová, P. - Nykl, P. - Sakmár, M. - Vlk, M. - Kozempel, J. - Nespesna, L.: **Hydroxyapatite nanoparticles labelled with medicinal radionuclides.** In: The 22nd International Symposium on Radiopharmaceutical Sciences (ISRI 2017). Dresden. New York: J. Wiley, 2017, p. 446. vol. 60. ISSN 0362-4803.

Kukleva, E. - Vlk, M. - Kozempel, J.: **Alfa a beta zářiče v terapii**. In: Osmančíková, P. - Hanušová, T. eds.: Kutnohorský experiment - Studentská konference radiologické fyziky 2017. Kutná Hora. Praha: ČVUT, Fakulta jaderná a fyzikálně inženýrská, KDAIZ, 2017, p. 25. (in Czech).

Kukleva, E. - Vlk, M. - Kozempel, J.: **Hydroxyapatite Nanoparticles Labelled with ^{18}F.** In: Czech Chemical Society, Symposium Series 2. 18th Radiochemical Conference, Mariánské Lázně. Praha: Česká společnost chemická, 2018, vol. 16, p. 236. ISSN 2336-7202.

Kukleva, E. - Vlk, M. - Kozempel, J. - Suchánková, P.: **Dota Decorated Hydroxyapatite Nanoparticles Labelled with ^{68}Ga.** In: Symposium Scientific Programme and Collection of Abstracts. 13th International Symposium on the Synthesis and Application of Isotopically Labelled Compounds, Praha. Praha: Česká společnost chemická, 2018, p. 107. ISBN 978-80-86238-89-0.

Málková, E. - Mičolová, P. - Vlk, M. - Marešová, L. - Jandová, L. - Nagy, R. - Hrubý, M. - Kozempel, J.: **In vivo Studies with [^{223}Ra]HANPs on Nu-Nude mice and B16-F10 melanoma.** In: XXXIX. Pracovní dny Radiofarmaceutické sekce České společnosti nukleární medicíny. Kroměříž, Praha: ČLS JEP, 2017. (in Slovak).

Micolova, P. - Kukleva, E. - Nykl, P. - Sakmár, M. - Vlk, M. - Nespesna, L. - Kozempel, J.: **Titanium Dioxide - Perspective Nanocarrier Material for Medicinal Nuclides Delivery Systems.** In: The 22nd International Symposium on Radiopharmaceutical Sciences (ISRI 2017). Dresden. New York: J. Wiley, 2017, p. 283. vol. 60. ISSN 0362-4803.

Mihóková, E. - Popovich, K. - Procházková, L. - Pelikánová, I. T. - Čuba, V. - Jakubec, I. - Tomanová, K. - Dědic, R. - Nikl, M.: **Novel Scintillating Nanocomposites for X-Ray Induced Photodynamic Therapy.** In: Lumdetr 2018 Book of Abstracts. Praha: České vysoké učení technické v Praze, Fakulta jaderná a fyzikálně inženýrská, 2018. ISBN 978-80-01-06479-5.

Neužilová, B. - Múčka, V.: **Decrease of the Radiation Sensitivity of the Microorganisms Irradiated with the UV-radiation in the Presence of Scavengers of OH Radicals.** In: ChemZi. 69. zjazd chemikov, Vysoké Tatry, Horný Smokovec. Bratislava: Chemicke zvesti, 2017. ISSN 1336-7242. (in Czech).

Neužilová, B. - Múčka, V. - Ondrák, L.: **Ethanol as a Modifier of Radiation Sensitivity of Living Cells Against UV-radiation.** In: XL. Dny radiační ochrany, sborník abstraktů. XL. Dny radiační ochrany, Mikulov. Praha: Czech Technical University in Prague. 2018, p. 164. ISBN 978-80-01-06503-7. (in Czech).

Neužilová, B. - Múčka, V. - Ondrák, L. - Čuba, V.: **Influence of Gamma Radiation Dose Rate and Some Other Parameters on the Radiation Protection of Microbial Cells by OH Radical Scavenging.** In: Czech Chemical Society, Symposium Series 2. 18th Radiochemical Conference, Mariánské Lázně. Praha: Česká společnost chemická, 2018, vol. 16, p. 221. ISSN 2336-7202.

Nový, Z. - Petřík, M. - Gurská, S. - Kozempel, J. - Vlk, M. - Lobaz, V. - Kučka, J. - Hrubý, M. - Drymlová, J. - Hajdúch, M.: **Preparation of ^{99m}Tc-labelled hydroxyapatite nanoparticles and their in vitro/in vivo characterization**. In: XXXIX. Pracovní dny Radiofarmaceutické sekce České společnosti nukleární medicíny. Kroměříž, Praha: ČLS JEP, 2017. (in Czech).

Ondrák, L. - Múčka, V.: **Modification of Eukaryotic Cells´ Radiation Sensitivity by Various Hydroxyl Radical Scavengers.** In: Czech Chemical Society, Symposium Series 2. 18th Radiochemical Conference, Mariánské Lázně. Praha: Česká společnost chemická, 2018, vol. 16, p. 222. 16. vol. 2. ISSN 2336-7202.

Ondrák, L. - Vachelová, J. - Davídková, M. - Neužilová, B. - Múčka, V.: **Protection of Cells against Ionizing Radiation Using Hydroxyl Radicals Scavengers.** In: XL. Dny radiační ochrany, sborník abstraktů. XL. Dny radiační ochrany, Mikulov. Praha: Czech Technical University in Prague. 2018, p. 152. ISBN 978-80-01-06503-7. (in Czech).

Pejchal, J. - Barta, J. - Kucerkova, R. - Beitlerova, A. - Nikl, M.: **Luminescence and Scintillation Properties of Rare-Earth-Doped $LaAlO_3$ Single Crystals.** In: Lumdetr 2018 Book of Abstracts. Praha: České vysoké učení technické v Praze, Fakulta jaderná a fyzikálně inženýrská, 2018, p. 139. ISBN 978-80-01-06479-5.

Pokorný, M. - Hupka, I. - Zavadilová, A.: **Study of Europium Speciation Using Time-resolved Laserinduced Luminiscence Spectroscopy.** In: Czech Chemical Society, Symposium Series 2. 18th Radiochemical Conference, Mariánské Lázně. Praha: Česká společnost chemická, 2018, vol. 16, p. 81. ISSN 2336-7202.

Popovich, K. - Šípková, M. - Čuba, V. - Procházková, L. - Nikl, M.: **Luminescent Properties of Cerium-Doped YSO/LSO/LYSO microcrystals prepared via Room Temperature Sol-Gel Route.** In: Lumdetr 2018 Book of Abstracts. Praha: České vysoké učení technické v Praze, Fakulta jaderná a fyzikálně inženýrská, 2018, p. 140. ISBN 978-80-01-06479-5.

Popovich, K. - Tomanová, K. - Procházková, L. - Jarý, V - Nikl, M. - Mihokova, E. - Jakubec, I. - Čuba, V.: **LuAG:Pr^{3+} - Based Nanohybrid Systems for Singlet Oxygen Generation.** In: SCINT 2017 - Abstracts: Poster Session 2. SCINT 2017 - 14th Int. Conference on Scintillating Materials and their Applications, Chamonix. Genéve: CERN, 2017.

Prášek, T. - Němec, M.: **Preparation of Fluoride Target Matrices for ^{236}U AMS Measurement.** In: Czech Chemical Society, Symposium Series 2. 18th Radiochemical Conference, Mariánské Lázně. Praha: Česká společnost chemická, 2018, vol. 16, p. 162. ISSN 2336-7202.

Prášek, T. - Němec, M.: **Preparation of Fluoride Target Matrices for ^{236}U AMS Measurement.** In: Czech Chemical Society Symposium Series 5. 70. Sjezd českých a slovenských chemických společností. Praha: Česká společnost chemická, 2018, vol. 16. ISSN 2336-7202.

Prášek, T. - Neufussová, I. - Němec M.: **Preparation of Target Materials with Fluoride Matrix for ^{236}U Determination by Means of Accelerator Mass Spectrometry.** In: ChemZi. 69. zjazd chemikov, Vysoké Tatry, Horný Smokovec. Bratislava: Chemicke zvesti, 2017. ISSN 1336-7242. (in Czech).

Procházková, L. - Čuba, V.: **Radiation-induced preparation of ZnO:Ga-Based Scintillators with Band Gap Modulation.** In: Czech Chemical Society, Symposium Series 2. 18th Radiochemical Conference, Mariánské Lázně. Praha: Česká společnost chemická, 2018, vol. 16, p. 224. ISSN 2336-7202.

Procházková, L. - Čuba, V. - Nikl, M.: **Tailoring of ZnO Luminescence Properties by Controlled Doping.** In: The 5th International Conference on the Physics of Optical Materials and Devices. BOOK OF ABSTRACTS. Igalo, Montenegro. Beograd: Institut za nuklearne nauke "Vinča" Beograd, 2018. ISBN 978-86-7306-141-2.

Procházková, L. - Vaněček, V. - Čuba, V. - Nikl, M.: **Luminescent ZnO:Ga Nanopowder: Surface Passivation and Limiting the Particle Agglomeration.** In: SCINT 2017 - Abstracts: Poster Session 3. SCINT 2017 - 14th Int. Conference on Scintillating Materials and their Applications, Chamonix. Genéve: CERN, 2017.

Procházková, L. - Vaněček, V. - Martinez-Turtos, R. - Nikl, M. - Čuba, V. - Auffray, E.: **ZnO:Ga-Core-Shells Embedded in Polystyrene Matrix.** In: Lumdetr 2018 Book of Abstracts. Praha: České vysoké učení technické v Praze, Fakulta jaderná a fyzikálně inženýrská, 2018, p. 197. ISBN 978-80-01-06479-5.

Sakmár, M. - Vlk, M. - Kozempel, J. - Kukleva, E. - Suchánková, P.: **Surface modification of ^{99m}TC-HAp-NPs.** In: Czech Chemical Society, Symposium Series 2. 18th Radiochemical Conference, Mariánské Lázně. Praha: Česká společnost chemická, 2018, vol. 16. ISSN 2336-7202.

Sakmár, M. - Vlk, M. - Kozempel, J.: **Application of ^{11}C, ^{13}N and ^{15}O Short-lived Positron Emmitters in Nuclear Medicine.** In: Osmančíková, P. - Hanušová, T. eds.: Kutnohorský experiment - Studentská konference radiologické fyziky 2017. Kutná Hora. Praha: ČVUT, Fakulta jaderná a fyzikálně inženýrská, KDAIZ, 2017, p. 29. (in Slovak).

Sakmár, M. - Vlk, M. - Suchánková, P. - Kukleva, E. - Kozempel, J. - Hrubý, M. - Lobaz, V.: **In Vitro and In Vivo Studies of ^{223}Ra Labelled HAp Nanoparticles Modificated with Phosphonic Acids.** In: Symposium Scientific Programme and Collection of Abstracts. 13th International Symposium on the Synthesis and Application of Isotopically Labelled Compounds, Praha. Praha: Česká společnost chemická, 2018, p. 117. ISBN 978-80-86238-89-0.

Shashkova, E. - Vlk, M. - Bildziukevich, U. - Šusteková, J. - Šaman, D. - Wimmer, Z. - Kozempel, J.: **Complexes of Stigmasterol Hemiesters with L, D-Tryptophan.** In: Symposium Scientific Programme and Collection of Abstracts. 13th International Symposium on the Synthesis and Application of Isotopically Labelled Compounds, Praha. Praha: Česká společnost chemická, 2018, p. 121. ISBN 978-80-86238-89-0.

Sobkuliaková, Z. - Valová, V. - Kukleva, E. - Sakmár, M. - Mokhodoeva, O. - Vlk, M. - Kozempel, J.: **Labelled Superparamagnetic Iron Oxide Nanoparticles.** In: Czech Chemical Society, Symposium Series 2. 18th Radiochemical Conference, Mariánské Lázně. Praha: Česká společnost chemická, 2018, vol. 16, pp. 236-237. ISSN 2336-7202.

Tomanová, K. - Čuba, V. - Procházková, L. - Jakubec, I. - Bárta, J. - Mihóková, E. - Turtos, R. M. - Auffray, E. - Nikl, M.: **Blue-Emitting $CsPbBr_3$ Nanocrystals with Ultrafast Decay.** In: Lumdetr 2018 Book of Abstracts. Praha: České vysoké učení technické v Praze, Fakulta jaderná a fyzikálně inženýrská, 2018, p. 143. ISBN 978-80-01-06 479-5.

Tomanová, K. - Popovich, K. - Jakubec, I. - Procházková, L. - Nikl, M. - Mihokova, E. – Čuba, V.: **Silica Coating of Scintillating Nanoparticles.** In: SCINT 2017 - Abstracts: Poster Session 2. SCINT 2017 - 14th Int. Conference on Scintillating Materials and their Applications, Chamonix. Genéve: CERN, 2017.

Urbanová, K. - Seifert, D. - Vlk, M. - Ucar, E. - Kozempel, J.: **Galium-68 Labelling on the Microfluidic Systems.** In: Symposium Scientific Programme and Collection of Abstracts. 13th International Symposium on the Synthesis and Application of Isotopically Labelled Compounds, Praha. Praha: Česká společnost chemická, 2018, p. 125. ISBN 978-80-86238-89-0.

Valová, V. - Kukleva, E. - Mičolová, P. - Kománková, L. - Mokhodoeva, O. - Vlk, M. - Kozempel, J.: **Superparamagnetic 'Core-shell' Nanoprobes.** In: XXXIX. Pracovní dny Radiofarmaceutické sekce České společnosti nukleární medicíny. Kroměříž, Praha: ČLS JEP, 2017. (in Czech).

Valová, V. - Sobkuliaková, Z. - Kukleva, E. - Mokhodoeva, O. - Vlk, M. - Kozempel, J.: **Magnetic nanoparticles labelled with ^{68}Ga and ^{18}F.** In: 55. Dny Nukleární Medicíny. Mikulov. Praha: Česká lékařská společnost J. E. Purkyně, 2018. p. 12. ISSN 1805-1146. (in Czech).

Valová, V. - Sobkuliaková, Z. - Kukleva, E. - Sakmár, M. - Mokhodoeva, O. - Vlk, M. - Kozempel J.: **Theranostic Superparamagnetic Iron Oxide Nanovectors.** In: Symposium Scientific Programme and Collection of Abstracts. 13th International Symposium on the Synthesis and Application of Isotopically Labelled Compounds, Praha. Praha: Česká společnost chemická, 2018, p. 126. ISBN 978-80-86238-89-0.

Vencovský, V. - Vetešník, A.: **Theoretical Study on Onset of Cubic Distortion Product Otoacoustic Emissions.** In: To the Ear and Back Again - Advances in Auditory Biophysics: Proceedings of the 13th Mechanics of Hearing Workshop. St. Catharines. Melville. NY: AIP Publishing, 2018, p. 1-7. AIP Conference Proceedings. vol. 1965. ISSN 0094-243X. ISBN 978-0-7354-1670-3.

Vencovský, V. - Vetešník, A. - Rund, F.: **The Relationship Between SFOAEs and Tuning of Cochlear Filters in a Model of the Human Cochlea.** In: To the Ear and Back Again - Advances in Auditory Biophysics: Proceedings of the 13th Mechanics of Hearing Workshop. St. Catharines. Melville. NY: AIP Publishing, 2018, p. 1-7. AIP Conference Proceedings. vol. 1965. ISSN 0094-243X. ISBN 978-0-7354-1670-3.

Višňák, J. - Sobek, L.: **Multilinear Analysis of Time-Resolved Laser-Induced Fluorescence Spectra of U(VI) Containing Natural Water Samples.** In: EPJ Web Conferences. Theoretical and Experimental Studies in Nuclear Applications and Technology, Adana, Les Ulis Cedex A: EDP Sciences - Web of Conferences, 2017, vol. 154.

Višňák, J. - Steudtner, R. - Kassahun, A. - Hoth, N.: **Multilinear Analysis of Time-Resolved Laser-Induced Fluorescence Spectra of U(VI) Containing Natural Water Samples.** In: EPJ Web Conferences. Theoretical and Experimental Studies in Nuclear Applications and Technology, Adana, Les Ulis Cedex A: EDP Sciences - Web of Conferences, 2017, vol. 154.

Višňák, J. - Steudtner, R. - Kassahun, A. - Hoth, N. - Sobek, L.: **Uranyl - Carbonate - Ca(2+)/Mg(2+) Aqueous System Spectroscopic Experimental and Theoretical Study - Molecular Modelling Meets Environmental Protection.** In: Czech Chemical Society, Symposium Series 2. 18th Radiochemical Conference, Mariánské Lázně. Praha: Česká společnost chemická, 2018, vol. 16, p. 117. ISSN 2336-7202.

Višňák, J. - Veselý, P.: **Quantum Algorithms for Computational Nuclear Physics Revisited, Particular Case of Second Quantized Formulation.** In: EPJ Web Conferences. Theoretical and Experimental Studies in Nuclear Applications and Technology, Adana,. Les Ulis Cedex A: EDP Sciences - Web of Conferences, 2017. vol. 154.

Vlk, M. - Mokhodoeva, O. - Micolova, P. - Valova, V. - Malkova, E. - Maresova, L. - Slouf, M. - Kozempel, J.: **Preparation and In Vivo Evaluation of [^{223}Ra]@Fe_3O_4 Nanoparticles - Novel Vehicles for Targeted Alpha Particle Therapy.** In: The 22nd International Symposium on Radiopharmaceutical Sciences (ISRI 2017). Dresden. New York: J. Wiley, 2017, p. 609. vol. 60. ISSN 0362-4803.

Vlk, M. - Nykl, P. - Sakmár, M. - Málková, E. - Kukleva, E. - Mičolová, P. - Lobaz, V. - Šlouf, M. - Hrubý, M. - Kozempel, J.: **Nanocarrier Stabilization prior to the ^{99m}Tc, ^{68}Ga and ^{223}Ra Labelling.** In: XXXIX. Pracovní dny Radiofarmaceutické sekce České společnosti nukleární medicíny. Kroměříž, Praha: ČLS JEP, 2017. (in Czech).

Vlk, M. - Valová V. - Sobkuliaková Z. - Kozempel J.: **Multimodal Magnetic Nanoprobes.** In: 55. Dny Nukleární Medicíny. Mikulov. Praha: Česká lékařská společnost J. E. Purkyně, 2018. p. 12. ISSN 1805-1146. (in Czech).

REPORTS

Čubová, K. - Baborová, L. - Němec, M. - John, J.: **Speciation of Radionuclides under the Conditions of Repository for Wastes Unacceptible to LLW/ILW Repository.** [Research Report] Praha 1: Správa úložišť radioaktivních odpadů, 2017. Report no. SÚRAO TZ 207/2017. (in Czech).

Večerník, P. - Drtinová, B. - Bárta, J. - Brázda, L. - Havlová, V. - Kittnerová, J. - Kolomá, K. - Rosendorf, T.: **Transport Characteristics of Cementitious Materials III.** [Research Report] 2017. Report no. SÚRAO TZ 209/2017. (in Czech).

Němec, M. - Sochor, J.: **Report on MEET-CINCH Project Survey about Nuclear Chemistry Educational Videos.** MEET-CINCH Project Deliverable D1.5, 2018.

Němec, M. - John, J. - Šácha, M. - Scully, P.: **Functional Requirements for the MEET-CINCH E-learning Platform.** MEET-CINCH Project Deliverable D2.3, 2018.

Scully. P. - Němec, M. - John, J. - Šácha, M.: **Potential Options for Design and Hosting of an E-learning Platform.** MEET-CINCH Project Deliverable D2.4, 2018.

PATENTS

Adámek, K. - Šebesta, F. - Vlk, M. - Fialová, K. - Kozempel, J. - Kukleva, E.: **Sorbent for Radionuclide Generator ^{68}Ge/^{68}Ga.** Functional Sample. 2018 (in Czech).

Čuba, V. - Bárta, J. - Popovich, K. - Procházková, L.: **Inorganic Powder Scintillator for LSC.** Functional Sample. 2017 (in Czech).

Čubová, K. - Němec, M. - Straka, M. - Szatmáry, L.: **Method of Removing Cobalt from Aqueous Solutions.** Patent Application (in Czech).

Kovařík, P. - Navratil, J.D. - John, J.: **A Method of Processing Hazardous and Radioactive Waste.** Czech Republic. Patent CZ 306880. 2017-07-12 (in Czech).

Kozempel, J. - Vlk, M. - Mičolová, P. - Kukleva, E. - Jandová, L. - Merhautová, H. - Ficenzová, K.: **A Combination for Radionuclide Therapy for the Use as a Medicine.** Czech Republic. Patent CZ 307369. 2018-05-23 (in Czech).

Kozempel, J. - Vlk, M. - Mičolová, P. - Kukleva, E. - Fialová, K. - Kománková, L. - Bajzíková, A. - Podlaha, J.: **A Method of Ac Isolation from a Mixture of Radium, Actinium and Thorium.** Czech Republic. Patent CZ 306722. 2017-04-12 (in Czech).

Kukleva, E. - Kozempel, J. - Vlk, M.: **[^{18}F]F-nHAp.** Functional Sample. 2017.

Kukleva, E. - Kozempel, J. - Vlk, M. - Sakmár, M. - Fialová, K. - Lobaz, V. - Hrubý, M.: **[^{99m}Tc]HAp-PEG.** Functional Sample. 2017.

Kukleva, E. - Sakmár, M. - Kozempel, J. - Vlk, M. - Suchánková, P. - Lobaz, V. - Hrubý, M.: **[^{99m}Tc]HAp-PEOX.** Functional Sample. 2017.

Popovich, K. - Čuba, V. - Bárta, J. - Procházková, L.: **An Automated Device for the Continuous Photochemical Preparation of Nanoparticles of Metals or Metal Oxides from Aqueous Solutions.** Czech Republic. Utility Model CZ 31858. 2018-06-19 (in Czech).

THESES

Author, **Title**, *Supervisor, Year*

DOCTORAL / DISSERTATION

Distler, P.

Study of Extraction Systems for Lanthanoids and Minor Actinoids Partitioning

John, J. / Štamberg, K., 2017

Kužel, F.

Optimization of přípravy [^{18}F] fluorocholine preparation

Adam, J. (ÚJV Řež, a. s.), 2017

Blaha, P.

Induction of HPRT Mutations in Mammalian Cells After Irradiation with Heavy Ions

Múčka, V. / Koshlan, I. (JINR Dubna), 2017

Procházková, L.

Nanocomposite Scintillators Based on Zinc Oxide with Band Gap Modulation

Čuba, V., 2018

MASTER / DIPLOMA

Hupka, I.

Determination of Low Uranium Concentration in Presence of Complexing Agents by Laser Induced Fluorescence Method

Zavadilová, A., 2017

Kittnerová, J.

Sorption of Radium on Cementitious Materials

Drtinová, B., 2017

Kománková, L.

Preparation and Characterization of the Material for Bone Tissue Engineering

Vetrik, M. (IMC ASCR), 2017

Neužilová, B.

The Use of Scavengers of Radicals in Cultures Irradiated under Various Conditions

Múčka, V., 2017

Nykl, P.

Plant Uptake and Translocation of Labelled Nanoparticles

Vlk, M., 2017

Pastorek, A.

A Study on Synthesis of Biogenic Molecules´ Formation by the Effects of Ionising Radiation

Civiš, S. (JH IPC ASCR), 2017

Reimitz, D.

Synergy of Ionizing Radiation with Platinum and Rhuthenium-Based Chemotherapeutic Drugs in DNA Damage Induction

Davídková, M. (INP ASCR), 2017

Adámek, K.

Development and Testing of Radionuclide Generator ^{68}Ge - ^{68}Ga

Šebesta, F., 2018

Beck, P.

Radiation Preparation of Metal Nanoparticles (Ag, Pt) in the Associative Colloids

Silber, R., 2018

Florianová, M.

Energetic Ion Interaction with Graphene Based Materials

Macková, A. (INP ASCR), 2018

Kuzár, M

Synthesis and Characterization of Multi-Component Exotic Garnets

Bárta, J., 2018

Ondrák, L.

A Modification of Radiation Sensitivity of Eucaryotic Cells

Múčka, V., 2018

Palušák, M.

Preparation and Characterization of Structures Based on Oxidised Graphite

Kozempel, J., 2018

Pelikánová, I. T.

Investigation of Nanomaterials for Singlet Oxygen Production

Procházková, L., 2018

Pokorný, M.

The Study of Europium Complexation with Selected Agents

Zavadilová, A., 2018

Sakmár, S.

Composite Carriers for Novel Multiphase Teranostics

Vlk, M., 2018

Tomanová, K.

Synthesis of the Luminescent Core-Shell Materials

Čuba, V., 2018

Valová, V.

Synthesis of "Core-Shell" Magnetic Theranostic Nanoprobes

Vlk, M., 2018

Vaněček, V.

Core-Shell Scintillators Based on ZnO/ZnMgO

Procházková, L., 2018

BACHELOR

Beňová, K.

Photoinitiated Affinity Probes - Mechanism and Pharmacologic Effect of Radiation Theraphy

Šulc, M. (FS CU), 2017

Jeziorská, V.

The Study of Complexation of Selected Actinides and Lanthanides with Agents Promising for Advanced Nuclear Fuel Cycles

Zavadilová, A., 2017

Kujan, J.

Immobilisation of Actinoids by Materials Based on ZrC

John, J., 2017

Patočka, A.

Diffusion of Radionuclides in Barrier Materials

Vopálka, D., 2017

Shashkova, E.

Teranostic Carriers of Radionuclides

Vlk, M., 2017

Šalplachtová, M.

Utilization of UV Radiation for Removal of Heavy Metals from Aqueous Solutions

Drtinová, B., 2017

Šebesta, J.

Partitioning of Minor Actinoids and Lanthanoids by Using N-donor Compounds

Distler, P., 2017

Šobová, T.

Radionuclide Separation in the Processes of Decontamination and Decommissioning

Špendlíková, I., 2017

Urbanová, K.

Study of Structural Materials Corrosion in the Environment of the Storage of Spent Nuclear Fuel

Dobrev, D., 2017

Vodehnal, O.

Kinetic Aspects of Actinoids Partitioning by Microfluidic Systems

Distler, P., 2017

Bilous, M.

Ultratrace Analysis of Fission and Activation Products

Němec, M., 2018

Burešová, M.

Recycling of Decontamination Media

Němec, M., 2018

Grapa, M.

Synthesis and Luminescent Properties of Quantum Dots

Čuba, V., 2018

Mindová, M.

Extracting Compounds for Advanced Nuclear Fuel Cycles

Distler, P., 2018

Sedmidubská, B.

Postradiation Reactions of Biomolecules

Davídková, M. (INP ASCR), 2018

Suchá, A.

Preparation of Inorganic Materials in Non Aqueous Systems

Čuba, V., 2018

Skálová, M.

Surface Modification of Silicon by the Covalent Attachment of Organic Molecules Using Grignard Reaction

Kozempel, J., 2018

PROJECTS, GRANTS AND CONTRACTUAL RESEARCH

Title, Code, Donator/Contractor; Chief Scientific Investigator(s)

EU PROJECTS

GENIORS - GEN IV Integrated Oxide Fuels Recycling Strategies, CA 730227, EC H2020 Euratom; John, J.

MEET-CINCH - A Modular European Education and Training Concept In Nuclear and RadioCHemistry, CA 754972, EC H2020 Euratom; Němec, M.

CEBAMA - Cement-based Materials, Properties, Evolution, Barrier Functions, CA 662147, EC H2020 Euratom; Vopálka, D.

EU STRUCTURAL AND INVESTMENT FUNDS

RAMSES - Ultra-trace Isotope Research in Social and Environmental Studies Using Accelerator Mass Spectrometry, CZ.02.1.01/0.0/0.0/16_019/0000728, ESIF Operational Programme Research, Development and Education; Němec, M.

CAAS - Center for Advanced Applied Sciences, CZ.02.1.01/0.0/0.0/16_019/0000778, ESIF Operational Programme Research, Development and Education; Čuba, V.

CAP - Centre of Advanced Photovoltaic, CZ.02.1.01/0.0/0.0/15_003/0000464, ESIF Operational Programme Research, Development and Education; Kozempel, J.

NSSF - Nuclear Safety, Security and Forensics, CZ.02.2.69/0.0/0.0/16_018/0002367, ESIF Operational Programme Research, Development and Education; John, J.

NSSF-Labs – Laboratories for Nuclear Safety, Security and Forensics, CZ.02.1.01/0.0/0.0/16_017/0002370, ESIF Operational Programme Research, Development and Education; Vlk, M.

Upgrade of Practical Training of Students, CZ.02.2.67/0.0/0.0/16_016/0002357, ESIF Operational Programme Research, Development and Education; Čuba, V.

NATIONAL PROJECTS

Research of Ionic Liquids for Application in Separation Processes, TH01020381, Technology Agency of the CR; Čubová, K.

Novel Composite Materials for Medical Radionuclides Separation, TJ01000334, Technology Agency of the CR; Vlk, M.

New Multistage Nanodiagnostics for Cancer Imaging and Prediction of Antiangiogenic Therapy Efficacy, NV16-30544A, Ministry of Health, Czech Republic; Kozempel, J.

Composite Filters for the Treament of Rinse Solutions, VI20172020106, Ministry of the Interior of the CR; Čuba, V.

Recyclable Decontamination Solution for Decommissioning of Nuclear Facilities, FV10023, Ministry of Industry and Trade, Czech Republic; Němec, M.

Research and Development of Technological Methods for Radiation-induced Production of Advanced Nanomaterials, FV30139, Ministry of Industry and Trade, Czech Republic; Bárta, J.

Synthesis, Characterization and Tailoring the Properties of Luminescent Nanocomposites, GA17-06479S, Czech Science Foundation; Čuba, V.

Support of the Activities in the Division of Nuclear and Radiochemistry (DNRC) EuCheMS, LTV17008, Ministry of Education, Youth and Sports, Czech Republic; John, J.

CTU GRANTS

Advanced Separation Techniques for Radionuclides, SGS18/192/OHK4/3T/14, CTU Prague; Fenclová, K.

Preparation of Theranostic Radionuclides Carriers for Nuclear Medicine, SGS16/251/OHK4/3T/14, CTU Prague; Mičolová, P.

Study of Speciation, Complexation and Migration of Critical Radionuclides, SGS16/250/OHK4/3T/14, CTU Prague; Baborová, L.

Partitioning of Selected Radionuclides in Advanced Nuclear Fuel Cycles, SGS15/216/OHK4/3T/14, CTU Prague; Distler, P.

Investigation of Advanced Nanostructures and Biomaterials, SGS17/195/OHK4/3T/14, CTU Prague; Procházková, L.

CONTRACTUAL RESEARCH

Research Support for Safety Assessment of Deep Geological Repository, 14SMN319, SÚRAO CZ, ÚJV Řež; Vopálka, D.

Safety Assesment of the Richard Repository, C1981-16-0, SÚRAO ČR; Amec Foster Wheeler s.r.o. Slovakia; Vopálka, D.

Research and Development of Chromatographic Materials for Medicinal Radionuclide Separation, 8301618D TRISKEM France; Kozempel, J.

Cerium-doped $Y_3Al_5O_{12}$ Nanocrystalline Material, 830-8301718D PRECIOSA - LUSTRY, a.s.; Čuba, V.

Determination of ^{235}U Abundance in a Sample of Metallic Uranium, 8301838D UJP Praha a.s.; Němec, M.

Absorber for Radiocaesium Determination, 8301839D WHOI USA; Šebesta, F.

RESEARCH FELLOWSHIPS / VISITING SCIENTISTS

OUTGOING:

Višňák, J.

Collaborative experiments at FZDR

FZDR Rossendorf, Germany, January – February 2017

Vetešník, A.

International Task Force GWFTS meeting „Modelling of GroundWater Flow and Transport of Solutes“

Stockholm, Sweden, May 2017

Procházková, L.

Collaborative experiments at CERN

Geneve, Switzerlan, May – June 2017

Vaněček, V.; Kittnerová, J.

Summer practice

Joint Institute for Nuclear Research (JINR), Dubna, Russian Federation, July 2017

Rosendorf, T.

PFLOTRAN Short Course

Barcelona, Spain, September 2017

Kittnerová, J.; Bartl, P.

I2EN Summer School: The back-end of the Nuclear Fuel Cycle

La Hague, Flamanville, Marcoule, France, September 2017

Kittnerová, J.

CEBAMA Intership in FZ Jülich

Jülich, Germany, January – April 2018

Fenclová, K.; Němec, M.

Collaborative experiments at VERA facility at University of Vienna

Vienna, Austria, February 2018

Fenclová, K.

Intercontinental Nuclear Institute (INI)

IAEA Fellowship Programme, Lowell, USA, June – July 2018

Bartl, P.

Summer practice

Joint Institute for Nuclear Research (JINR), Dubna, Russian Federation, July 2018

Kozempel, J.

Joint IAEA-JRC Workshop on the "Supply of Actinium-225“

IAEA Vienna, Austria, October 2018

Vlk, M.

IAEA Technical Meeting in Production and Quality Control of Theranostic Labelled Peptides

IAEA and Polatom, Warsaw, Poland, June 2018

Vlk, M.

IAEA Hands on Training: Diagnostic and Therapeutic Radioisotopes and Radiopharmaceuticals Application

World Council on Isotopes (WCI), Korea Atomic Energy Research Institute (KAERI), Seoul, Korea, October 2018

John, J.

Radiotracers and Sealed Sources Technologies and Applications in Industry

IAEA Project RER1020, Vienna, Austria, December 2018

INCOMING:

Evans, N. M.

Visiting professorship in Nuclear Chemistry
(Programme „Mobility" of the Ministry of Education, Youth and Sports of the CR)

Nottingham Trent University, UK, April – December 2018

Schumann, D.

Exotic radionuclides

Paul Scherrer Institute, Switzerland, February 2017

Kajan, I.

Chemistry of the nuclear reactor accidents

Paul Scherrer Institute, Switzerland, October 2017

Todd, T. A.

Nuclear fuel reprocessing in U.S.

Idaho National Laboratory, USA, December 2017

Harwood, L. M.

The development of ligand systems for separating minor actinides from lanthanides for nuclear fuel reprocessing

University of Reading, UK, November 2017

Synal, H. A.

Development of Accelator Mass Spectrometry

ETH Zurich, Switzerland, March 2018

Pike, S. M.

Fukushima Dai-ichi - a view from the ocean

Woods Hole Oceonagrpic Institution, USA, May 2018

Andris, B.

Management of sludges from the long-term fuel storage pond at A1 NPP

VÚJE Trnava, Slavakia, May 2018

Mothersill, C.

The implications of non-targeted effects for Radiation Biology and Radiotion Protection

McMaster University, Hamilton, Ontario, Canada, October 2018

DEPARTMENT SEMINAR

Below, the overwiev is given of invited opening lectures and the respective speakers at the Department seminar in 2017 and 2018. Since 2015 the seminar has been opened to broad nuclear chemistry community and is run in collaboration with the Nuclear Chemistry Working Group of the Czech Chemical Society (http://osjch.csch.cz/en/home/). The invited opening lectures are recorded, archived and openly accessible for the general public (subject to approval of the speaker) in the SlidesLive system at https://slideslive.com/seminar-kjch-fjfi-cvut-v-praze. Full programme of the seminars, including all the contributed lectures and their authors, can be found at the Department web at http://www.jaderna-chemie.cz/?vv=seminar_en

2017

Schumann, D.

Exotic radionuclides, what are they good for?

Paul Scherrer Institute, Switzerland, February 2017

Uhlíř, J.

History of the Oak Ridge National Laboratory: Manhattan Project and post-war period

ÚJV Řež, March 2017

Sovová, H.

Increasing possibilities of supercritical carbon dioxide applications

Institute of Chemical Process Fundamentals CAS, April 2017

Štuller, J.

National action plan for the development of nuclear energy in the Czech Republic and its implementation

Ministry of Industry and Trade of the CR, May 2017

Kajan, I.

Chemistry of the nuclear reactor accidents

Paul Scherrer Institute, Switzerland, October 2017

Todd, T. A.

The past and present of nuclear fuel reprocessing in U.S.

Idaho National Laboratory, USA, November 2017

Harwood, L. M.

The development of ligand systems for separating minor actinides from lanthanides for nuclear fuel reprocessing

University of Reading, UK, December 2017

2018

Hanus, V.

Unique approaches and technologies in management of the chemistry of NPP Temelín

NPP Temelín, February 2018

Synal, H. A.

History and development of Accelator Mass Spectrometry

ETH Zurich, Switzerland, March 2018

Evans, N. M.

The Fate of Technetium in UK Radioactive Waste Disposal

Nottingham Trent University, UK, April 2018

Pike, S. M.

Fukushima Dai-ichi - a view from the ocean

Woods Hole Ocenographic Institution, USA, May 2018

Andris, B.

Management of sludges from the long-term fuel storage pond at A1 NPP

VÚJE Trnava, Slavakia, May 2018

Mothersill, C.

From Biophotons to Bystander Effect : The implications of non-targeted effects for Radiation Biology and Radiotion Protection

McMaster University, Hamilton, Ontario, Canada, October 2018

Janata, J. A.

Greatest Discovery: Of interest to anybody who cares about energy and its impact on environment

Georgia Institute of Technology, Atlanta, Georgia, USA, December 2018

Evans, N. M.

What were they thinking of? Radioactive Quackery.

Nottingham Trent University, UK, April 2018

PERSONNEL

Head of the department:
prof. Ing. Jan John, CSc.

Vice head:
doc. Ing. Mojmír Němec, Ph.D.

Registrar:
Ing. Alois Motl, CSc.

Project Manager / Economist:
Mgr. Štěpánka Maliňáková

Secretary:
Marie Kotasová

SEPARATION AND RADIOANALYTICS

prof. Ing. Jan John, CSc.
Ing. Kateřina Čubová, Ph.D.
RNDr. Martin Daňo
Ing. Alois Motl, CSc.
doc. Ing. Mojmír Němec, Ph.D.
Ing. Miroslava Semelová, Ph.D.
doc. Ing. Ferdinand Šebesta, CSc.
Ing. Irena Špendlíková, Ph.D.
Ing. Alena Zavadilová, Ph.D.

Ph.D. students:
Ing. Pavel Bartl
Mgr. Kateřina Fenclová
Ing. Ivan Hupka
Ing. Kamil V. Mareš
Ing. Michal Pokorný
Ing. Tomáš Prášek

Part time:
RNDr. Ing. Petr Distler, Ph.D.&Ph.D.

Technician:
Jana Steinerová

SPECIATION AND MIGRATION

doc. Mgr. Dušan Vopálka, CSc.
Ing. Barbora Drtinová, Ph.D.
doc. Ing. Karel Štamberg, CSc.
Mgr. Aleš Vetešník, Ph.D.
RNDr. Eva Viglašová, Ph. D.

Ph.D. students:
Mgr. Lucie Baborová
Ing. Eva Hofmanová
Ing. Jana Kittnerová
Ing. Iveta Kroulíková
Ing. Tomáš Rosendorf
Ing. Jakub Višňák

Part time:
Ing. Helena Filipská, Ph.D.

Technician:
Olga Múčková

RADIATION CHEMISTRY

prof. Ing. Viliam Múčka, DrSc.
Ing. Jan Bárta, Ph.D.
doc. Ing. Václav Čuba, Ph.D.
Ing. Lenka Procházková, Ph. D.
doc. Ing. Rostislav Silber, CSc.

Ph.D. students:
Ing. Barbora Neužilová
Ing. Iveta T. Pelikánová
Ing. Kseniya Popovich
Ing. Kateřina Tomanová

Technician:
Alena Matyášová

RADIOPHARMACEUTICAL CHEMISTRY

doc. RNDr. Ján Kozempel, Ph.D.
RNDr. Martin Vlk, Ph.D.

Ph.D. students:
Mgr. Klára Belešová
Ing. Kateřina Fialová
Ing. Ekaterina Kukleva
Ing. Lukáš Ondrák
Ing. Michal Sakmár
Ing. Petra Suchánková

Technician:
Ing. Šárka Hráčková

Redaction and technical support: Marešová, B.
Foto p. 67 © Drtinová, B.